FINAL REPORT

UXO Navigation Technology

SERDP Project MM-1441

OCTOBER 2008

Dr. John Foley
Robert Mehl
Dr. Nicolas Lhomme
Sky Research, Inc.

REPORT DOCUMENTATION PAGE

Form Approved
OMB No. 0704-0188

1. AGENCY USE ONLY (Leave blank)	2. REPORT DATE	3. REPORT TYPE AND DATES COVERED
	October 2008	Final Report, 2007-2008

4. TITLE AND SUBTITLE
"UXO Navigation Technology, Draft Final Report"

5. FUNDING NUMBERS
SERDP MM-1441

6. AUTHOR(S)
Dr. John Foley, Sky Research, Inc.
Robert Mehl, Sky Research, Inc.
Dr. Nicolas Lhomme, Sky Research, Inc.

7. PERFORMING ORGANIZATION NAME(S) AND ADDRESS(ES)
Sky Research, Inc
445 Dead Indian Memorial Road,
Ashland, OR 97520

PERFORMING ORGANIZATION REPORT NUMBER

9. SPONSORING/MONITORING AGENCY NAME(S) AND ADDRESS(ES)
SERDP
901 North Stuart Street, Suite 303,
Arlington, VA 22203

10.SPONSORING/MONITORING AGENCY REPORT NUMBER

11. SUPPLEMENTARY NOTES

12a. DISTRIBUTION/AVAILABILITY STATEMENT
Unclassified/Unlimited

12b. DISTRIBUTION CODE

13. ABSTRACT (Maximum 200 words)

This report documents the goals, objectives, materials, methods and analysis associated with the SERDP MM-1441 "UXO Navigation Technology" research and development project. Over the 3+ years of the project, three laser-based positioning systems were evaluated for performance, and technology was developed associated with expanding laser positioning capabilities for UXO applications. Technologies developed as part of this project will significantly impact the DoD by facilitating deployment of new and emerging UXO discrimination tools where precise sensor location and orientation data are required. This project investigated three similar laser-based positioning technologies providing real-time 3D positional accuracy at the millimeter level. Only one of the systems was integrated with an inertial measurement unit (IMU) and two systems were integrated with the EM61-HH for hand-held applications. This new technology was tested and results presented in this report. The new Trimble SPS930 with its low latency and jitter, and 10 Hertz sampling rate is the instrument that proved to be the most feasible instrument for hand-held and wooded survey deployments.

14. SUBJECT TERMS
Positioning accuracy
UXO discrimination
Navigation systems

15. NUMBER OF PAGES
145

16. PRICE CODE

17. SECURITY CLASSIFICATION OF REPORT	18. SECURITY CLASSIFICATION OF THIS PAGE	19. SECURITY CLASSIFICATION OF ABSTRACT	20. LIMITATION OF ABSTRACT
Unclassified	Unclassified	Unclassified	Unlimited

NSN 7540-01-280-5500

Standard Form 298 (rev. 2-89)
Prescribed by ANSI Std 239-18

TABLE OF CONTENTS

LIST OF TABLES

LIST OF FIGURES

ACRONYMS

µs	microsecond(s)
3D	three-dimensional
cm	centimeter(s)
DAS	Data Acquisition System
DoD	Department of Defense
EDM	Electronic Distance Measurement
EM	Electromagnetic
EMI	Electromagnetic Induction
EOD	Explosive Ordnance Disposal
ERDC	Engineer Research and Development Center
ESTCP	Environmental Security Technology Certification Program
FPGA	Field Programmable Gate Array
GHz	Gigahertz
GNSS	Global Navigation Satellite System
GPS	Global Positioning System
GUI	Graphical User Interface
HH	EM61HH-MK2
Hz	Hertz
IMU	Inertial Measurement Unit
IR	Infrared
km	kilometer(s)
LED	Light Emitting Diodes
LOS	Line of Sight
m	meter(s)
mg	milligravity
mgon	milligon
MHz	Megahertz
mm	millimeter(s)
ms	millisecond(s)
m/s	meter(s) per second
ppm	parts per million
RMS	Root Mean Square
RPC	Remote Procedure Calls
RTK GPS	Real Time Kinematic Global Positioning System
RTS	Robotic Total Station
s	second(s)
SERDP	Strategic Environmental Research and Development Program
SON	Statement of Need
SPEC	Stratton Park Engineering Company Inc.
UHF	Ultra High Frequency
UXO	Unexploded Ordnance

EXECUTIVE SUMMARY

This report describes the research conducted under Strategic Environmental Research and Development Program (SERDP) project MM-1441 titled "UXO Navigation Technology". The main objective of this research project was to explore different laser-based positioning technologies and evaluate their performance when applied to hand-held technology integration and limited line-of-sight environment surveying. Laser positioning systems have been in use by land surveyors for many years. Geophysical surveying has used the systems in limited capacities, which include surveying near wooded boundaries, buildings, along cleared wooded path with a heavy canopy or other areas where GPS does not work effectively. Laser-based positioning technology has a positional accuracy in the millimeter range and a small spherical error, both of which provide the positional accuracy needed for anomaly parameter recovery through inversion techniques.

Several different systems by two different manufacturers (Leica and Trimble) were tested. As the project evolved it became clear that the Leica TPS1200 system could not provide a positioning solution at either the speed or with the timing consistency as the newer Trimble SPS930 unit. The Trimble was a superior instrument for the following reasons:

1 Latency and dither: The Trimble SPS930 has a small dither (4 ms) that makes correcting the timestamp of the positions a simple calculation.
2 Faster update rate; The SPS930 has a 10 Hz sample rate with a possibility of 20 Hz in the future.
3 Active Prism: The flashing LED of the prism provides a glow that the gun identifies and tracks even when multiple prisms are in use. Also the LED provides a glow that the gun uses to locate the prism after the line-of-sight has been interrupted.
4 Firmware Stability: The firmware of the SPS930 was more stable and reliable when compared to the firmware of the TPS1200. However, some glitches were noticed during the wooded tests. The SPS930 is a new instrument so some glitches are expected.

For hand-held sensor integration the dither and sample rate are the key points. Sensor integration tests with the Leica system did not provide the necessary positional data quality needed for successful inversion. The Trimble provided the necessary positional quality for the reliable inversion of geophysical sensor data, making it the instrument of choice for sensor integration.

Wooded environments contain many obstructions for line-of-sight laser positioning methods. One potential solution is to deploy multiple guns with the expectation that more of the site will be visible from two gun positions. Deploying a multi-gun system requires software to monitor gun status and send instructions to the guns to establish lock when prism lock is lost. Both Leica and Trimble provide system monitoring and instruction commands to control gun operations. A man-machine interface called PrismTracker was developed to monitor and control gun operations. PrismTracker monitored gun status and when the gun lost prism lock, the software used prism location data from the locked gun to point and reestablish lock on the unlocked gun.

Successfully surveying in a wooded environment is difficult as there are many issues to consider including tree density, placement, cross sectional area, gun placement, survey speed, and stop

points. At tree densities of less than 6 trees per 5 m by 5 m (25 m^2 or 2400 trees per hectare), dual-laser guns appear to provide sufficient coverage as long as the guns are placed intelligently. When the tree density exceeded the limit cited above there were multiple problems with the prism tracking. Firstly, the prism would be obscured from one, or both guns, for large portions of the site. When one gun was tracking the prism, it would instruct the other gun to point to the prism. The second problem was encountered when this location was in another shadow area as the software would have to point the gun again. In theory, if the software had an idea of where the shadows were it could intelligently point the gun to a non-obscured position.

In conclusion, the Trimble SCS930 provides an extremely accurate and reliable positioning sensor suitable for deployment in open and wooded areas with tree densities less than 6 trees per 25 m^2. Above this density, accurate positions can only be obtained over a small fraction of the site. Therefore, we conclude that laser systems are a partial, but not complete, solution for surveying in wooded areas.

1. INTRODUCTION

This report documents the goals, objectives, materials, methods and analyses associated with the SERDP MM-1441 "UXO Navigation Technology" research and development project.

1.1. Background

Technologies developed as part of this project will positively influence the Department of Defense (DoD) by facilitating deployment of new and emerging UXO discrimination tools where precise sensor location and orientation data are required. Data requirements for positioning accuracy for UXO discrimination were defined by the Strategic Environmental Research and Development Program (SERDP) and Environmental Security Technology Certification Program (ESTCP) during the SERDP Electromagnetic Induction (EMI) Workshop held in Annapolis, Maryland in February 2004. Seventy authorities specializing in all aspects of EMI-based UXO discrimination reached verbal consensus that 2-3 centimeter (cm) level positional accuracy is needed to apply current discrimination techniques.

The essential requirement for positional accuracy when applying UXO discrimination technologies to geophysical data has been clearly demonstrated through focused research and development efforts sponsored by SERDP and ESTCP. For example, Foley et al. (2002) shows an 11% root mean square (RMS) change in recorded EM-61 target signatures due to 10 cm X, Y positional errors. Barrow & Nelson (2001) show through numerical simulation and testing with recorded field data that target signatures corrupted with modest positional errors produce erroneous discrimination results. Bell (2005) demonstrated that discrimination with a Geonics EM-61 hand-held device required positional precision on the order of 1 cm.

The need for "near-laboratory-quality" measurements must be met through the development of robust and precise positioning technologies. This requirement influences several system design considerations as well as practical survey deployment issues. Thus, efficient development of appropriate data positioning technologies must recognize and fully exploit the well-established components of the UXO mapping, analysis, relocation, and excavation process.

This project investigated three similar laser-based positioning technologies providing real-time three-dimensional (3D) positional accuracy at the millimeter (mm) level (±5 mm + 2 parts per million [ppm]). Only one of the systems was integrated with an inertial measurement unit (IMU). The results of tests using this latter, new technology are presented in this report.

New positioning technologies must be flexible in terms of multiple modes of operation, sensor integration, and applicability in vegetated and wooded terrains. Additionally, these systems must be small, lightweight, rugged, and inexpensive. Furthermore, these systems must have a low metal content to minimize interference with proximally located metal detecting sensors. A significant added challenge is the need for technology readily transferable to the UXO remediation industry at low unit-cost. Logical, achievable, and cost-effective solutions can be based on existing laser positioning technology. Therefore, this project brings together experts in

data positioning, laser tracking, and system electronics to solve this problem by leveraging existing technology.

This project extends the application of laser positioning technology to meet the SERDP objectives of Statement of Need (SON) UXSON-05-02. Table 1 outlines the stated objectives of UXSON-05-02, the current laser positioning system capability, and the technology improvements researched, developed, and demonstrated in this project. Performance specifications were developed and based on existing and proposed sensor deployment strategies and on the data quality requirements for target detection and discrimination. This project leverages research and development work previously conducted as part of ESTCP Project UX-0129 ("Innovative Navigation Systems to Support Digital Geophysical Mapping") and further explored in SERDP Project UX-1310 ("Sensor Orientation Effects on UXO Geophysical Target Discrimination").

Table 1. SERDP Statement of Need 05-02 and MM-1441 Project Objectives

Performance Goals from UXSON-05-02	Current RTS System Capability	Technology Needs
Handheld or man-portable • Suitable size • Weight • Power requirements	• 12 cm prism • Less than 0.4 kg • Passive on rover, simple base station power solutions	• None • None • None
Compatible with geophysical sensors	EM61, EM61-MKII, G858, TM4 integration completed	Rigorous clock synchronization via master/slave configuration
Handheld or cart mounted	Simple mounting completed	Low or no-metal prism components
Operate in rough, vegetated terrain, where GPS fails	Effective in light to moderate trees	Leapfrog capability to reduce set-ups. More sophisticated tracking for dense-tree environments
Dual-mode navigation tools • Same basic technology • Operator selectable	• Coarse/fine capability demonstrated (Phase III) • Not implemented	• None • System software
Coarse Mode • Min: ±0.3 m RMS error • Desired: ±0.1 m (X,Y)	±0.309 m Phase II results	• Improved RTS system configuration
Fine Mode • Min: ±0.1 m RMS error • Desired: ±0.01 m (X,Y)	• ±0.05 m Phase III tests	• Improved RTS system configuration

1.2. Objectives

The goal of this laser positioning project is to develop the technical modifications to integrate laser technology with man-portable survey platforms. Integration will satisfy the requirements of geophysical surveys for precise sensor location and orientation data, enabling marked improvements in both UXO target detection and discrimination. Furthermore, the developed capabilities will be transitioned directly to the UXO community through new product development.

The following are the objectives of this project:

1. Identify and quantify specific applicability of laser positioning technologies under a suite of field conditions, including wooded areas and areas with significant topographic variability.
2. Modify existing laser-based technologies and integrate with industry-standard sensors for man-portable survey platforms as specified in SERDP UXSON-05-02.
3. Provide the UXO community with a robust, flexible and inexpensive navigation technology that solves the navigation problem for hand-held, pushcart, and vehicle systems, in detection and interrogation modes in both open and wooded areas.

During Year 1, an initial laser assessment was conducted to meet the first objective and significant progress made to modify and deploy the technology to meet the second objective. The main conclusion drawn from the assessment is that laser positioning technology with its millimeter-level precision is highly applicable for UXO detection and discrimination applications. The core optical capability of the technology provides the necessary precision, update rates, and repeatability specified in the SERDP SON.

Year 2 saw comparative testing of three different laser-based systems with an industry standard satellite-based position system at the Engineer Research and Development Center (ERDC) Test Stand in Vicksburg, Mississippi. After this comparative testing, issues with the Leica instrument's timing became apparent. The multi-gun control software underwent further development, modification and testing. Lastly, one of the Leica instruments was integrated with an industry-standard electromagnetic (EM) sensor designed for hand-held deployments.

In Year 3, instrument testing shifted from Leica to the more stable and better performing Trimble platform. Utilizing lessons learned from the previous years, a characterization study measured the performance specifications of the Trimble platform. Trimble released a new laser-based system in late summer of 2007 and Sky acquired two systems as part of an evaluation of the system. During the evaluation, several issues were identified and presented to Trimble engineers. These issues included prism list addition and several man-machine interface command problems.

Trimble instrument availability and the identified hardware issues in 2007 slowed progress of the project. After a conference call with Trimble engineers in mid-December 2007, the issues were resolved and testing commenced in early 2008.

1.3. Report Outline

This final report discusses, in detail, the results of this multi-year project. Section 2 discusses the laser assessment tests that were designed to measure the performance and operational parameters of the different laser-based positioning systems. Section 3 discusses the integration of the laser systems with the EM61HH-MK2, which was one of the primary objectives of this project. This section also provides a detailed analysis of the performance of the system through a parameter analysis using geophysical inversion. Section 4 discusses the multi-gun positioning system tests and results. These tests measured the operational parameters of the laser-based sensors and their ability to track a prism as it moves along a line with intermittent line-of-sight. This section also discusses the results of the forest testing which is another one of the primary objectives of this project. Section 5 discusses the line-of-sight model was used to establish the optimal location of the guns in a forested area. This model also provided an analysis into the performance of a system based on some key operational parameters. Lastly, the report concludes with a summary of the project and possible future directions. Appendix A presents the data in tabular format, and Appendix B presents an assessment of the Leica firmware.

2. LASER ASSESSMENT

Through the duration of the project, assessment of the performance and operational parameters of the different laser-based positioning systems was necessary. The most important parameters to assess are positional accuracy, latency and dither. Both the Leica and Trimble have the same static positioning accuracies of 5 mm ± 2 ppm, however the sampling intervals and timing latencies are very different. Over the course of the project the focus of the assessment shifted from positional to timing accuracies because this proved to be a more critical component affecting system performance.

In Year 1, the Leica positional and operational parameters were assessed using simple techniques. In Years 2 and 3, the timing capabilities of the instruments were tested by using a test track to measure the absolute prism position and comparison with the positions measured by the gun.

2.1. Materials

2.1.1. Leica TPS 1100/Leica TPS 1203

The Leica Robotic Total Station (RTS) unit is a laser-based 3D positioning technology providing millimeter-level positional accuracy. The Leica utilizes the concept of standard optical total station surveying; the RTS is set at a known location with a reference angle established relative to a second known location. Angle and distance measurements calculate the XYZ position of the prism. The system is capable of measuring 14 positions per second (s) in a wired configuration and eight positions in a wireless configuration. Figure 1 shows the equipment, including the base station optical tracking system (gun), and mobile prism. The RTS has a library of functions that provide low-level access to control the gun's operation. These functions allow the development of third-party software to assume control of the gun. An assessment of the Leica firmware was conducted as part of the equipment's evaluation, see Appendix B for these results.

Figure 1. Leica TPS 1203 and 360° passive prism.

2.1.2. ArcSecond

ArcSecond (Figure 2) is a laser positioning system that uses a minimum of three guns with rotating pulsed lasers and a range pole with light detection sensors. A constellation of guns are set up within 150 feet of each other. When the gun is powered on, laser light is emitted in a fan in 360°; the light detector measures the arrival of the light and uses triangulation to calculate the position of the detector. There are two different light detector configurations, a tetrahedron and a gradient bar. This system is unique in that it is able to calculate the angle at which the pole is positioned by measuring the arrival time of the different pulses and calculating the angles based on the fixed sensor geometry. The system is able to collect XYZ, and pole angles at 10 Hertz (Hz).

+

Figure 2. ArcSecond gun with rotating laser and flashing LED array (left) and the laser light detector which acts as the prism (right).

2.1.3. Trimble ATS600

The Trimble ATS600 instrument (Figure 3) utilizes the concept of standard optical total station surveying. The ATS600 is set at a known location with a reference angle established relative to a second known position. The system uses an active prism emitting an Infrared (IR) light source (a ring of pulsating light emitting diodes [LED] located one inch below a ring of mirrors) and calculates the XYZ position of the prism based on horizontal and vertical angle measurements and distance measurements. The active prism requires an external power source to operate the LED ring. The maximum update rate for the Trimble ATS600 is 6 Hz.

Figure 3. The Trimble ATS600 (left) searches and tracks the IR glow from the ring of LED lights on the active prism (right).

2.1.4. Trimble SPS930

In August 2007, Trimble released the SPS930 Universal Total Station, capable of collecting data at 20 Hz with an accuracy of ±5 mm +2 mm ppm. The SPS930 Universal Total Station (Figure 4) uses Trimble's MultiTrack technology, allowing the instrument to track a passive prism (mirror-only) or active prism (mirrors with an IR light source), and Trimble's MagDrive fourth generation servo technology. The MagDrive technology uses magnetic levitation to eliminate friction in the system producing smooth horizontal and vertical angular measurements accurate to 1 milligon (mgon) (Trimble 2007). The hardware also has a man-machine interface allowing the creation of third party software to access the low-level functions to control gun operations. The active prism has a ring of mirrors with two LED rings above and below the mirrors. The LED emits an IR source that the SPS930 uses to sense and track the prism location. The active prism requires a battery to operate the LED ring. The SPS930 uses a 2.4 gigahertz (GHz), 115,200 baud radio to receive data and transmit commands.

Figure 4. The new Trimble SPS930 (left) uses radio modems to send commands and position data to and from a portable controller while tracking an active prism (right) that has an IR glow from the ring of LEDs above and below the ring of mirrors.

2.1.5. Platform Test Track

The platform test track is a 0.8 meter (m) long aluminum track with a stepper motor that moves a trolley up and down the track via a belt. A stepper motor is a motor controlled by a microprocessor that can operate the motor one step at a time. The stepper motor counts 780 "ticks" from the start to the end of the track; the motor can accurately place the trolley to within 1.0 mm. Software counts the number of ticks to calculate the distance the trolley has traveled.

2.1.6. Sky Research Hardware DAS

The Sky Research Hardware Data Acquisition System (DAS) provides the means to accurately time stamp asynchronous data streams to a common time base. The DAS employs a Field Programmable Gate Array (FPGA) and a Linux operating system to process incoming serial data streams and send new data streams to a host computer for storage and display.

2.1.7. Trimble RTK GPS

For comparison of positioning accuracy, this project utilized Trimble Real Time Kinematic Global Positioning System (RTK GPS) technology for testing (Figure 5). GPS utilizes the United States Global Navigation Satellite System (GNSS) consisting of a network of 24 satellites which transmit radio signals containing time data. The GPS receiver calculates its position by measuring the distance between itself and three or more GPS satellites. Measuring the time delay between transmission and reception of each GPS radio signal gives the distance to each satellite, since the signal travels at a known speed. The signals also carry information about the satellite's

location. By determining the position of, and distance to, at least three satellites, the receiver can compute its position using trilateration. RTK GPS utilizes a differential method where a GPS receiver is setup over a known point and a radio modem connected to the base receiver transmits correction values to a second GPS receiver. The RTK also uses a carrier phase measurement. Trimble RTK GPS can provide horizontal positioning accurate to ± 10 mm + 1 ppm and vertical positioning accurate to ± 20 mm + 1 ppm.

Figure 5. Base-station setup used to provide corrections to a rover that operates in RTK mode.

A complete RTK GPS system includes two GPS receivers, one radio modem capable of transmitting differential corrections, one radio modem capable of receiving the differential corrections, and an interface to control the GPS equipment (either a laptop or survey controller). For the testing conducted for this project, the following Trimble RTK GPS equipment was utilized:

- Trimble R7 GPS receiver with Zephyr Geodetic antenna (base GPS unit);
- Trimble R8 GPS receiver with integrated antenna and receive radio modem (rover GPS unit);
- Trimble Trimark 3 Ultra high frequency (UHF) (450-470 megahertz [MHz]) transmit radio modem; and
- Trimble TSC2 survey controller.

2.1.8. ERDC Test Stand

The ERDC Test Stand is a 3 × 4 m platform area with a nearly unobstructed view of the sky. The ERDC Test Stand facility makes it possible to move sensors in a highly repeatable pre-programmed pattern. Robotic motors control the movement of the sensor arm. An ASCII control file defines the location and duration at each point, enabling both static and dynamic data collection at the Test Stand. These capabilities and the ability to position sensors with millimeter precision make the Test Stand an ideal testing platform for comparing the performance of various positioning technologies.

2.2. RTS Assessment 2005

Field experiments for assessing the accuracy and performance of the Leica TPS1200 RTS under a variety of conditions were conducted in Ashland, Oregon, using the Sky Research test site. These tests measured the operational distance between the gun and prism, 3D measurement accuracy and limited line-of-sight tracking capabilities.

2.2.1. Distance

Cloudy Conditions: Cloudy skies are the ideal conditions for RTS operations. The maximum effective tracking distance on the day of the test was approximately 850 m. The test consisted of placing the RTS at one end of the Ashland Municipal Airport runway and walking until lock was lost. A problem experienced during the test that was not expected was a disruption in radio communications between the gun and remote control unit at a distance of approximately 750 m. To resolve this problem, the antenna was placed 0.5 m higher so that it was not blocked by the operator or the metal casing of the gun.

Sunny Conditions: Sunny skies provide less than optimal conditions for RTS operations; performance issues are related to radiant heating of the ground, which results in a high temperature gradient close to the ground surface. This heat gradient refracts light and reduces the tracking capabilities of the RTS. The maximum effective tracking distance of the RTS on the day of the test in these conditions was approximately 440 m.

2.2.2. Accuracy

XY Accuracy: To measure the accuracy of the RTS, a circular path was established for the prism to traverse. A 0.5 m diameter wheel established the path and the wheel was manually spun at various speeds. The distance between the gun and prism was set at three distances: 7, 21 and 85 m. The test resulted in a cloud of points surrounding the actual path. On average, the RTS measured the position of the moving prism to within 5 mm of the actual path (Table 2). The error increased when the rotational speed increased. The error also increased the farther the RTS gun was positioned from the prism. This increase in error is caused by the spreading of the laser beam over distances and is documented in the product's technical specifications. The error also appears to be reduced at the 0°, 90°, 180°, and 270° positions, and is greater at 45° complement angles; this can be seen in Figures 6 and 7. This is explained by analyzing what the gun is doing

at those positions. At 90° and 270°, the rotation of the gun is slowing and about to change directions. Therefore, the position becomes a function of Electronic Distance Measurement (EDM) because the rotation and the vertical measurements are nearly constant. At the 0° and 180° positions, the positions become a function of the rotation angle because the EDM and vertical measurement are nearly constant. The error from all three measurements increases as the prism moves through the 45° complement angles (Figure 8).

Table 2. Summary of X-Y Accuracy

Statistic	7-Meter Test	21-Meter Test	85-Meter Test
Mean Error	0.005 m	0.005 m	0.007 m
Standard Deviation	0.004 m	0.004 m	0.007 m
Maximum Error	0.025 m	0.036 m	0.104 m

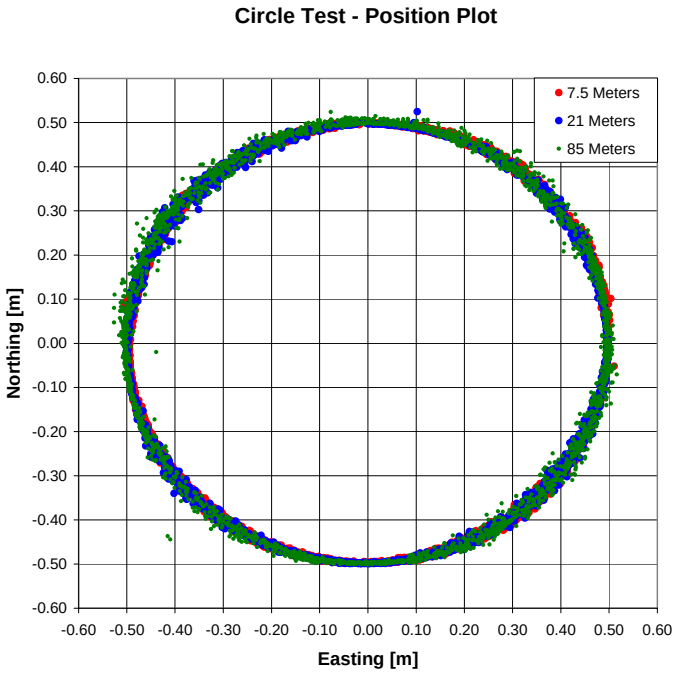

Figure 6. RTS measurements in a circular path.

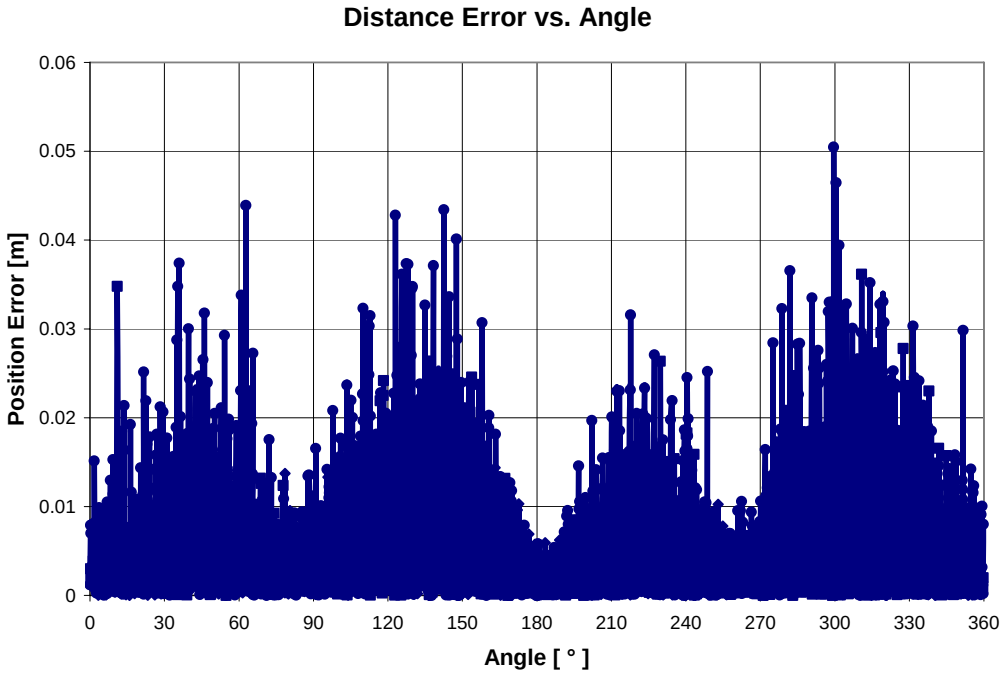

Figure 7. Distance error versus angle in the circular path test.

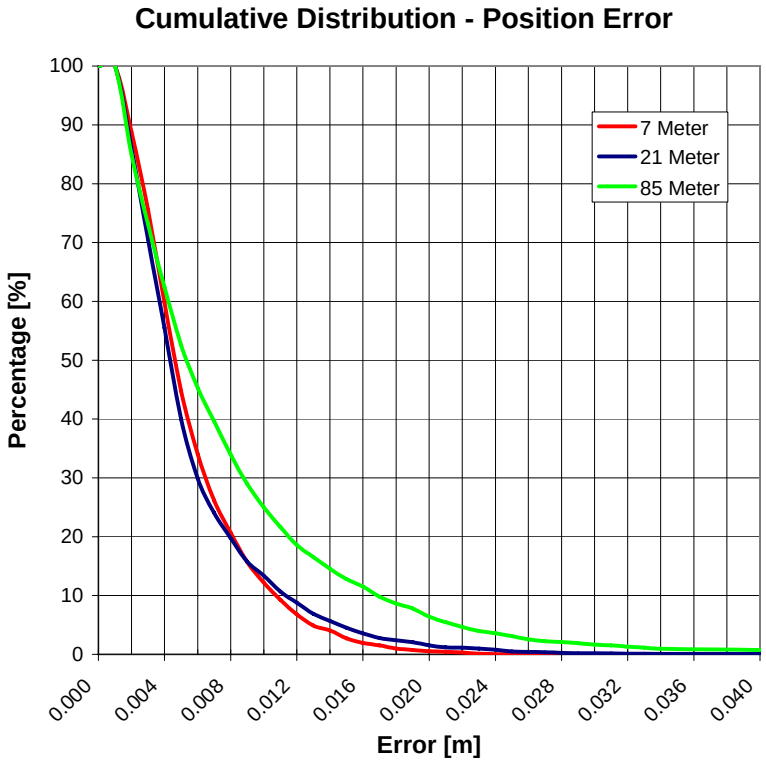

Figure 8. Distribution of positional error as measured during circular path test.

2.2.3. Elevation Test

To quantify the elevation accuracy, the rotating platform was tilted, allowing for approximately 0.02 m of elevation change around the circle. The results of the test are summarized in Table 3. The amount of error was related to where in the path the prism was located. Contrary to the X-Y error, the elevation error is greatest at 90° and 270° (Figure 9). Elevation measurements are solely a function of the vertical measurement axis and at these angles the vertical movement is greatest. As gun and prism distance increases, the movement in the vertical plane is small and error increases because of the instrument's inability to detect very small changes in vertical movement. This error, however, is still less than 2 cm.

Table 3. Summary of Elevation Accuracy

Statistic	7-Meter Test	21-Meter Test	85-Meter Test
Mean Error	0.001 m	0.000 m	0.004 m
Standard Deviation	0.001 m	0.000 m	0.003 m
Maximum Error	0.016 m	0.005 m	0.019 m

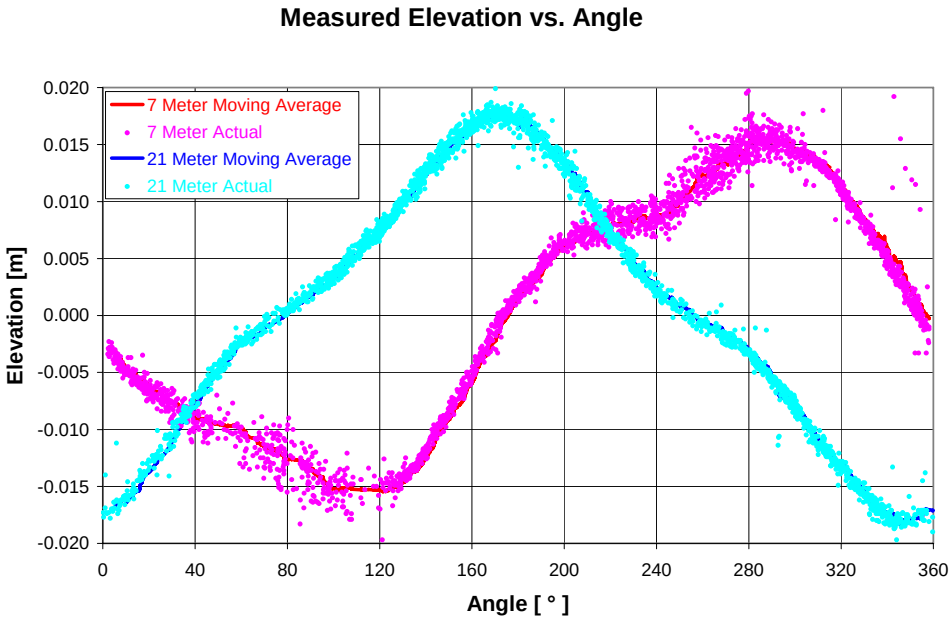

Figure 9. Elevation error as measured on a tilted platform.

2.2.4. Line of Sight Test

A test was conducted in a forested environment to assess the ability of the RTS to track and measure the location of the prism in conditions with limited line-of-sight. The major factors affecting the performance of the RTS in limited line-of-sight conditions are tree width, proximity of trees to the gun, tree density, and the distance between trees.

For this test, the RTS was set up in a clearing amongst the trees and used to survey the locations of all the trees within a 35 m radius. Project personnel then cleared several paths between the trees allowing safe passage along the paths and configured the RTS search window to allow for optimal lock recovery as the handheld prism traversed the cleared paths in the forest.

Figure 10 shows the results of the test with interesting areas outlined. As expected, a large-diameter tree close to the gun creates a large shadow zone; once the prism enters the shadow zone it is no longer tracked. The gun is able to predict the prism location but only for a couple of seconds, after which it stops and manual positioning is required. Area 1 of Figure 10 shows one of these trees close to the gun creating a large shadow. Area 5, however, creates the same effect as Area 1 but is accomplished with 3 trees close together effectively mimicking a single large tree.

Area 3 shows how tree density adversely effects the position measurements. There is cluster of 9 trees that severely hampers the ability of the RTS to track the prism. The RTS successfully tracked the prism on paths 2 and 3; however, tree density compromised the positions on paths 1 and 4.

During this test, when the gun lost prism lock it approximated the prism's position using the last velocity vector. It did this for a user-defined amount of time after lock was lost. When the prism re-emerged from the shadow, the gun regained lock and resumed measuring distances within a second once the prism was in the field of view of the gun. However, when the trees were too close together, the gun did not have enough time to lock onto the prism. The two trees within the boundary of Area 4 were roughly 3 m apart in easting (radially) but were only 0.5 m apart in the northing direction. These trees were too close together and the gun did not have enough time to establish lock before entering the next shadow.

Area 6 had low lying branches which disrupted prism tracking. The gun was able to track the prism but the hemlock needles prevented the gun from locking onto the prism. Typically in forested survey sites, the brush and limbs are removed to a height of 2 m allowing for safe passage.

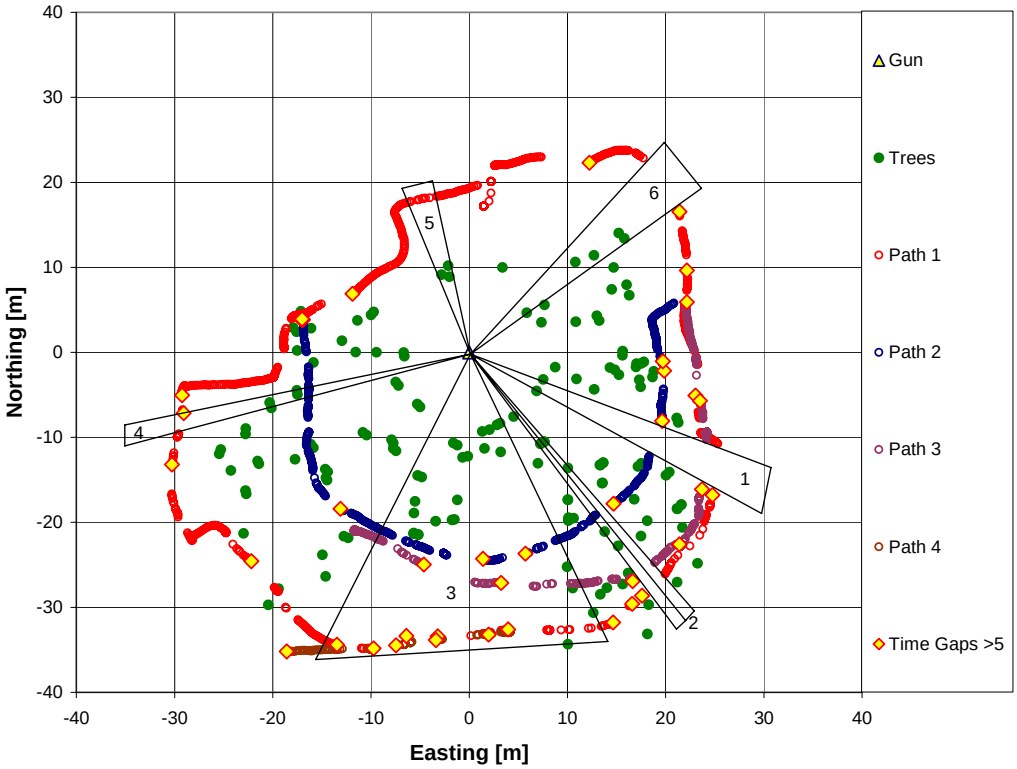

Figure 10. Line-of-sight test results following four paths in a forested environment with six areas indicating shadow zones of obstructed line-of-sight.

When surveying in wooded areas, the operator of the RTS adjusted the gun's search area and automatic prism search parameters to optimize performance. In an area with little topographic change and many line-of-sight obstructions, a vertical search range of ±2° was sufficient where the horizontal search range has a much larger angle defined, such as ±15°. After the gun lost prism lock, it predicted the location for a user-defined period of time ranging from 1 to 5 seconds. In wooded environments, we found that the 5 s setting allowed the surveyor enough time to clear the tree(s) before the gun entered the uninterruptible search algorithm. Figure 10 shows all the locations where the gun entered the search algorithm. As expected, the farther the prism was from the gun, the higher the chances that there was a tree between the prism and gun, which increased the likelihood that the gun would enter search mode. Area 3 shows the greatest number of search modes per unit length for path 1 because the number of trees in this area caused the most interruptions in line-of-sight.

2.2.5. Discussion

The Leica RTS performed well and within the instrument's specifications. These tests were designed to quantify the basic optical performance and the timing capabilities of the RTS. In hindsight, the instrument sampling rate and latency/dither, which are summarized in Section 2.4, are far more important issues than the optical performance. A positioning system can have great

optical performance but if the timing is off and variable, then the positions will have increased error relative to the prism's velocity.

Since gun placement is important, the surveyor can, with some success, select an optimal location in the survey area to place the gun. This is done by placing as many trees as possible in a line and minimizing shadow zones. This works well when setting up one gun position; however, the n-gun case, with n > 1, is extremely difficult to solve in the field. After performing the line-of-sight test it was clear that a potential survey site would require computer modeling to select the best location for the n-guns. Using different search parameters for the wooded survey as input into the model would aid surveyors in properly configuring the instrument prior to each instrument setup. This issue is explored in section 5.1.

2.3. ERDC Test Stand - 2006

After initial assessment, the laser positioning capabilities were tested in 2006 at the ERDC Test Stand (Figure 11) to compare the positioning accuracies of laser navigation versus RTK GPS technologies. These tests were executed to better define the capabilities of the laser technology and to evaluate the sources of positional errors that affect RTS technology. During winter of 2006, tests were conducted using an older model of the Leica system (TPS1100) and the dynamic test results were somewhat ambiguous; therefore, at the request of the SERDP Program Office, additional testing was conducted in Fall 2006 at the Test Stand.

Figure 11. ERDC Test Stand in Vicksburg, Mississippi.

2.3.1. Testing Method

The three types of tests conducted at the Test Stand were static, dynamic east-west (Figure 12) and dynamic north-south (Figure 13). To test data repeatability, each of the dynamic tests completed 10 movements. A test sequence consisted of a 5 minute static measurement, a north-south movement of 13 parallel north-south orientated lines, a 5 minute static measurement, an east-west movement of 16 parallel east-west orientated lines and a final 5 minute static measurement. The 5 minute interval for the static tests provided an adequate length of time to perform statistics because of the differences in the sampling interval between the GPS (1 Hz) and the laser-based systems (5 to 7 Hz). A smaller time window would favor the laser-based systems.

The dynamic north-south test moved the sensor platform along north-south azimuth lines spaced 0.25 m apart. The width of the survey area was 3 m, which equates to 13 survey lines. The dynamic east-west test moved the sensor platform along east-west azimuth lines spaced 0.20 m apart. The length of the survey area was 3 m which equates to 16 survey lines. The Test Stand moved the sensor to the same relative position for the static measurements. The position was not the same for all measurements but was within the tolerances of the Test Stand. These methods were used for both deployments.

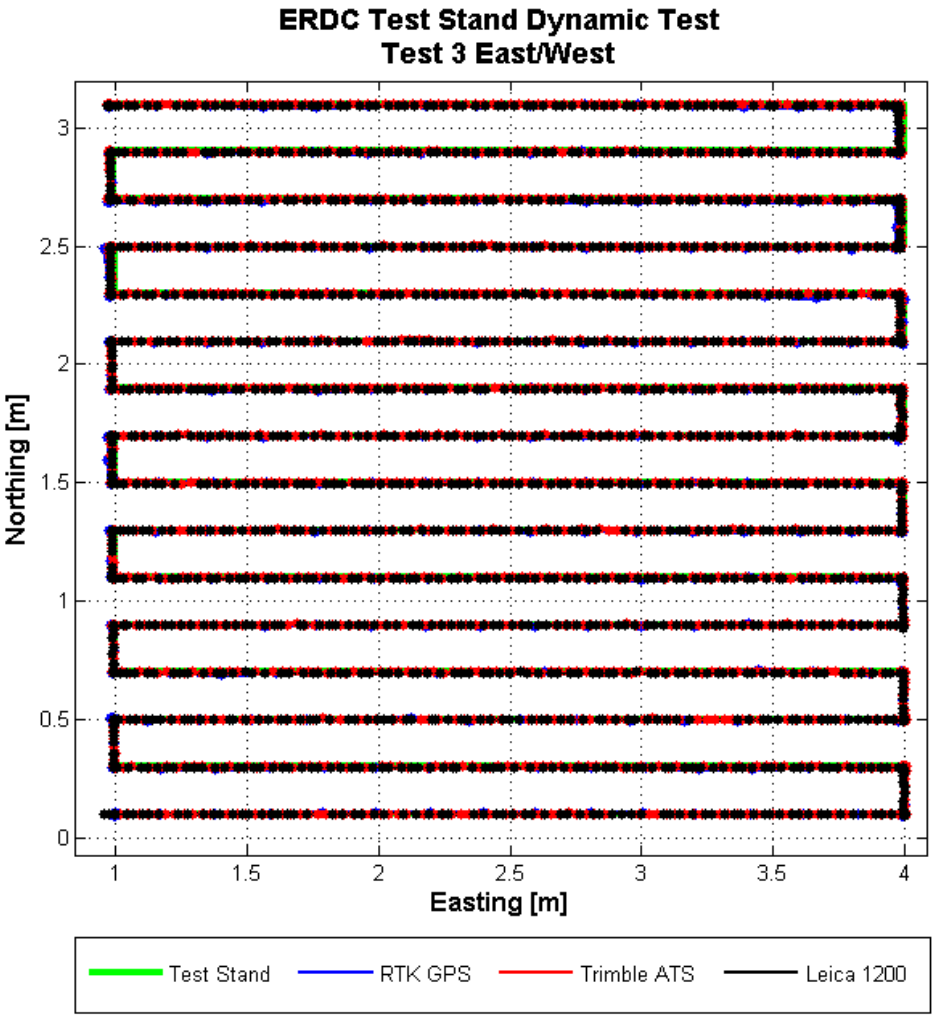

Figure 12. ERDC Test Stand East/West test positions.

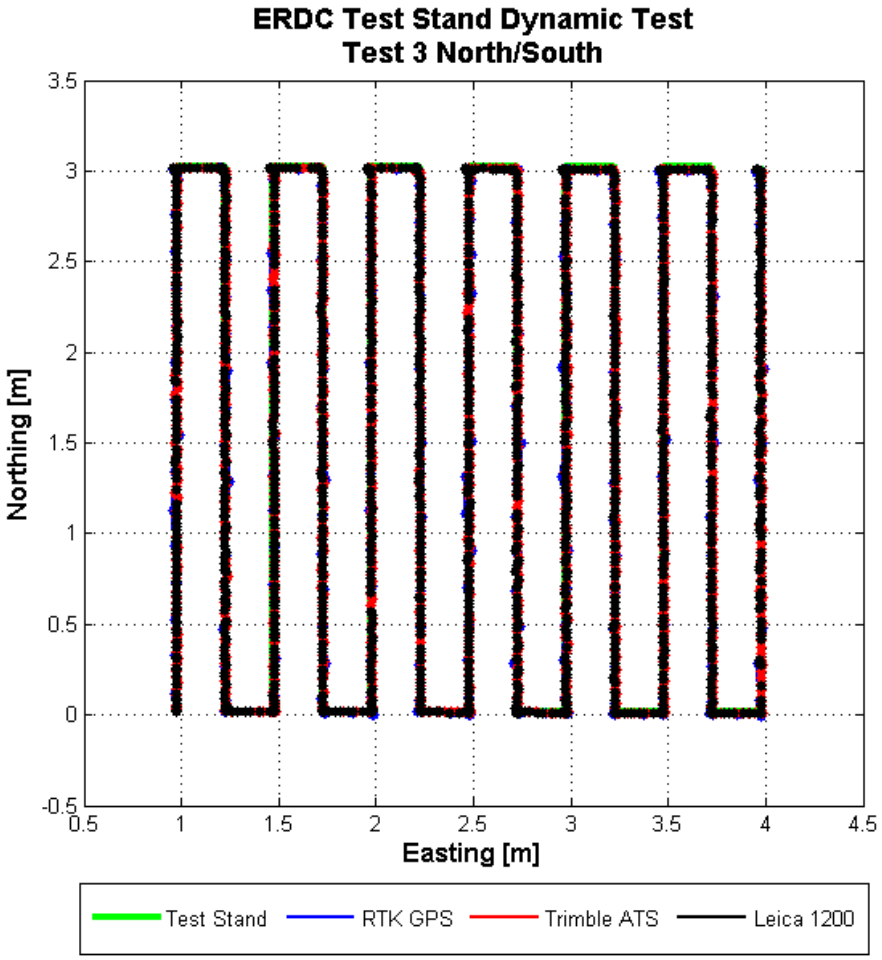

Figure 13. ERDC Test Stand North/South test positions.

2.3.2. Data Processing

The instruments were configured using an arbitrary local coordinate system for the laser-based systems and geodetic coordinates for the GPS. Datum translations and rotations applied to the data transformed them from their respective coordinate systems to the local Test Stand coordinate system, in which the southwest corner was (0, 0). The southwest and northeast values provided the necessary vector needed to properly position the data. Since the data sequence contained all five tests, the data was broken into individual tests. Individual instrument data for each run were broken into lines where a small rotation adjusted the azimuth of each line to orient them north-south. Microsoft Excel spreadsheets were used to format, analyze, and develop statistics from the data.

In viewing all the datasets overlaid atop each other, it became apparent that there was an additional rotation required to remove the systematic error of the Test Stand. Once all the translations and rotations were complete the data could be compared. All data from both deployments were processed using these same general procedures.

2.3.3. Winter 2006

In winter of 2006, tests were conducted at the ERDC Test Stand using three positioning technologies: Leica TPS1100, ArcSecond and a Trimble RTK GPS. The ArcSecond system setup was problematic and obtaining valid data from all of the tests proved difficult due to the unfamiliarity with the system. Even the person with the most experience with the system had difficulty configuring the system properly after several calls to experienced users. Due to the data problems with the ArcSecond system, the data are not presented here.

2.3.3.1. Instrument Setup

The RTK GPS base station was set up over the closest survey monument to the test stand which was less than 0.5 kilometer (km) away. The Leica RTS was set up approximately 20 m north of the test-stand This position gave the RTS a clear line-of-sight to the entire platform. The ArcSecond guns were set up around the test stand and far enough away to give the guns a clear line-of-sight to the light detectors. A 3-tiered mount constructed from clear Plexiglas secured the ArcSecond detectors, prism and GPS antenna to the sensor platform (see Figure 14).

2.3.3.2. Static Summary

The typical range of positions measured during the static tests using the RTS 1100 varied ±1 mm in X and Y and ±1 mm in Z. The greatest static deviations were -9 and 10 mm.

The Trimble RTK GPS system typically is accurate to ±1 cm in X and Y and ±2 cm in Z. The results from all the static tests conducted at the Test Stand confirm these accuracies. Thirty static tests were performed over the two days of testing at the Test Stand. Some tests had very good results while others had a larger spread of points from the mean. The variations in the spread are due to changes in satellite constellations and the interference of the nearby trees and other features. As noted, no useful data were collected from the ArcSecond system.

2.3.3.3. Dynamic Test Summary

The RTS1100 dynamic test accuracies were an order of magnitude higher than the static tests. The cause of this discrepancy was the timing error in measuring the horizontal angles. Because of this timing error the positional errors were on the same level if not greater than the RTK GPS errors which were in the 1 to 2 cm range.

2.3.3.4. Discussion

These tests yield useable static results but the dynamic results did not properly reflect the abilities of laser positioning systems to properly measure the prism's location in space. These tests were repeated in Fall 2006 with the updated equipment to properly quantify the performance of the laser systems.

Figure 14. The tiered mount held the ArcSecond detector (top), the GPS antenna (middle) and Leica prism (bottom) securely to the trolley of the test stand.

2.3.4. Fall 2006

In Fall 2006 at the ERDC Test Stand tests were conducted using three positioning technologies: the Leica TPS1203, the Trimble ATS600 and the Trimble RTK GPS (Figure 15). The results for the tests were computed using all of the information collected during the tests. Systematic errors were removed by documented data processing scripts and may not be reflected in the following summary tables.

Figure 15. Leica TPS1203 (left) and Trimble ATS (right) stationed to the northwest of the ERDC Test Stand for laser assessment tests.

2.3.4.1. Instrument Setup

The instruments were set up at the Test Stand, with the RTK GPS base station to the northwest of the Test Stand and both laser systems stationed north of the Test Stand. A jig held both the R8 antenna/GPS receiver and the active prism (Figure 16). Because the ATS system can only use the active prism, it was selected as the reflective surface for both of the laser-based systems. Although the active prism is not a standard prism to use with the Leica system, it was used for this test in order to place the laser systems in the optimal location. This prism substitution introduced approximately an additional 2.5 mm error in order to get the best line-of-sight. The exact error is unknown since the prism offset was not documented on the prism in use. Prism offset is a function of the index of refraction of the glass used and prism design. Typical prism offsets vary from 25 to 30 mm.

2.3.4.2. Static Measurements Test Results

The typical range of positions measured during the static tests using the Trimble ATS varied ±3 mm in X and Y and ±1 mm in Z. The greatest static deviations were -9 and 10 mm. Figure 17 summarizes the results of the static tests for the Trimble ATS.

The Leica TPS1203 measured positions during the static tests in varied ±2 mm in X, Y, and Z. The greatest static deviations were 8 and 9 mm. Some of the errors of the Leica system are systematic errors due to the use of a non-standard prism; these were left uncorrected because they are truly unknown and are on the millimeter scale. The standard Leica prism was substituted for the Trimble active prism so ATS measurements could be taken concurrently. The active prism has multiple reflective surfaces that could reflect the Leica laser at different times thus increasing the error. Figure 18 summarizes the results of the static tests for the Leica TPS1203.

Figure 16. 3-Tiered Plexiglas mounting platform (left) and up close photo of the active prism (right). Below the reflective glass prism is a ring of LEDs that pulsate making this an active prism.

The Trimble RTK GPS system typically is accurate to ±1 cm in X and Y and ±2 cm in Z. The results from all the static tests conducted at the Test Stand confirm these accuracies. Thirty static tests were performed over the two days of testing at the Test Stand. Some tests had very good results while others had a larger standard deviation. The variations are due to changes in satellite constellations and the interference of the nearby trees and other features. Figure 19 summarizes the results of the static test for the RTK GPS.

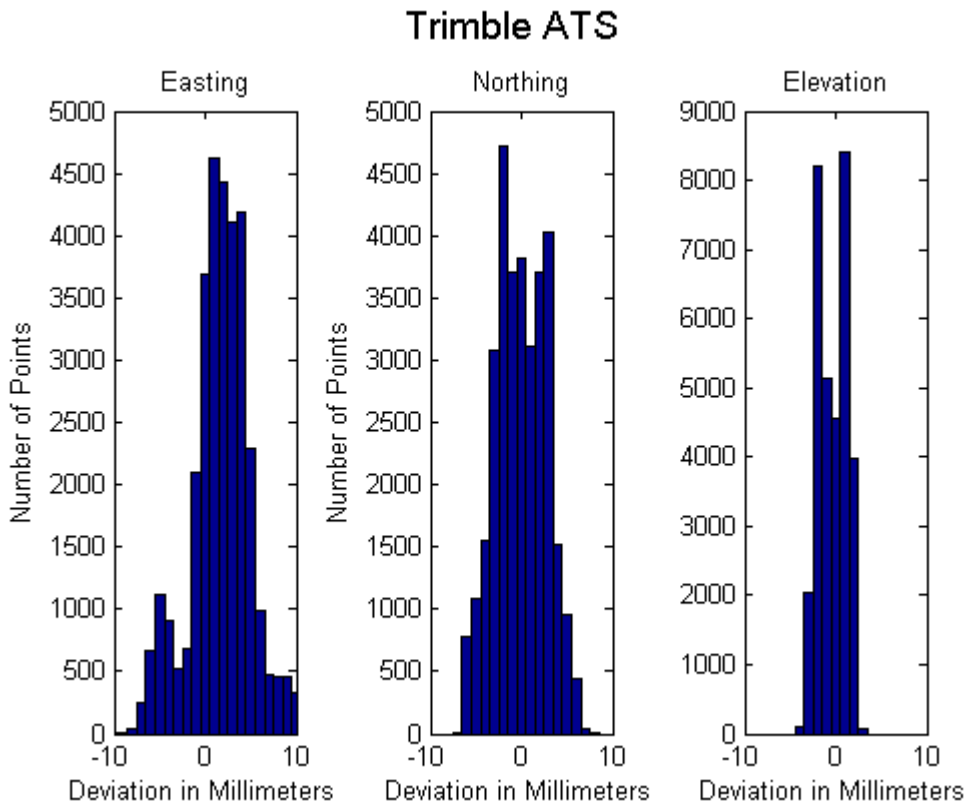

Figure 17. Summary statistics for the Fall 2006 Trimble ATS static measurements.

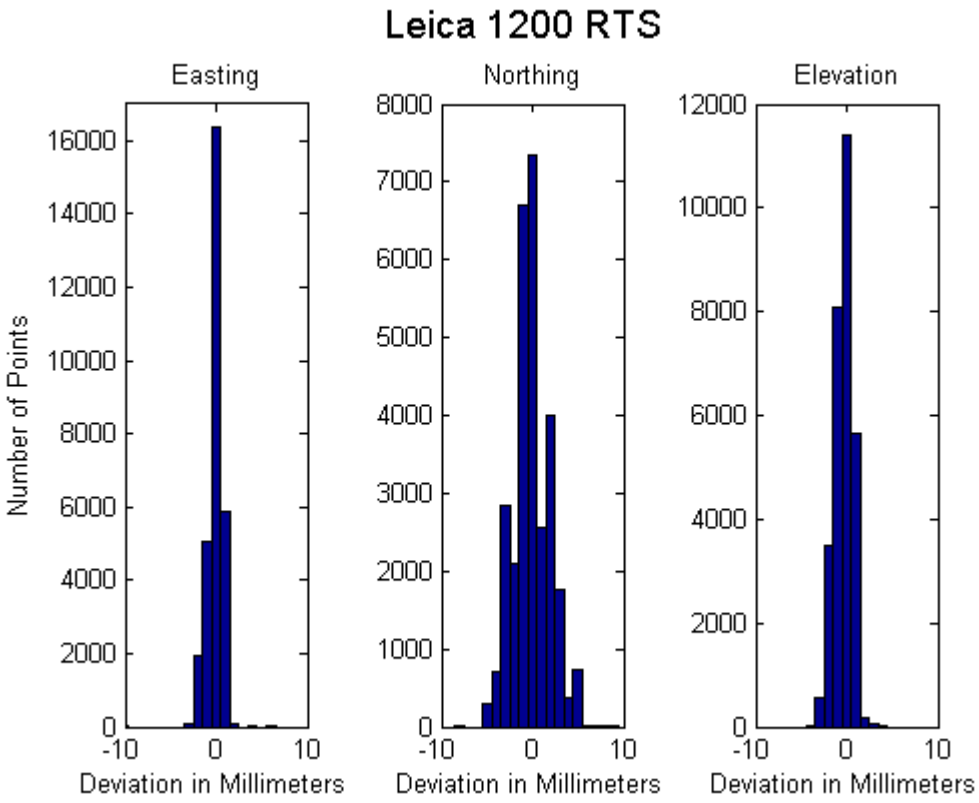

Figure 18. Summary statistics for the Fall 2006 Leica TPS1203 static measurements.

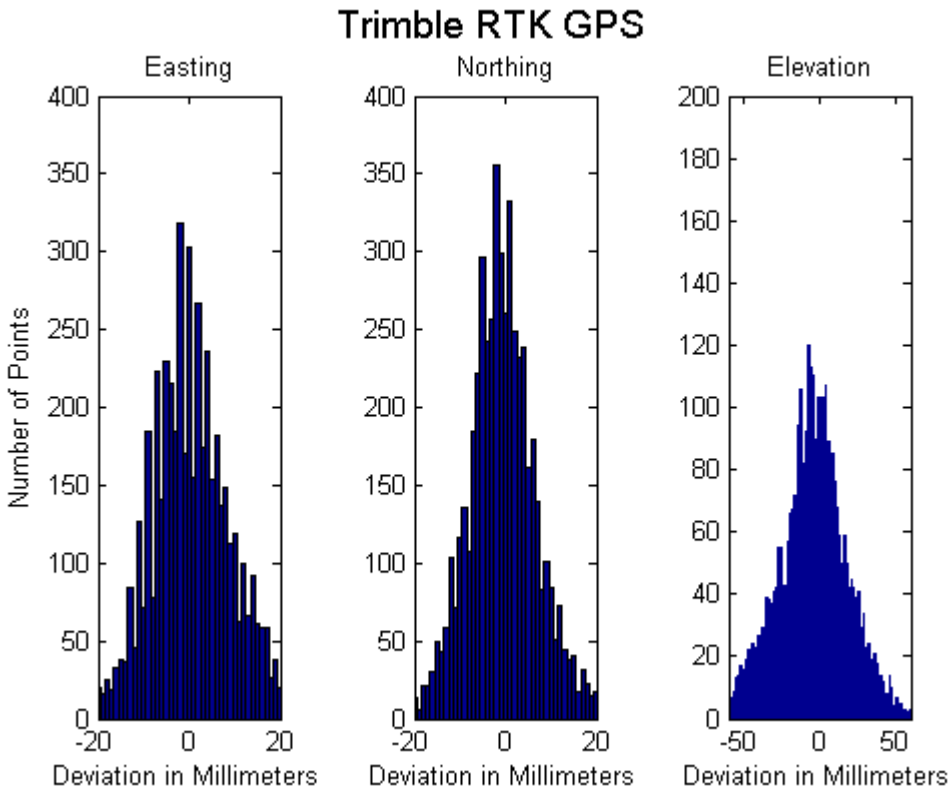

Figure 19. Summary statistics for the Fall 2006 RTK GPS static measurements.

2.3.4.3. Dynamic Measurements Test Results

It should be noted that during the motion of the trolley down the sensor arm in the north-south tests, the trolley wobbled. Upon closer inspection of the trolley, it was discovered that the wooden wheels that the trolley rolls on are not smooth. As the wooden wheels turn, the trolley wobbles and the lever arm amplifies the motion.

The Trimble ATS performed very well in the north-south motion tests. The standard deviation calculated for all the runs averaged to 1 mm (Figure 20). However, the averaged range of values for all the tests is a bit misleading. Sensor trolley wobble and the abnormal tracking contributed to the values in the range column. Another key observation is the difference in the Test Stand position relative to the ATS. The difference is sub-millimeter after the removal of systematic error. The Trimble ATS also performed very well in the east-west motion tests (Figure 21). The standard deviation calculated for all the runs averaged 2 mm. The averaged range of values for all the tests is less than in the north-south tests. The abnormal tracking of the ATS was primarily in the east/west direction so the error caused by the tracking affects the axis not used for this analysis. The absence of the sensor wobble makes these tests more accurate than the results from the north-south tests.

The Leica RTS performed similarly to the Trimble ATS system. In dynamic tests in the north-south direction, the average standard deviation for all the tests was 1 mm (Figure 20). The sensor trolley wobble is detectable in the range column of the table below. The differences in the Test Stand positions relative to the Leica were on the order of the standard deviation. For east-west dynamic testing, the average range in positioning has been cut in half compared to the north-south data due to the lack of trolley wobble (Figure 21). The differences in the Test Stand positions relative to the Leica were on order of the standard deviation.

The dynamic test results for the Trimble RTK GPS were within the expected range (Figures 20 and 21). Comparing the Test Stand against the GPS easting values, the average easting values measured ±2 mm of true. However, looking at the range of possible errors, the GPS recorded positions as far as 40 mm away with the average deviation of 24 mm. If taking into account the amplified wobble of the sensor trolley in the north-south direction, the average deviation would most likely decrease. No analysis was performed on the elevation errors, but using the results from the static tests one could assume the elevation error would be about twice that of the easting-northing errors. The most noticeable difference between the north-south and east-west test results is the lack of sensor trolley wobble. The lack of wobble is clearly seen in the average range during the east-west tests, 18 mm compared to 25 mm. The absence of the wobble shows up in the standard deviation as well. See Table 4 for the tabular standard deviations for the static and dynamic tests.

2.3.4.4. Discussion

The ERDC Test Stand in Vicksburg, Mississippi provided a platform for reproducing motion to quantify the accuracy of three positioning instruments. The static tests held the instruments still for 5 minutes while positions were recorded. The RTK GPS had the greatest variance followed by the ATS and then the Leica. The ATS positioning results were more variable because of the issues related to tracking of the active prism. However, overall the laser-based positioning systems performed better than the satellite-based system.

The motion tests moved the prism and antenna around the test platform in north-south and east-west directions. Again, the laser-based systems outperformed the GPS. The north-south tests had error associated with the wobble of the sensor trolley as it moved north and south down the sensor arm. The lever arm created by the sensor mount amplified the wobble. This error increased the spread of values for the laser-based and GPS systems by factors of 2 and 1.5, respectively. Lower sampling rates and lesser accuracy caused the GPS to be less affected by the wobble.

In conclusion, laser-based positioning systems can achieve millimeter-level positional accuracy in both static and dynamic positioning. The faster sampling of the laser-based technology provided better positional interpolations because there is less of a time gap between readings. Though the laser systems requires a clear line-of-sight between the gun and prism, the positions measured, in a wooded environment, are far better than the GPS positions in the open.

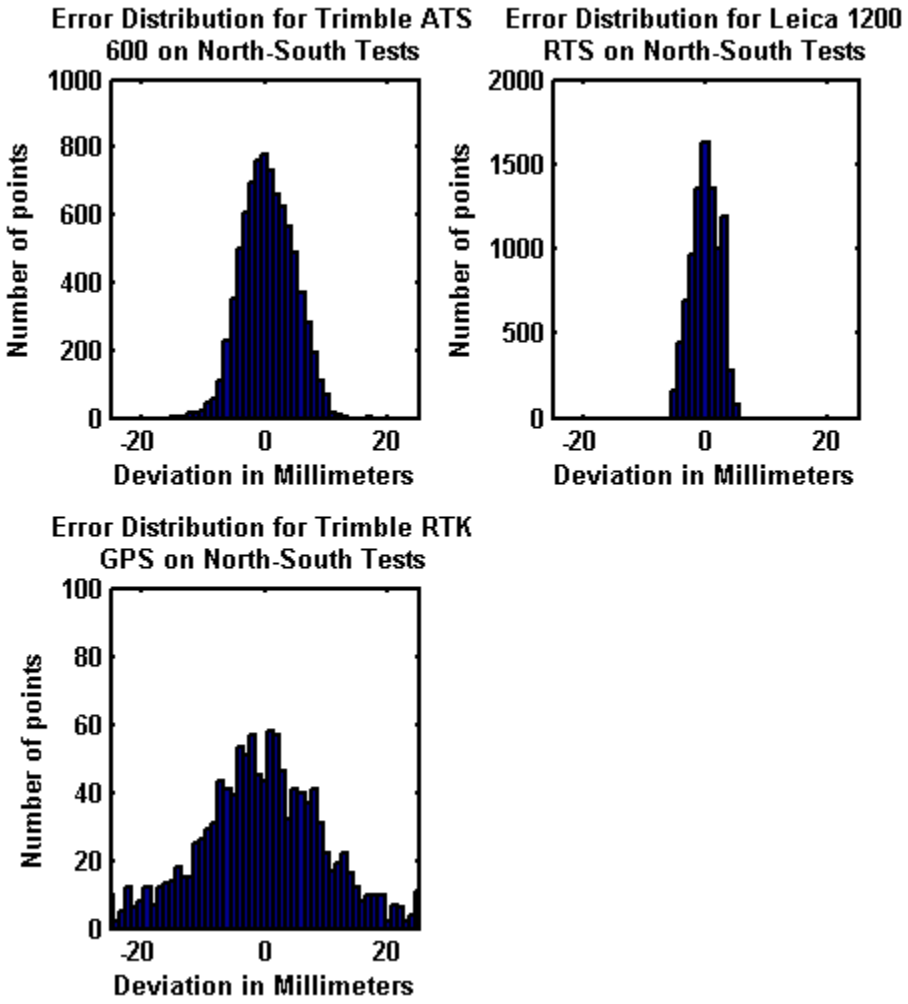

Figure 20. Error distribution for three positioning technologies in north-south tests of accuracy during testing at the ERDC Test Stand.

2.4. Latency and Dither Test

To precisely measure the latency and dither parameters, a linear test track (Figure 22) moved the prism back and forth. The track measures the location of a trolley as a function of the number of steps of the motor. Latency is calculated by comparing the test track trolley location and the measured prism location as a function of time and is an average of the timing offset between the trolley location and the laser measurement. Calculating the variance of the latency generates the dither. The track also measured the inter-sample variability by comparing the timestamps of the adjacent measurements.

The following is a description of the test methodology for each test performed using the platform test track.

1. Setup the gun five meters from the track.

2. Position the platform at one end of the track.
3. Send software commands to start platform motion and start data collection.
4. After reaching the end, send platform back to start position.
5. Repeat 5 times.

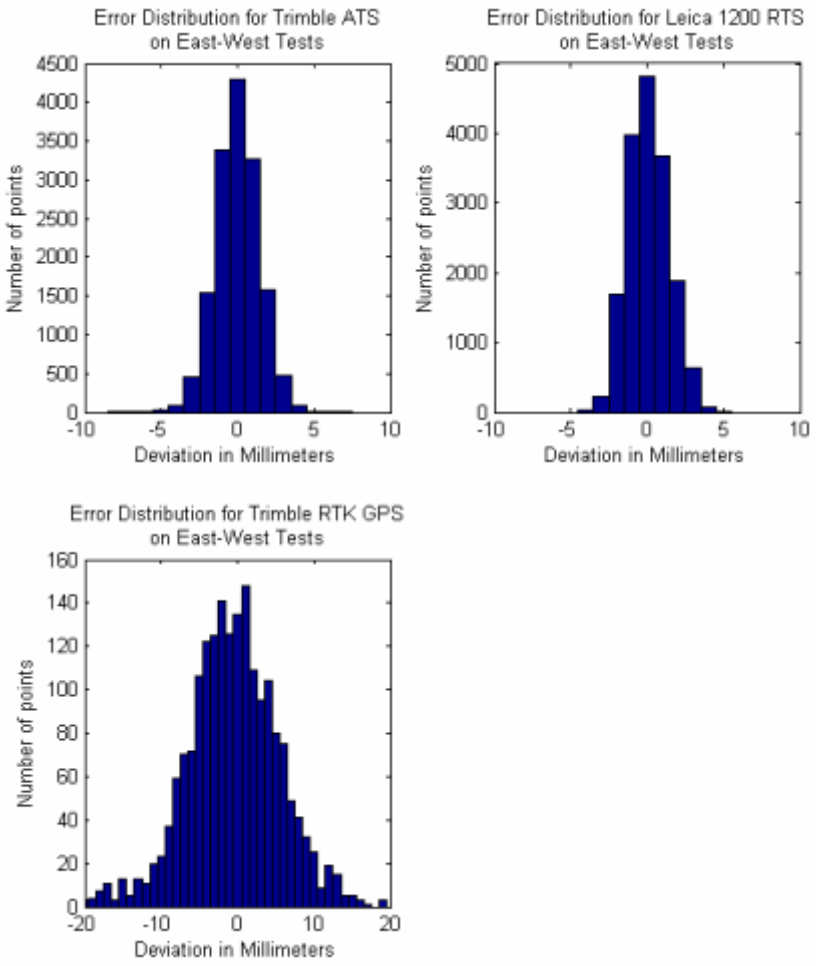

Figure 21. Error distribution for three positioning technologies in east-west tests of accuracy during testing at the ERDC Test Stand.

Table 4. Fall 2006 Static and dynamic results from the Test Stand.

	STD Easting (cm)	STD Northing (cm)	STD Vertical (cm)
Static – Leica RTS	0.1	0.1	0.1
Static – Trimble RTS	0.2	0.3	0.2
Static – Trimble GPS	0.6	0.7	2.0
Dynamic – Leica RTS	0.1	0.2	0.1
Dynamic – Trimble RTS	0.1	0.4	0.2
Dynamic – Trimble GPS	0.5	0.7	1.5

To carry out this test, the track was placed 5 m away and perpendicular to the direction of the gun. Given the speed of the platform and the distance from the gun to the prism, this simulated a moving prism at a distance of 30 m away traveling at about 1.2 meters per second (m/s). Prior to the start of the test, the prism was mounted on the moving platform and the platform was statically positioned at the starting location and then ending location, and the elevation, azimuth and distance relative to the gun was determined by polling the units for this information. Given these two measurements, and the knowledge that there were 780 equal steps between these two points, calculation each of the "step" positions can be derived (elevation, azimuth and distance, though only azimuth was used for the calculation in this test procedure) as the platform traversed the rail.

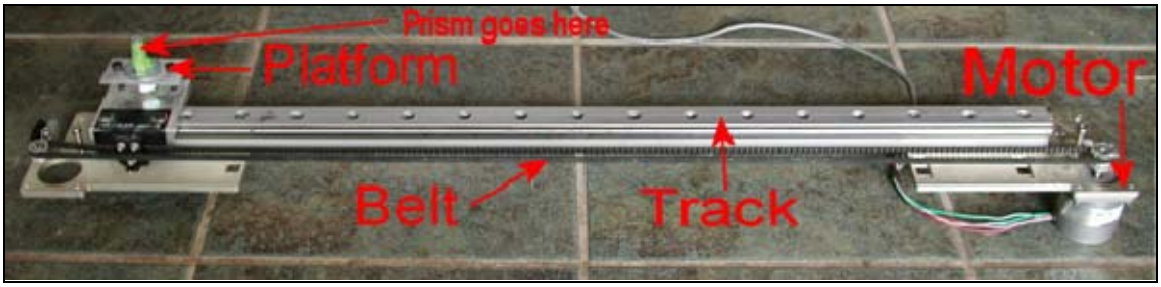

Figure 22. The stepper motor moves the test platform down the 0.83 m track in 11.8 seconds. The prism attaches to the platform while the DAS collects two platform position data streams from the microcontroller and the gun.

By controlling the travel speed of the trolley which was holding the prism, one could also calculate the travel time to each location following the start of trolley movement. To establish this "starting time," the microprocessor controlling the motor was further programmed to output a character just before beginning its left-right and right-left travel. The latency from the issuing of this character to when the trolley started moving averaged 1.74 milliseconds (ms).

The DAS was used to simultaneously capture two channels of serial data. The first channel was the single character output from the microprocessor. The second channel captured the reported azimuth, elevation and distance readings output by the laser system. The DAS system can accurately time the occurrences of these two events as its internal clocking system provides nearly 1 microsecond (μs) accuracy with regard to incoming serial data capture.

The actual testing was carried out by starting the microprocessor which repeatedly caused the trolley to traverse the track. During this time, the DAS continuously collected the resulting "start" character from the microprocessor and the coincident positional data reported by the laser unit. By measuring the "start" time of the platform movement (via the microprocessor "start" character) and knowing the true position of the prism at any given time (based on the repeatability of the motor driven platform and the knowledge of the starting and ending locations) it is a simple matter to determine the latency and jitter by comparing the "actual" position to the reported position.

Latency was measured as the average time interval between when the target was at a known azimuth position and when that position was subsequently reported. Note that because of our approach for time tagging the serial data, the time stamps applied to each of the two data streams

is measured from the receipt of the first character received for each measurement (rather than upon completion of receipt of a line of data). Jitter was measured as the variance from that average latency for individual time intervals.

Inter-sample reporting variability of the data returned from each of the laser units as part of these tests.

2.4.1. Leica Assessment 2007

2.4.1.1. Data Reporting Accuracy, Latency and Jitter

Figure 23 is a chart illustrating the latency and to a lesser extent the jitter of the Leica TPS 1200. The latency has a jitter of about 100 to 200 ms which makes it difficult to exactly determine the position of the prism when the prism is in motion as seen in Figure 24. This jitter along with a variability of 1 to 2 seconds in the sampling rate can add as much as a centimeter to the positions measured by the unit.

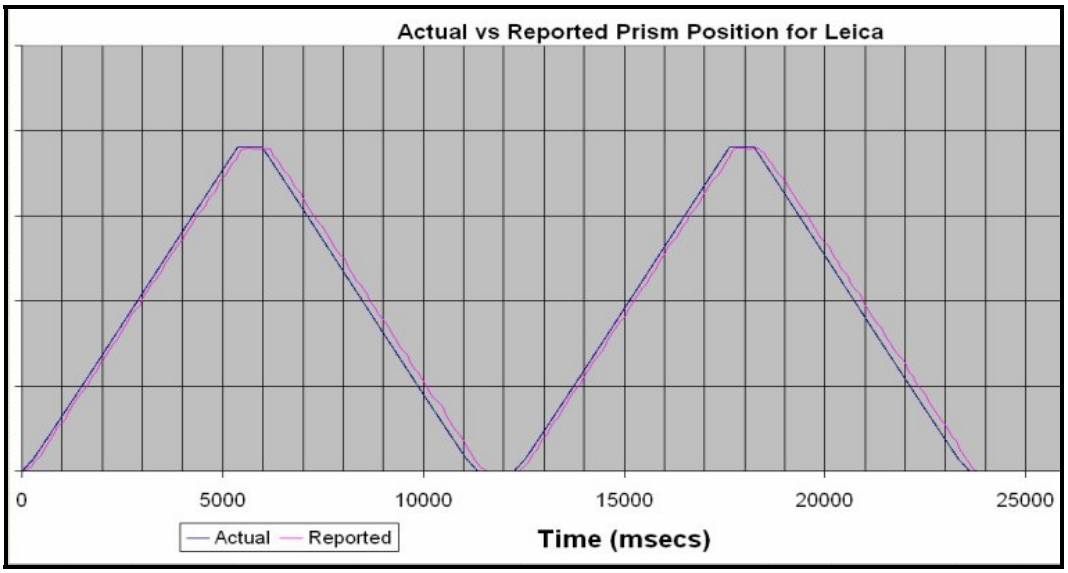

Figure 23. The actual (blue) and reported (red) positions of the prism for the Leica instrument. The difference of the position is the latency in the measurements.

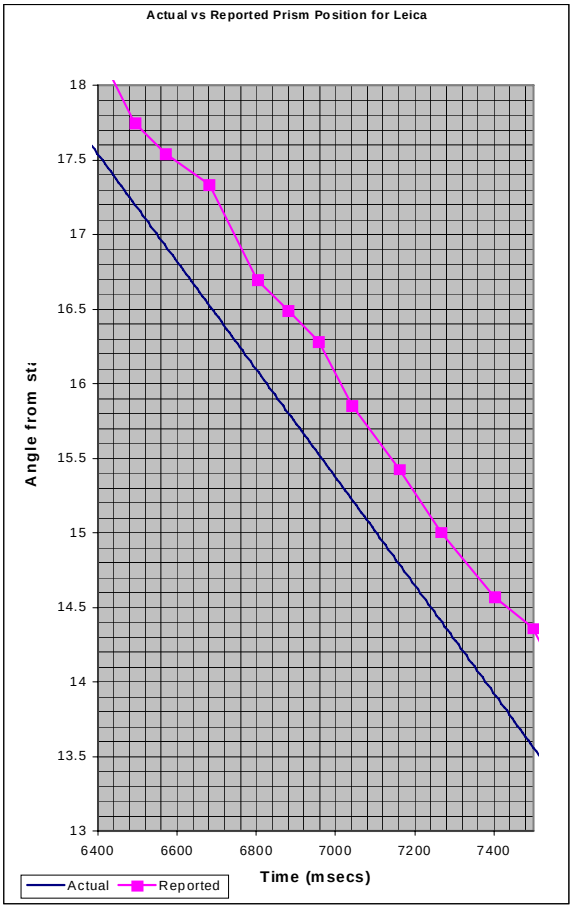

Figure 24. A zoomed-in view of the above figure that clearly shows the jitter in the Leica readings which is responsible for positional errors.

2.4.2. Trimble Assessment 2007

2.4.2.1. Lag and Lead Behavior of the Units

Figure 25 is a representative chart showing the relationship between the true target position and the reported position from the SPS930 tests. Similar results were obtained from the ATS600 unit. What this illustrates is the characteristic behavior of the gun as it follows a moving prism. The blue line represents the actual azimuth of the target relative to the gun, and the magenta line represents the eventual reporting of the prism's position. Note that near the start of movement (0, 7, and 14 seconds) the reporting of the position tends to lag more so than for the 5 or so seconds following these points. Also note that as the target reaches its final position on the track (around 12.5 seconds) that the reported position "overshoots" or leads the true position.

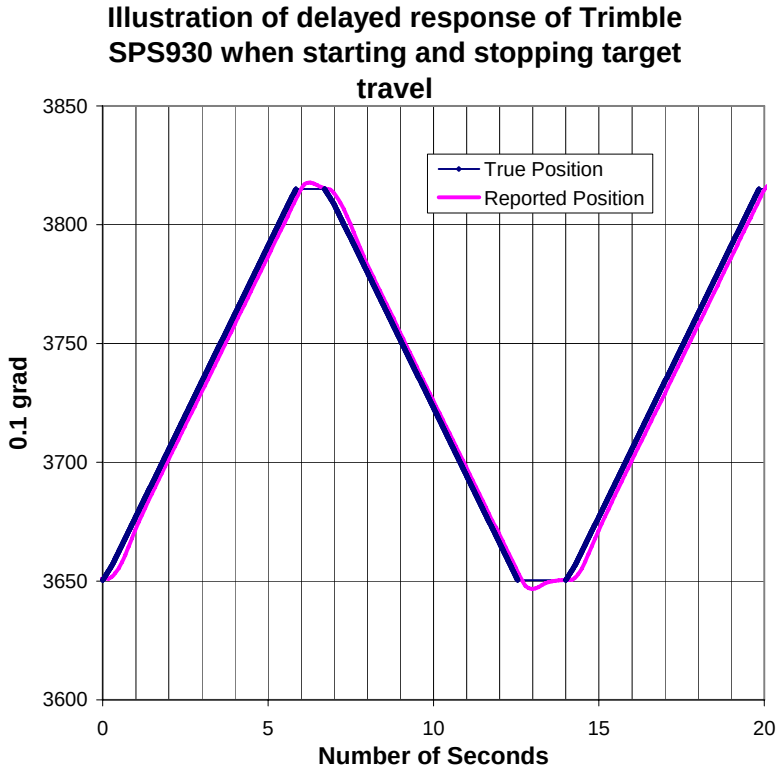

Figure 25. As the prism starts or stops to move, there is a lag in the response of the measured horizontal angle from the gun. This is simply the response time of the gun to responds to prism movements.

From these results, it is clear that the internal algorithm of the Trimble SPS930 (and similarly the ATS600) will lag in response at a sudden start, and will continue to presume continued movement when a sudden stop occurs. During steady movement, the tracking is more reliable. Consideration of this behavior is a must for future positional application involving the Trimble units.

2.4.2.2. Data Reporting Accuracy, Latency and Jitter

Figures 26 and 27 are two representative charts illustrating the latency and jitter of each of the two Trimble units. The samples are taken while the target is near the center of the track to avoid the Lag/Lead problems discussed above. The latency is the measure of the how long it takes the unit to report the target's position once a distance/angle measurement event occurs. The jitter is the variability in this latency.

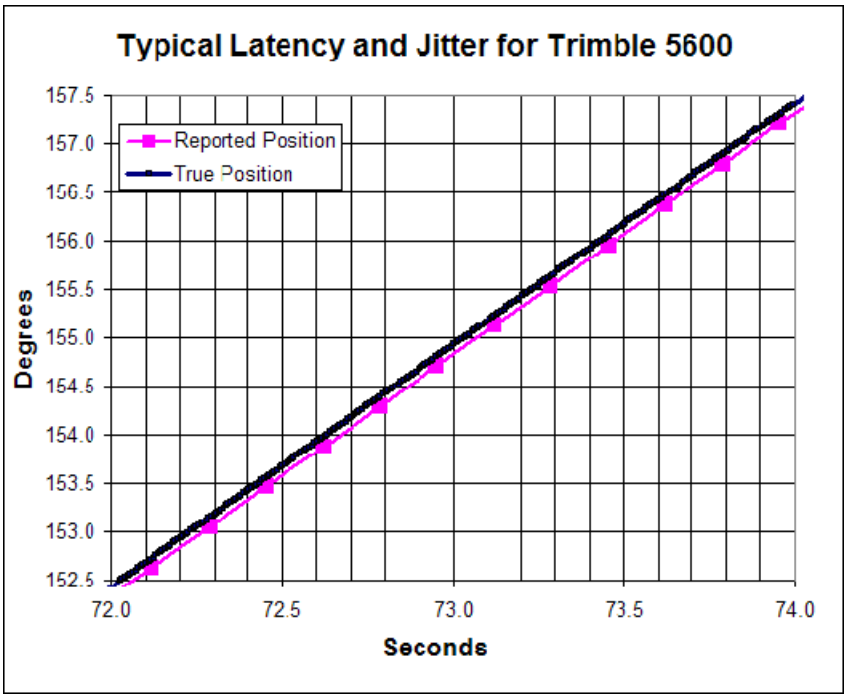

Figure 26. Lag and jitter of the angular measurement reported by the Trimble ATS600.

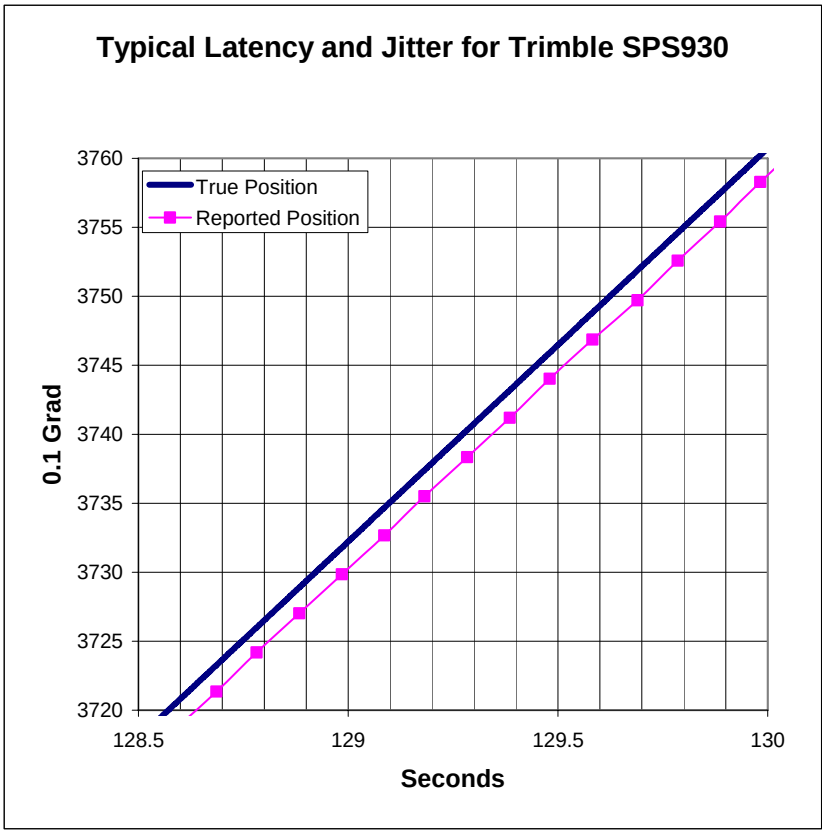

Figure 27. Lag and jitter of the angular measurement reported by the Trimble SPS930.

Figure 28 shows estimated (interpolated position between motor steps) target positions and times at angles identical to those reported by the SPS930 unit. In this way, the actual delay or latency of reporting the true position can be calculated for each of the reported points. These results are presented in Table 5 and indirectly represent the accuracy of the positional reporting.

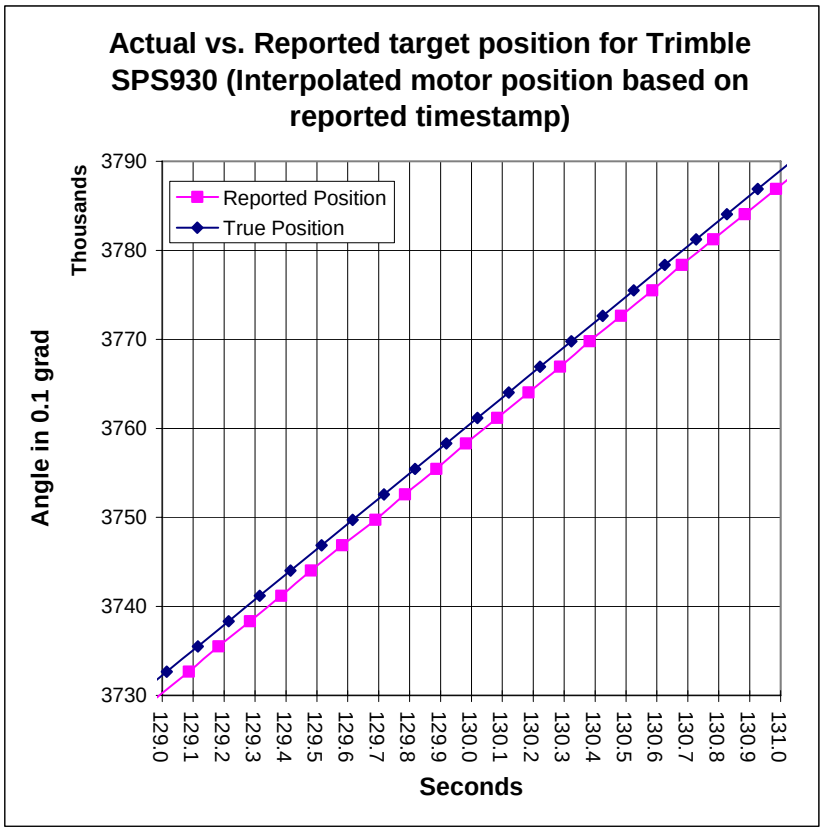

Figure 28. Interpolating the Trimble SPS930 measurement events onto the true positions simplifies the latency calculation.

The latency is not very significant because this can be removed when calculating positions. However, jitter is critical in the calculation of the target's position and cannot be easily removed like the systematic latency.

2.4.2.3. Inter-Sample Reporting Accuracy

The ATS600 and SPS930 can operator in a continuous mode where readings are returned automatically. The ATS600 and SPS930 returned 6 and 10 samples per second, respectively. These measurements gauge the variability in the time between consecutive samples and the table below reports the test results.

Table 5. Latency and Jitter values for the Trimble ATS600 and SPS930

Parameter	Leica TPS1200		Trimble ATS600		Trimble SPS930	
	Mean	St. Dev.	Mean	St. Dev.	Mean	St. Dev.
Latency (ms)	133	39	39	5	68	7
Inter-Sample Timing (ms)	88	19	166	3	99	4

2.5. Discussion

In general, the two Trimble units have the same measured accuracy in regards to this test whereas the Leica failed to provide positions in a timely manner. Certainly, the increase in the sampling rate for the SPS930 unit is an advantage for future applications. We believe it was the intention of Leica engineers to develop a system for static measurements only, where Trimble designed a system with dynamic measurement in mind since their hardware is meant to work on construction machinery.

The latency of the SPS930 unit is expectedly more than that of the ATS600 unit due to the use of data communication radios with the SPS930 device. These radios are a requirement of the SPS930 for receiving the data and transmitting commands. However, as mentioned, the latency of the data reporting can be accounted for during data processing. The radios may also contribute to the slightly higher jitter measurement in the SPS930 over that of the ATS600, though the difference may be negligible considering the sample size.

It should be noted that the SPS930 unit tested had just been released and had some initial problems that need to be addressed. These included 1) radio units needed adjustment by the manufacturer to be more consistent in performance, and 2) prism matching to the SPS930 gun. During SPS930 testing, a non-standard active prism was used for this test. Its performance was good, but not necessarily approved for use by the manufacturer. For future testing, the manufacturer will either supply an alternate and approved prism, or will validate the prism used during these test for use with the SPS930 unit.

Timing jitter is really an important issue and the Leica has a jitter five times larger than either of the Trimble units. A 1 ms jitter for a target traveling at 1 m/s translates into 1 mm of positional error. Timing jitters less than 10 ms is necessary to collect discrimination quality data. The Leica unit is too unstable to routinely use for interrogation data collection.

3. LASER POSITIONING INTEGRATION WITH HAND-HELD SENSOR

Global Positioning Systems are the industry standard positioning instrumentation, but they do not provide the required 1 cm of positional accuracy nor a high enough sampling rate needed by inversion algorithms to correctly recover target parameters. In the past, high quality data required by the algorithms were collected using static data collection methods. Static data collection is extremely time consuming and costly to clients. Finding a method of collecting interrogation quality data in a single pass is of the utmost importance. Laser positioning instruments measure 3D positions to within 5 mm and with increasing sampling rates. This section describes the equipment, methods and results from integrating two different laser-based positioning systems with a Geonics EM61HH-MK2 (HH) metal detector.

In 2006, the EM61HH-MK2 was integrated with the Leica RTS and a Crossbow AHRS 400 IMU to demonstrate the integration. Data collected over an anomaly showed that the RTS and IMU could provide positional data for the hand-held detector when moving in a moderately slow sweeping motion. These data were adequate for detection, however careful and control testing in 2007 showed these data were not adequate for discrimination.

3.1. Materials

3.1.1. Leica TPS 1203

As described in previous section

3.1.2. Trimble SPS930

As described in previous section.

3.1.3. EM61HH-MK2

The Geonics Limited HH is a smaller version of the popular EM61-MK2 time domain metal detector. Like the larger EM61-MK2, the HH has a transmit and receive coil and measures the secondary magnetic field over 4 geometrically spaced time gates. The instruments are unalike in that the HH has smaller (0.17 m in diameter) and offset coils with the receiver coil leading the transmit coil by 0.13 m (Geonics 2005). The smaller and offset coils improve the detection of smaller targets but are highly susceptible to changes in sensor orientation (roll, pitch and yaw).

3.1.4. Zigzag Board

The zigzag board was a 1.3 m × 1.3 m wood platform with a zigzag shaped track carved out of the surface. The platform was constructed using wood and contained no metal fasteners.

3.1.5. Crossbow IMU

The Crossbow AHRS400 IMU is an inertial measurement unit capable of measuring 3-axis acceleration and 3-axis rate information at 50 Hz. This instrument was used to augment the positioning information for the Leica unit.

3.2. Methods

The method used to test the hand-held sensor with the laser system was to follow a predetermined path over individual targets, a 2.125-inch steel sphere and a 37-mm projectile. The predetermined path was a zigzag pattern designed to mimic the waving of a sensor as performed by explosive ordnance disposal (EOD) technicians. The EM61 coil, IMU and prism were mounted to a jig which kept the instruments a fixed distance relative to each other. All of the instruments contained some metal so it was imperative to keep their relative locations constant. The bottom of the jig had a hole for a guide pin which kept the jig on track. Data collection started at the south-west corner and followed the zigzag to the end. Data collection occurred in March and September 2007. The RTS and SPS930 were tested in March and September, respectively.

The survey speed and zigzag pattern changed between Spring and Fall tests. The speed of the survey varied in the spring tests with the Leica but not in the Fall tests performed with the SPS930. Another reason for the change was the faster speed did not provide high enough data density to support inversion. For the Fall testing, the IMU was not used because it did not provide any useful information during the Spring tests. The zigzag pattern became tighter for the Fall tests. In the Spring, the data density of the slow tests marginally supported inversions, so the spacing was cut in half from 20 cm to 10 cm.

The targets depths varied between 12 and 42 cm with the 37-mm projectile positioned in vertical and horizontal orientations.

3.3. Analysis of Positional Accuracy of Leica RTS

The quality of positioning depends both on the accuracy of the positional measurement and the timing between the measurement and its recorded time-stamp. Here we assess the accuracy of positioning on a platform in which a zigzag has been drawn to set a fixed and repeatable path for the integrated sensor.

3.3.1. Accuracy of Positional Measurements

For a mobile survey, the positional error can be assessed by following a fixed path and measuring the deviation of the Leica-predicted positions from their nearest position on the fixed path. In that manner the effect of position and time can be separated. Our test was performed by having the prism mounted on a system that strictly followed a trajectory along a zigzag-shaped (Figure 29).

The standard deviation for the positions were 2.0 and 3.5 mm, for the “slow” survey (0.2 m/s) and “fast” survey (0.5 m/s), respectively (Figure 30).

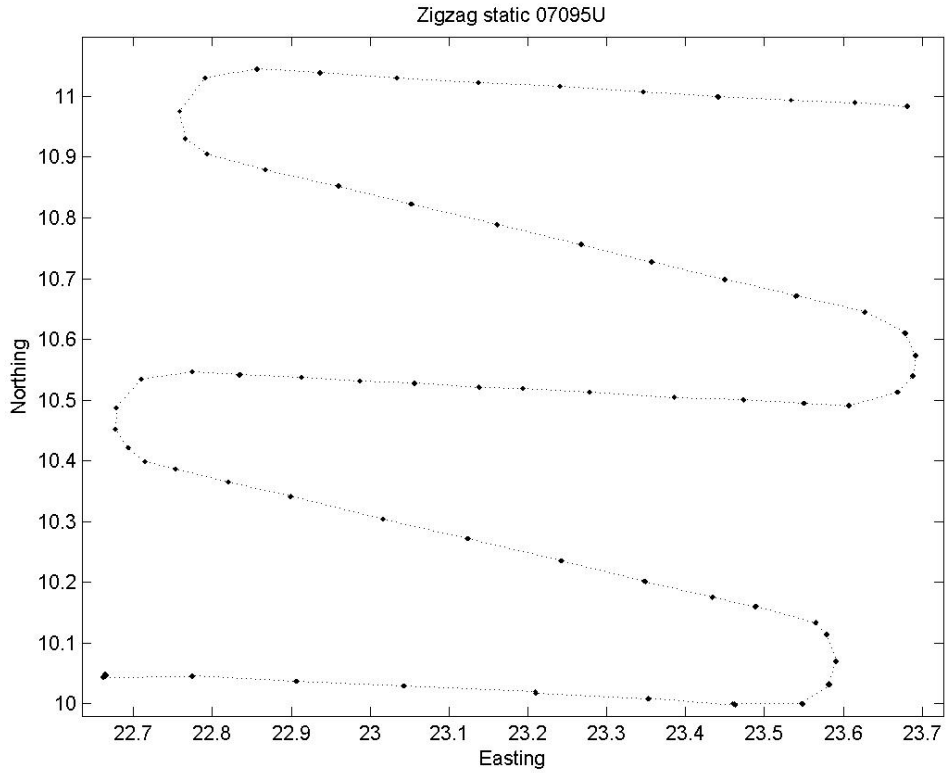

Figure 29. True path on fixed-zigzag survey platform. Reference trajectory based on static measurements.

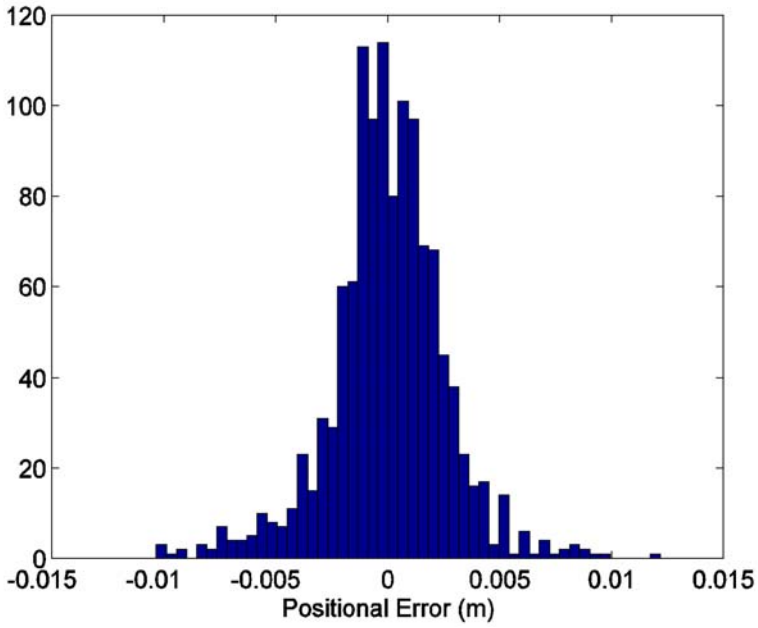

Figure 30. Positional error for the Leica RTS derived from measurements on the fixed zigzag survey taken for all speeds.

3.3.1.1. Time Latency

One key condition for an accurate positioning system is its ability to identify the time when a positional measurement is taken. Detailed scrutiny of the time-position relationship obtained from the Leica RTS revealed a time-stamping issue. These are detectable in the surveys over the fixed zigzag pattern at a semi-constant velocity because of the survey points stand out of the time-space trajectory (Figure 31). The time step also appears to be longer for those particular measurements.

These discrepancies arise when the RTS fails to measure and record a new position quickly enough, which causes a stutter. The cause of the problem is unknown to us but is suspected to be a firmware error. We refer to this issue as a delayed latency; the position provided by the RTS corresponds to an earlier time than the time recorded.

This problem was detected when inverting EM61 data, causing significant modeling problems. The issue is critical because position, orientation and sensor data are merged through their respective time stamps, thus the EM61 data is misallocated if the position-time relationship is erroneous. Figures 31-33 illustrate the issue.

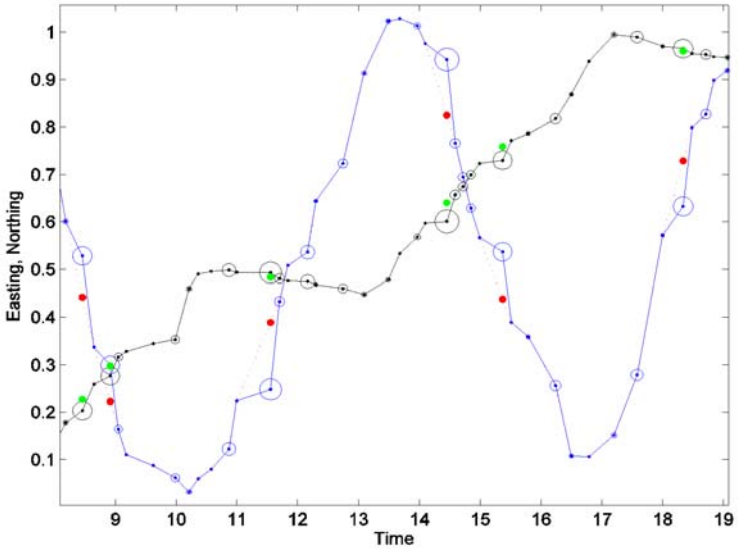

Figure 31. Predicted Easting and Northing as a function of time for a medium-speed survey over the zigzag path of Figure 29. Easting is in blue, Northing in black. Circles are proportional to the instantaneous speed: points with large speed are anomalous and correspond to problematic RTS updates. The position of these critical points for the RTS time can be interpolated by assuming constant velocity: the corrected position is indicated by red dots (Easting) and green dots (Northing).

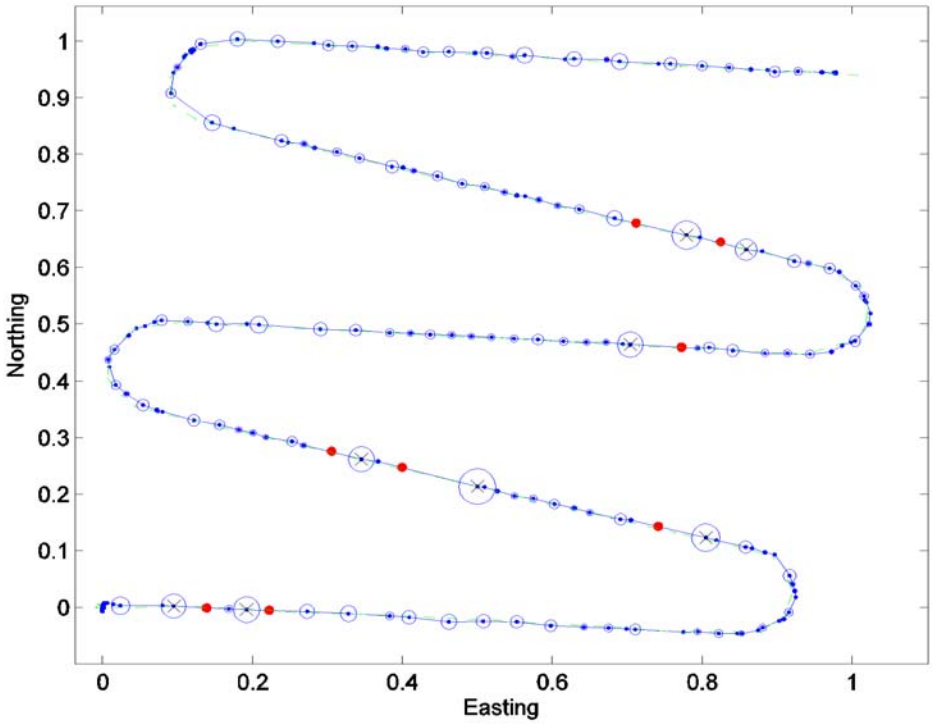

Figure 32. Same survey and symbols as previous figure (medium speed). Green dashed line indicates reference path. Measurements with erroneous time-position relationship (large circles) do not stand out of easting-northing trajectory, which suggests that positions are legitimate whereas recorded times are inadequate.

The positional error due to latency increases with the velocity of survey. For a fast survey the equivalent positional error can be as large as 0.30 m or 0.4 s in timing, as illustrated in the following figure by the measurement on the blue curve at 9 s.

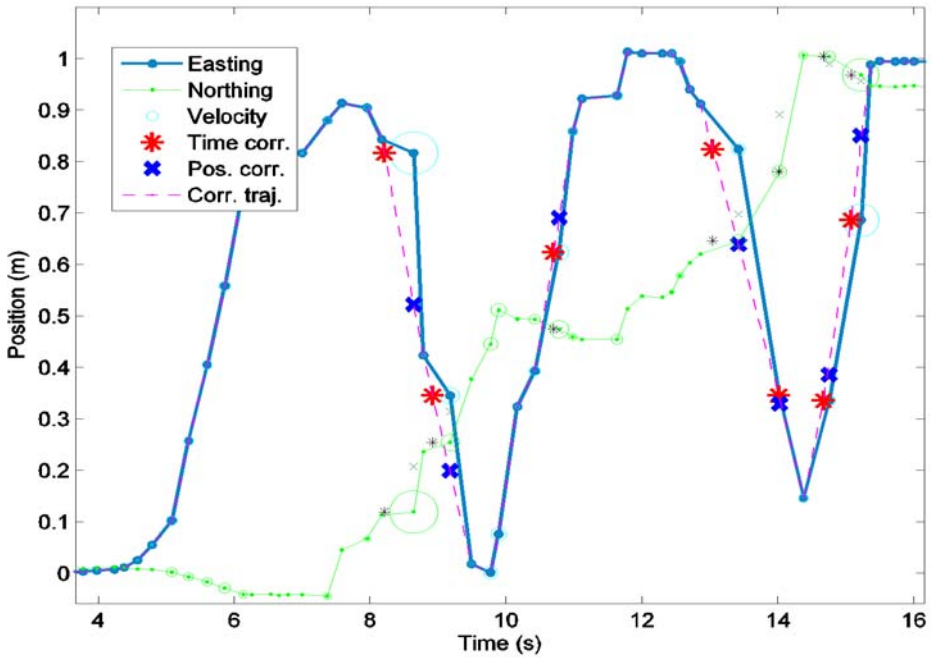

Figure 33. Easting and Northing as a function of time for a "fast" survey over a fixed zigzag.

Positional or timing error can be inferred on blue curve from distance between points associated with large circles and their correction: positional correction (blue x), time correction (red star).

Latency errors do not appear at predictable times or positions; they appear at random times and are usually associated with a variable time update. Figure 34 illustrates the large variability of the RTS update rate.

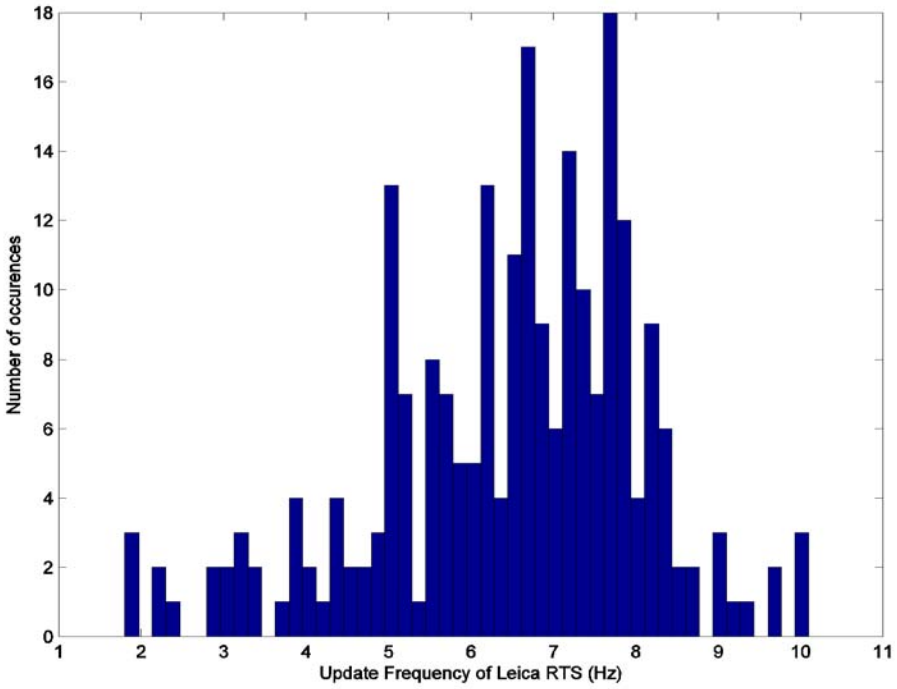

Figure 34. Typical example of update rate for Leica TPS1200.

3.3.1.2. Frequency of Positional Errors in RTS Data

Latency causes errors that can be interpreted as time or position errors.

- Viewed as positional error, we find that 3-6 % of RTS data have position off by more than 5 mm, depending on the velocity of survey. This result is illustrated by Figure 35.
- Viewed as a timing error, 5 % of RTS data have time off by more than 50 ms, as shown in Figure 36.

As seen in Figure 32, the RTS predicts positions that belong to the physical trajectory of the sensor in the survey (there are no points out of the fixed zigzag path). Therefore we believe that the error is due to latency and that RTS times require corrections. The converse point of view remains significant because the RTS positional data is merged with EM61 sensor data and IMU orientation data through their time channel. Therefore uncorrected timing errors effectively place the EM61 sensor at the wrong place for a given time and that error can be as large as 0.30 m (or 100 standard deviations) for a fast survey (Figures 35 and 36).

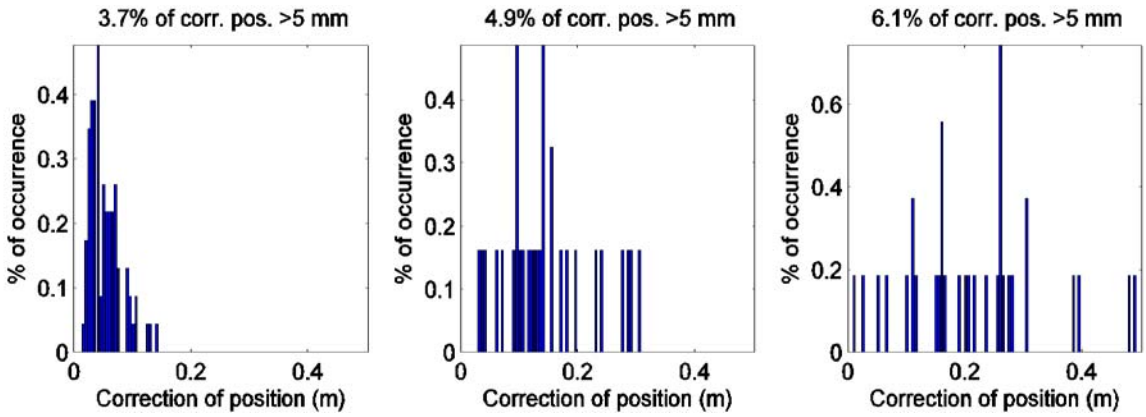

Figure 35. Frequency of errors larger than 5 mm for slow survey (left), medium-speed survey (center) and fast survey (right).

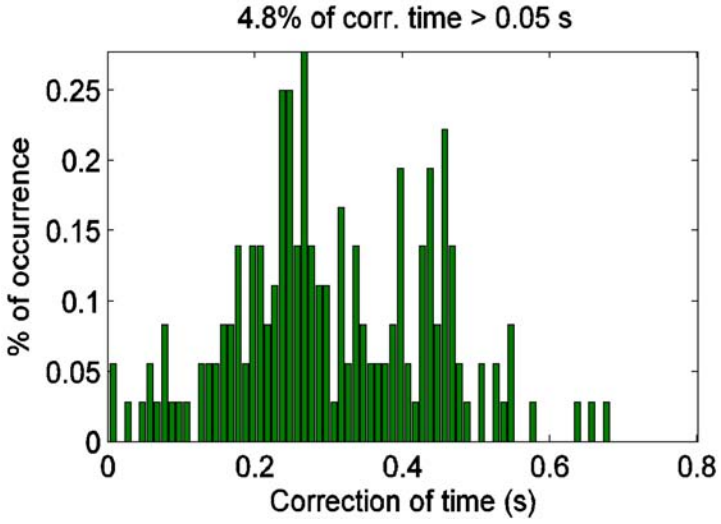

Figure 36. Frequency of timing errors larger than 0.05 s for all surveys.

3.3.1.3. Correction of Latency-Induced Positional Error

Time was corrected for any critical time-position pair by a linear interpolation method according to the distance traveled between the points before and after the erroneous point. We assume that the velocity is quasi-constant during a survey and therefore problematic points can be detected where both the velocity is more than three times as large as the average velocity and the time-step is more than 50 % of the average.

One additional advantage of this approach is that it does not introduce new positions that would not necessarily be located on the actual trajectory, had we chosen to correct position instead of time.

3.3.1.4. Discussion

Positioning with the Leica RTS has variable latency in its time-position update. Latency can introduce large errors for a hand-held sensor, which, by design, operates at a comparatively large speed. Errors are detectable because one can assume that a field operator surveys at a pseudo-constant pace without any erratic movements. Following that assumption and noting that latency issues are associated with irregular time stepping, timing errors can be corrected at first order by interpolation between other measurements. Higher order corrections would require information about the velocity between RTS updates. Such information could be derived from an IMU operating at a much higher frequency than that of the RTS. The following section details the potential of IMU systems.

3.4. Integration of Inertial Measurement Unit

Inertial measurement units measure the gyro rate and acceleration of a body upon which they are mounted. Some IMU systems also incorporate attitude information (roll, pitch and yaw); this is the case for the Crossbow AHRS400CD used in this study.

IMU data can be merged with positional systems (GPS, RTS) to improve accuracy of a positioning system and predict position between position updates if the IMU is used at a higher sampling rate. Merging methods are usually based on the integration of navigational equations and Kalman filtering.

IMU data are also essential for the discrimination of UXO because the attitude of the EM sensor can deviate from the horizontal when used over an uneven surface. Changes in orientation modify the intensity of the transmitted and received EM signals and must therefore be accounted in the modeling to maximize the chance of a successful inversion.

3.4.1. Presentation of IMU Data

The Crossbow AHRS400CD provides attitude (roll, pitch and yaw), angular rate (3-axis gyro), XYZ acceleration and magnetic field (3-axis magnetometer) measurements at a rate of up to 50 Hz. In “angle mode”, an internal Kalman filter implementation provides a continuous on-line gyro bias calibration, and an adaptive attitude and heading measurement that is stabilized by the long-term gravity and magnetic north (Rios and White 2001).

The IMU was strapped down onto the same structure as the EM61 sensor and placed right above it, as shown in Figure 37. The Sky DAS was used to log and time-stamp the RTS, IMU and EM sensor data.

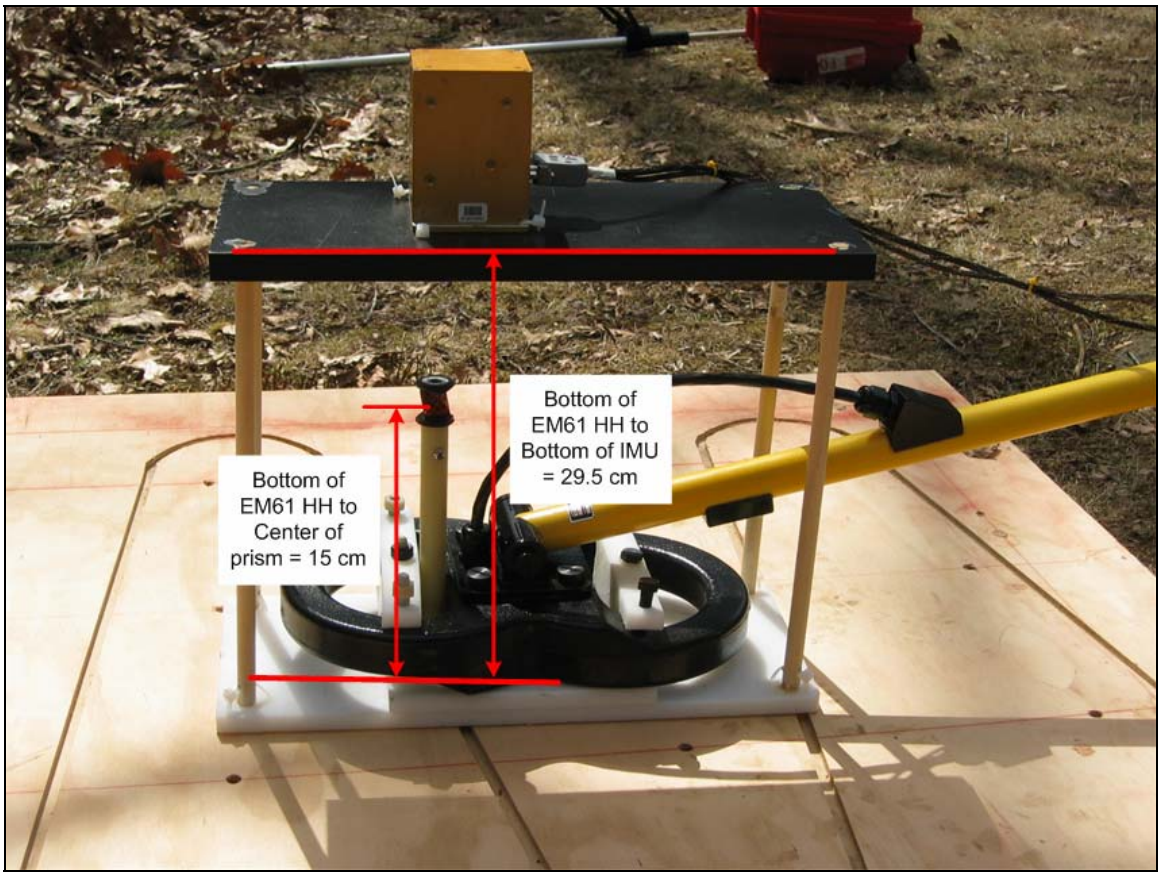

Figure 37. Hand-held sensor design: Geonics EM61HH-MK2 mounted with prism and Crossbow IMU. The sensor is here shown on the fixed zigzag survey.

Technical specifications include:

- Attitude, heading: dynamic accuracy < 3°, resolution < 0.1°
- Angular rate: bias < 0.05°/s, resolution < 0.025°/s
- Acceleration: bias < 12 milligravity (mg), resolution < 0.6 mg
- Data were collected at 10 Hz, which is a similar frequency to that of the RTS. Unfortunately the DAS was not reconfigured to accept data at the maximum update rate of 50 Hz for this Crossbow IMU.
- Data were noisy, especially gyro and acceleration data, as illustrated in Figure 38. This can be an artifact of the IMU, its operating mode, or its position relative to the EM sensor: if the IMU is exposed to the field of the EM sensor, interpretation of IMU data may be affected because the measurement of attitude relies on accurate determination of the magnetic North.

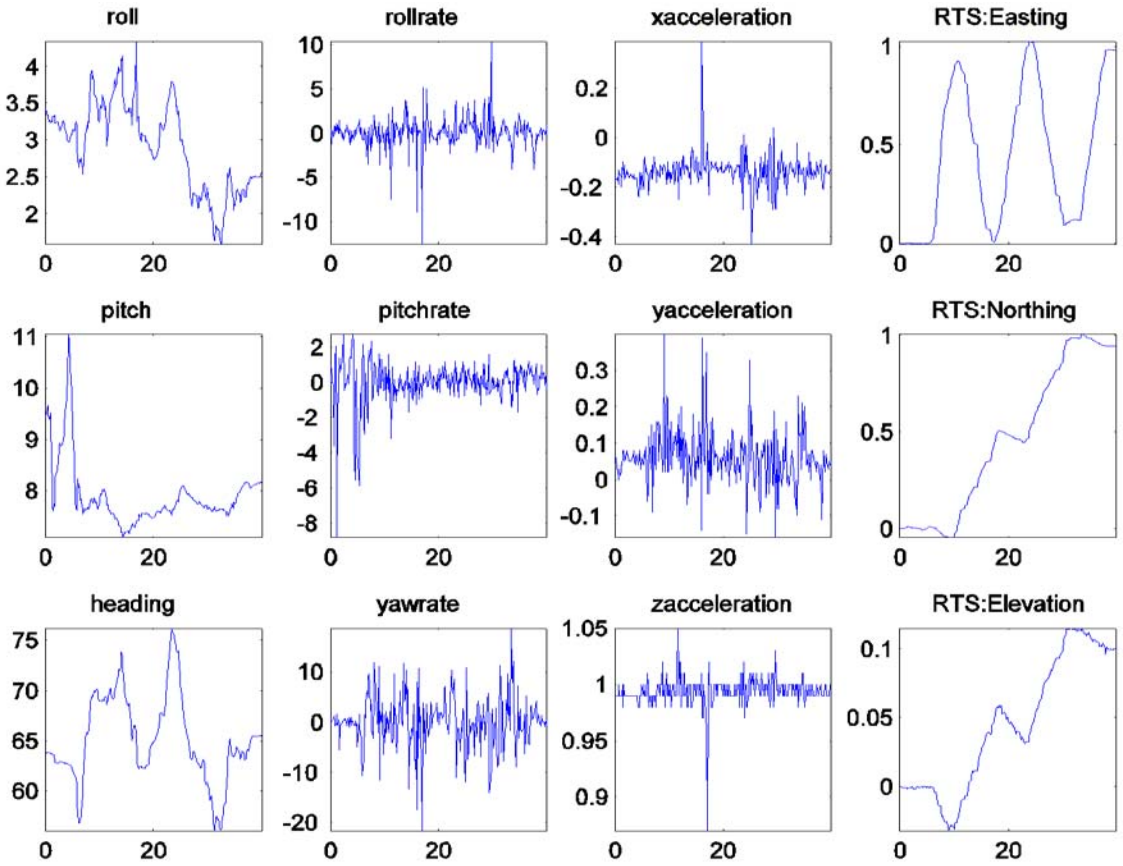

Figure 38. Example of IMU data (first three columns from left) and RTS data as a function of time (s): high frequency noise and large spikes (data for a slow-speed survey).

The gyro (angular rate) and acceleration data show large spikes and high frequency noise. Attitude data, also noisy, are necessary for the inversion of EM61 data because orientation of the EM61 sensor has a significant influence on the transmitted and received signals and any variations must therefore be accounted for (the transmitter and receiver loops are not collocated). High frequency variations are, however, not realistic because the operator cannot physically move the sensor at such a quick and erratic pace. Attitude data must therefore be filtered before being used for inversion with, e.g., a median filter (appropriate for non-linear noise). An example of filtered IMU data with a median filter of length 9 is illustrated in Figure 39. Most of the data acquired during our testing show similar features.

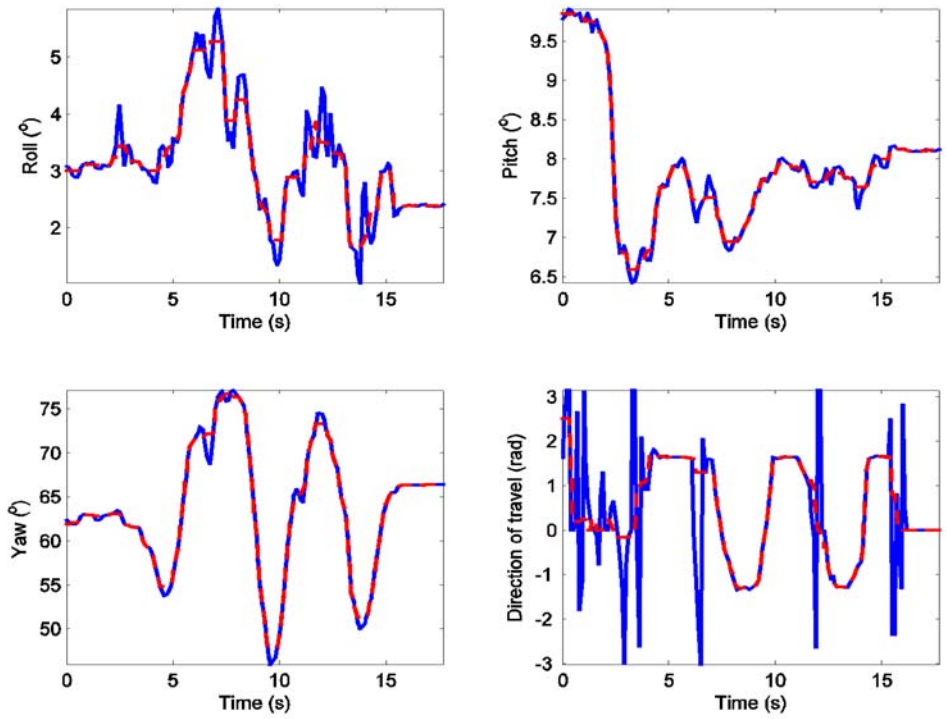

Figure 39. Filtering IMU attitude information: raw data (blue) and filtered data (red) using a 9-point median filter for roll, pitch and yaw, and 11 points for the direction of travel (a.k.a. azimuth).

3.4.2. Fusion of IMU and RTS Data

The IMU provides information about the attitude, gyro and acceleration of a body in motion. IMU and positional data can be combined to improve the accuracy of the positional system and predict positions between positional updates if the IMU has a faster update rate. Such systems have seen many applications for the navigation of helicopters and unmanned vehicles, cars and drones, using GPS and IMU. (e.g., Brandt and Gardner, 1998).

IMU data were collected in angle mode, which implies that the attitude data were already pre-processed internally by the IMU with a black-box Kalman filter (Kalman 1960), using gyro and accelerometer data to stabilize the attitude data.

A Kalman filter is combined with the navigation equation for a strap-down IMU. Taking positional data (GPS, RTS) as reference points, it integrates IMU data sampled at a faster rate to predict position and velocity between positional updates. Accounting for the expected errors in the reference positions and the IMU data, the method takes at each step a prior positional update to derive a prior estimate of the covariance of the position variables to weigh the new predicted position derived by integration of the IMU data, and corrects the position at a updated time (so that reference positions are corrected within their standard deviation).

Linear and non-linear formulations of a Kalman filter were tested. Maybeck (1979) and Welch and Bishop (1997) were used for the linear and non-linear filters with the Unscented Transformation to compute covariance according to Julier and Uhlmann (2004).

3.4.3. Algorithm

Algorithms were tested and validated on synthetic data, where levels of noise and positional error can be controlled. The following cases were tested: free falling object, rotation around a fixed axis, synthetic representation of a survey with a swinging sensor following a fixed zigzag pattern (Figure 40).

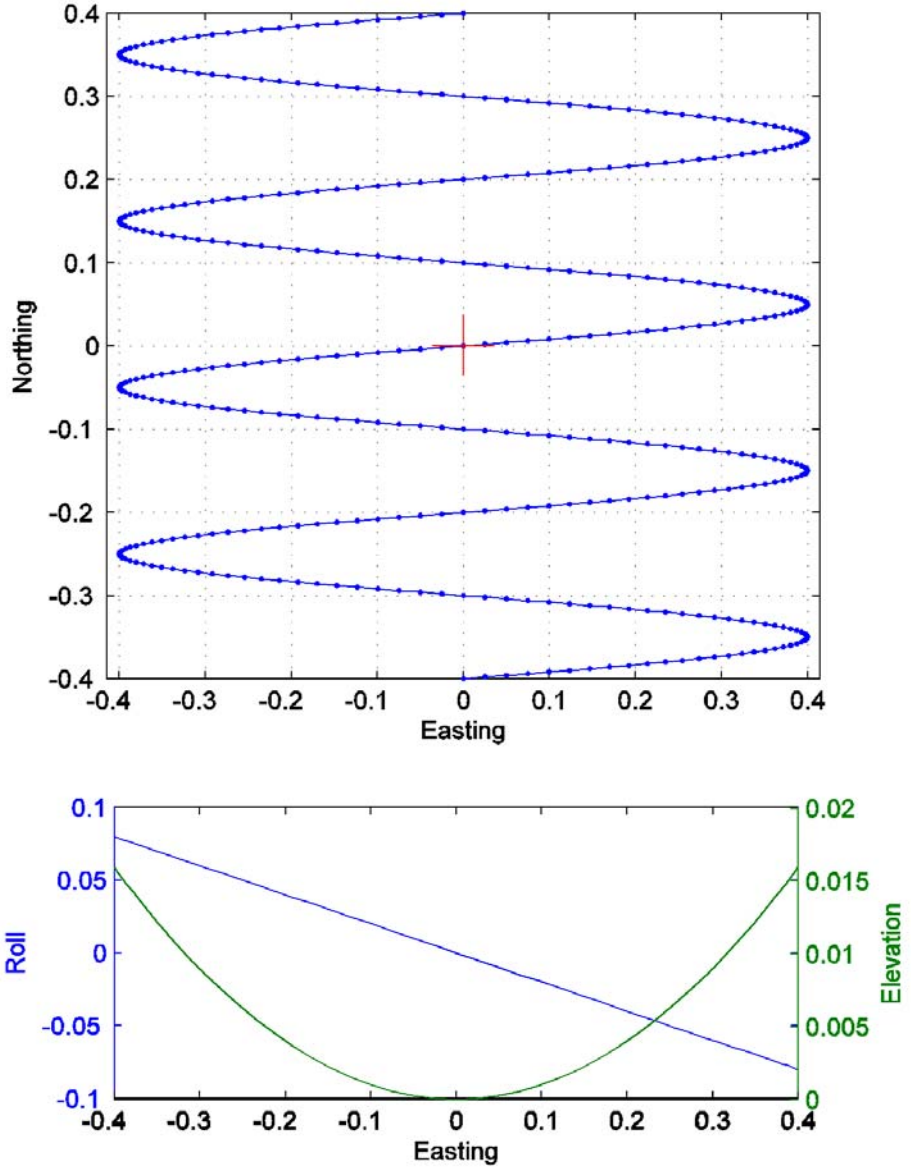

Figure 40. Synthetic path for a zigzag-type survey. Top panel: path and stations (dots). Low panel: roll and elevation when swinging the sensor from side to side in a survey. This survey mode is applied for the simulation of EM data in a later section.

Figure 41 shows the results of a synthetic test that uses the same characteristic errors as the RTS Leica and Crossbow IMU. The RTS is assumed to be placed at the top end of a boom, the IMU at the low end. Positional updates with the RTS occur at 1 s interval and stop after 6 s to illustrate drift; IMU updates at 10 Hz. The position of the RTS can be interpolated between its measurement updates by using the IMU (red line in middle panel, blue line shows linear interpolation) and the predicted position is close to the true position after the RTS updates stops (at 6 seconds). This result illustrates the stability of the Kalman filter algorithm.

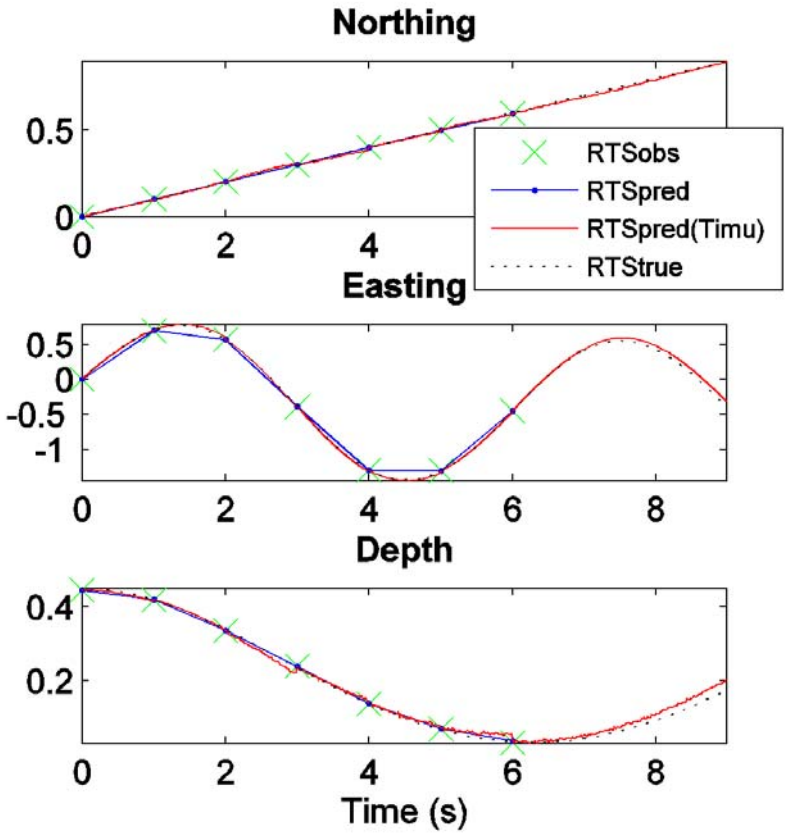

Figure 41. Synthetic test of integrating RTS and IMU data. RTS positions are assumed to be observed every second (RTS_{obs}) and predicted at the IMU update rate of 0.1 s (RTS_{pred} at 1 s using IMU, $RTS_{pred}(T_{imu})$ at 0.1 s interval using IMU). Horizontal axes: Time (s). Vertical axes: Northing, Easting and Depth (m).

3.4.4. Application to Field Data

Tests of integration with data collected in the field with the Crossbow IMU and Leica RTS were not successful because:

- There are large variations of time step for the RTS due to possible malfunction, causing random positional errors up to 0.30 m. This is a problem for the Kalman filter, which works best with a fixed time step; and,
- IMU data were found to have large levels of noise and were recorded at a low sampling rate.

In future deployments we expect those issues to be addressed to fully exploit the combination of positional and IMU data to obtain accurate positions at a fast update rate.

3.5. Inversion of EM Data

3.5.1. EM Model for Inversion

In time domain EM a loop of wire generates a time varying magnetic field that is used to illuminate a conducting target. This primary field induces surface currents on the target which then generate a secondary magnetic field that can be sensed above ground. With time, surface currents diffuse inward, and the observed secondary field consequently decays. The rate of decay and the spatial behavior of the secondary field are determined by the target's conductivity, magnetic permeability, shape, and size. The electromagnetic response of the target will be primarily dipolar for the target/sensor geometries of UXO surveys. The induced dipole is

$$M(t) = \frac{V}{\mu_o} A^T P(t) A b^P \qquad (1)$$

where V is the volume of the object, μ_o is the permeability of free space, A is the Euler rotation tensor, b^P is the primary field generated by the sensor transmitter loop, and P(t) is the magnetic polarization tensor. The shape and material properties (i.e., conductivity and magnetic susceptibility) of a target are contained in P. The time-dependent polarization tensor P(t) has the form

$$P = \begin{bmatrix} L3 & 0 & 0 \\ 0 & L2 & 0 \\ 0 & 0 & L1 \end{bmatrix} \qquad (2)$$

with L1 the largest eigenvalue, L3 the smallest, and L2(t)=L3(t) for axi-symmetric targets. In a typical survey, TEM soundings are acquired at a number of different locations by moving the transmitter and receiver along the surface, thereby illuminating the target at a number of different angles. This, in turn, causes different components of the polarization tensor to be preferentially excited.

For a Geonics EM61HH, the time decay of the scattered EM field is measured at four channels, corresponding to four time gates (0.216, 0.366, 0.660 and 1.266 ms) measured on a coil receiver placed in front and slightly above the transmitter coil (Figure 42). As a result the polarization tensor is to be resolved at four times. The orientation of the dipolar object remains the same at all times, therefore the rotation matrix A is constant and determined by three angles: φ, θ, γ. Thus the model, m, for the UXO parameterization can be written with 18 parameters (3 for position, 3 for orientation and 3×4 for polarization), under the form

$$m = [X; Y; Z; \varphi; \theta; \gamma; L1(t1); L1(t2); L1(t3); L1(t4); L2(t1); \ldots] \quad (3)$$

where X and Y denote the surface projection of the center of the body and Z is the depth of the object below the surface. The parameters are recovered by solving a least squares non-linear inverse problem that consists of minimizing the data misfit function

$$\Phi(m) = \left\| W(F[m] - d^{obs}) \right\| \quad (4)$$

subject to constraints if provided. The matrix W contains the standard deviations of the data (estimated noise and errors in the data), F is the forward modeling operator and d_{obs} is the observed data (details in Pasion 2007).

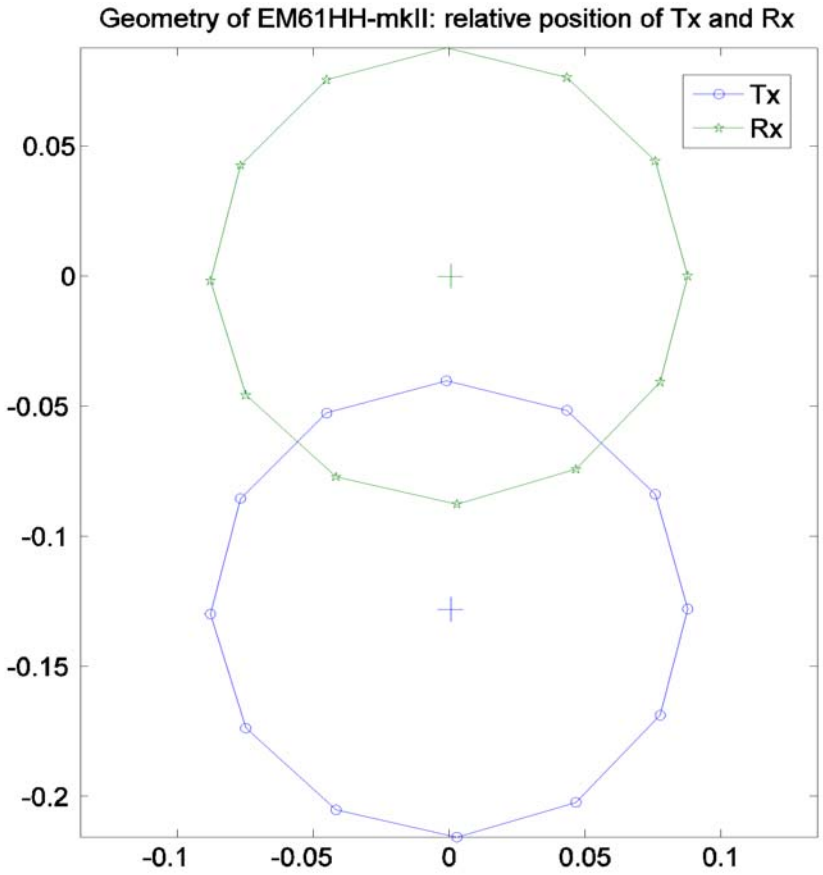

Figure 42. Geometry of EM61HH-MK2 sensor. The transmitter and receiver coils are not collocated; therefore it is critical to know the attitude of the sensor to accurately predict the primary field and the recorded scattered field.

3.5.2. Survey Speed and EM Anomaly

The receiver of the EM61HH-MK2 measures the voltage in the receiver loop V = dB/dt caused by the secondary field of a conductive, buried object. The measurement is not instantaneous and therefore the sensor records the integral of V over a time window. In dynamic acquisition mode the sensor moves during a measurement, therefore the voltage may vary during the time window.

If that occurs the integral of V(t) during the measurement is smaller than the peak value of the signal and the recorded amplitude will decrease for a fast survey (Figure 43).

When inverting EM data collected in dynamic mode the sensor motion should be accounted for, if significant. If accurate positioning were available with a faster update rate, the position of the EM61 sensor could be located during the measurement sweep. However, with degraded accuracy, such an attempt is unwarranted; therefore we assume for the modeling that the measurement is instantaneous to compare the peak amplitudes among a given type of surveys. The assumption appears to be in line with the recorded amplitudes displayed in Figure 43.

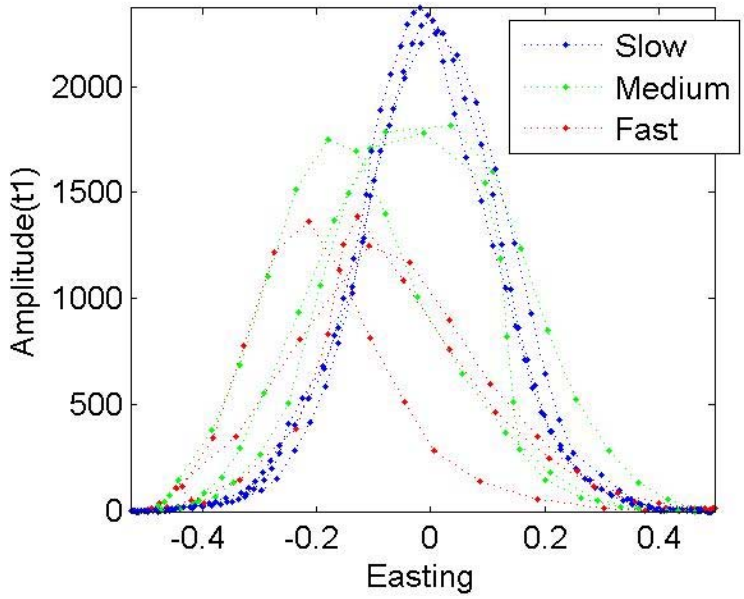

Figure 43. Amplitude of measured EM signal for surveys at slow, medium and fast pace over the same object.

3.5.3. Survey Design for Improved Discrimination: Synthetic Tests

Simulations were performed by generating synthetic data to assess the conditions under which a hand-held sensor could collect data of sufficient quality for EM inversion and discrimination. The conditions of the field are applied:

- the size of the buried object to identify: here the 2.125-inch steel ball used in the field;
- the depth of the target: here 0.10 m.

The survey mimics the zigzag drawn in the field with a tighter separation between lines, as in Figure 41. Some of the key parameters to examine include:

- the positional accuracy: depends on the positional sensor (std. dev. dr = 0, 2, 5 mm) and the orientation sensor (std. dev. dθ = 0, 1, 2); and,
- the station spacing (DX = 2.5, 5 cm, equivalent to survey velocity), line spacing (DY = 10 cm) and relative position of the target with respect to the survey line (Note: in the first

round of field tests there are only two lines passing over the anomaly, which provides limited coverage for inversion).

By varying the position and depth of the target, and the positional error of the sensor, hundreds of Monte Carlo simulations were made to test the effect of the survey design on the quality of an inversion and the possibility to discriminate. The success of these inversions is measured by the deviation from the actual position of the target and the recovered polarization (Figure 44) and the predicted depth (Figure 45).

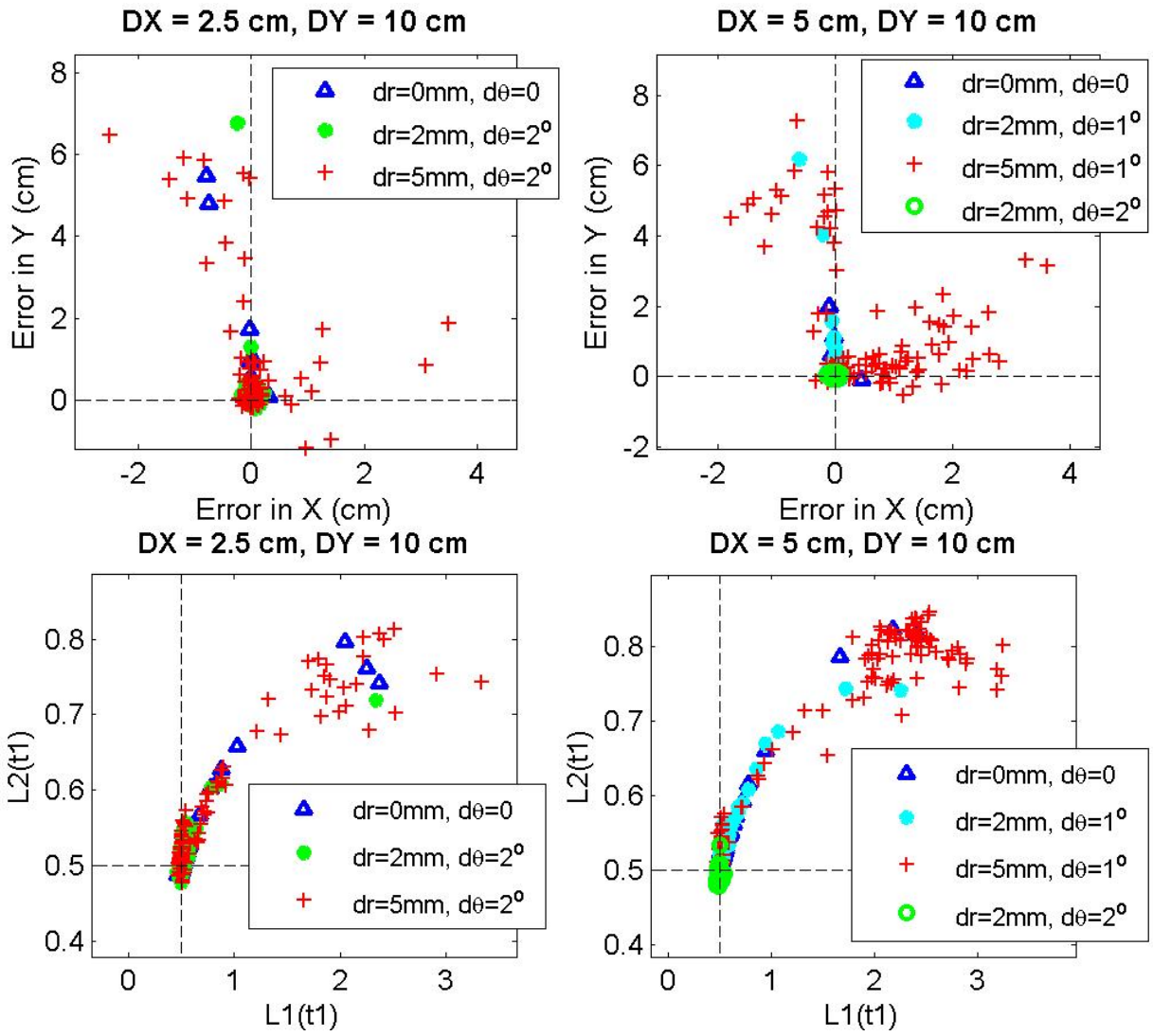

Figure 44. Results from inversion of synthetic data. Top panels: Difference between true and predicted position of target for different qualities of surveys. Bottom panels: Recovered first and second components of the polarization tensor at first time channel. The true value is 0.5 for each.

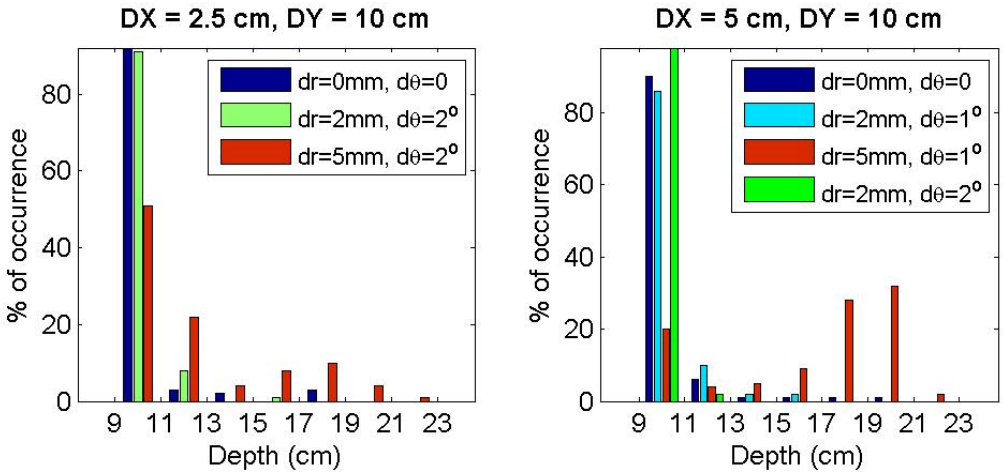

Figure 45. Predicted depth. True value is 10 cm.

Interpretation of these results can be done by considering the depth alone. Indeed, because the amplitude of an anomaly depends on the size or depth of a buried target, there is often an ambiguity between the size and depth of a target, and therefore the predicted size is correct if the recovered depth is accurate, whereas an item predicted too deep appears larger than it is.

Results show that all surveys with a positional error of 0-2 mm provide acceptable recovery of depth in most cases. There are few instances where depth estimates are inaccurate despite minimal positional error; this occurs when the position of the target relative to the two nearest survey lines causes an ambiguity in the target location. When that error reaches 5 mm with 1-2 degree on IMU (comparatively still a small error), then results become unstable, especially when station spacing increases to 5 cm (Figure 45). Given that 5 and 10 cm spacing for stations and lines constitute a dense survey to deploy in the field, these results suggest that high accuracy on the position and orientation of the sensor is critical for the discrimination of buried items.

3.5.4. Inversion of EM Data with Leica Positioning System

Figure 46 shows the result of an inversion for which the positions derived from the Leica system are not corrected. With positional errors, the recorded EM data are mis-located. The inversion fails because the model cannot reproduce the discrepancy between the positions given by the RTS and the spatial decay of the EM signal.

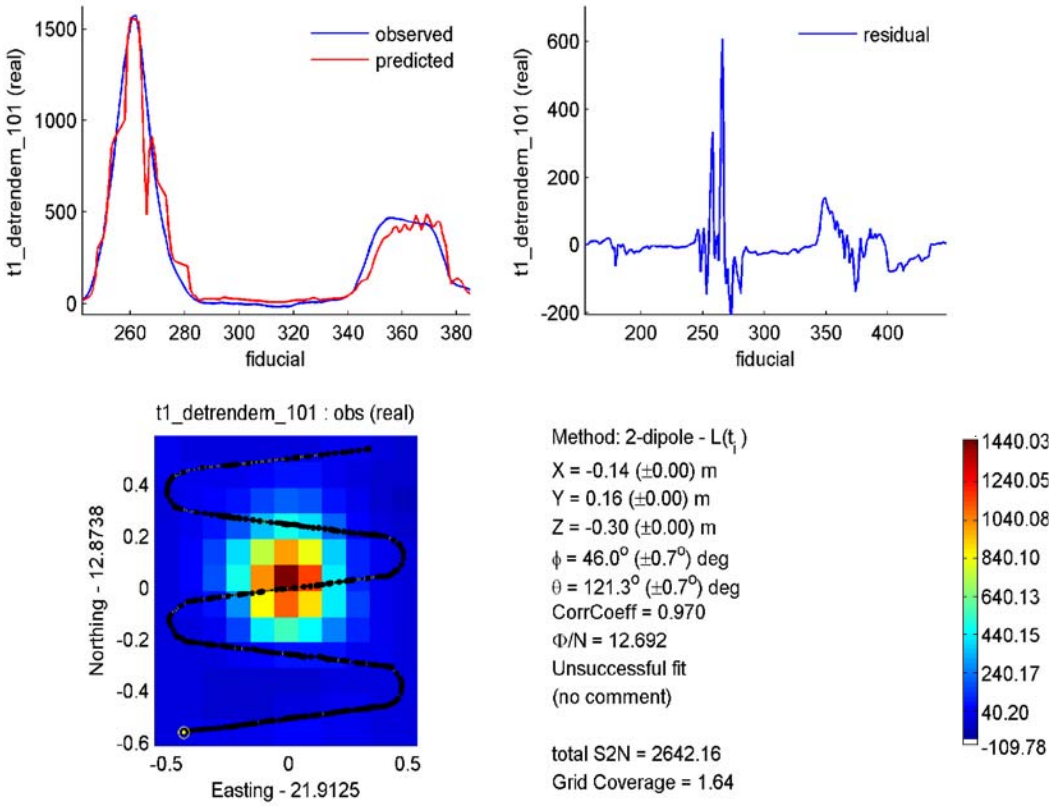

Figure 46. Inversion result for uncorrected positions. In the upper left window, the positions obtained from the RTS do not correspond to the physical spatial decay of the observed EM signal. Using those positions for the inversion, the dipole model fails to accurately predict the unphysical EM signal. In the upper panels, fiducial corresponds to the sequential data point number, while the ordinates are the detrended and drift-corrected data for the first time channel (the EM-61 sensor measures a relative amplitude that needs to be calibrated and drift-corrected so that background signal is close to zero in free space).

Following the method to correct positions that is proposed in the previous sections, EM61 data are re-merged with position and orientation data. Then inversion can be applied to all survey modes: static survey with the operator stopping at stations separated by an arbitrary distance; sweeping mode at slow, medium and fast speed. Figures 47 to 50 show examples of inversion results for the 37-mm projectile surveyed with the fixed zigzag pattern in the static, slow, medium and fast pace modes, respectively.

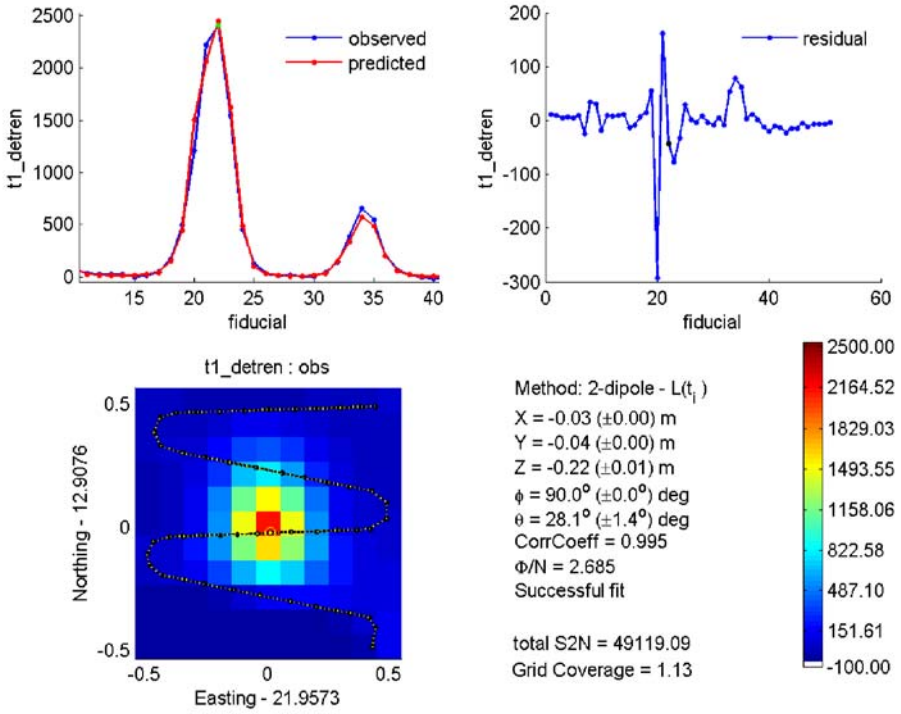

Figure 47. Inversion above 37-mm projectile, static survey mode. True depth is 8 cm, predicted depth is 22 cm. Despite a successful fit, the inversion fails because the station spacing is too large to provide a strong constraint on the depth of the object. Same legend as Figure 46.

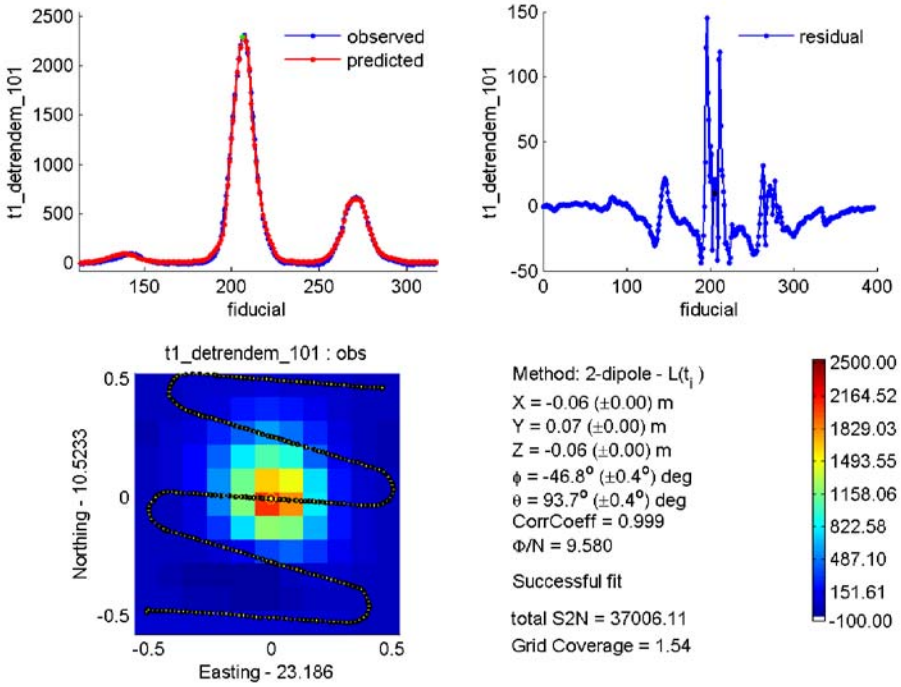

Figure 48. Inversion for slow survey mode. Here the predicted depth is 6 cm, observed is 8 cm. The inversion is successful because the slow survey allowed a high sampling rate along lines. Same legend as Figure 46.

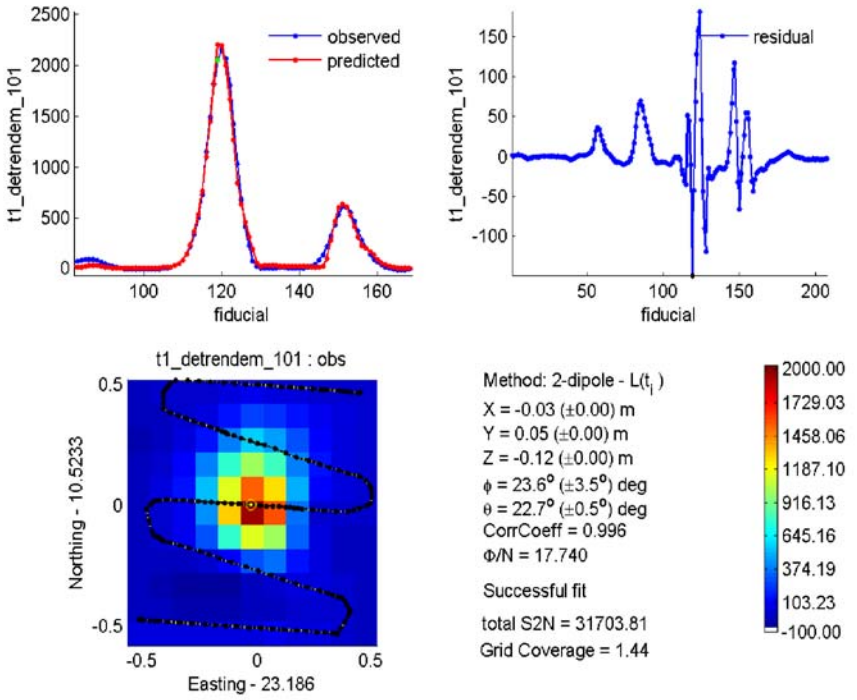

Figure 49. Inversion for medium speed. Here the result starts degrading (12 cm instead of 8 cm), because a faster survey mode effectively increases the spatial sampling rate. Same legend as Figure 46.

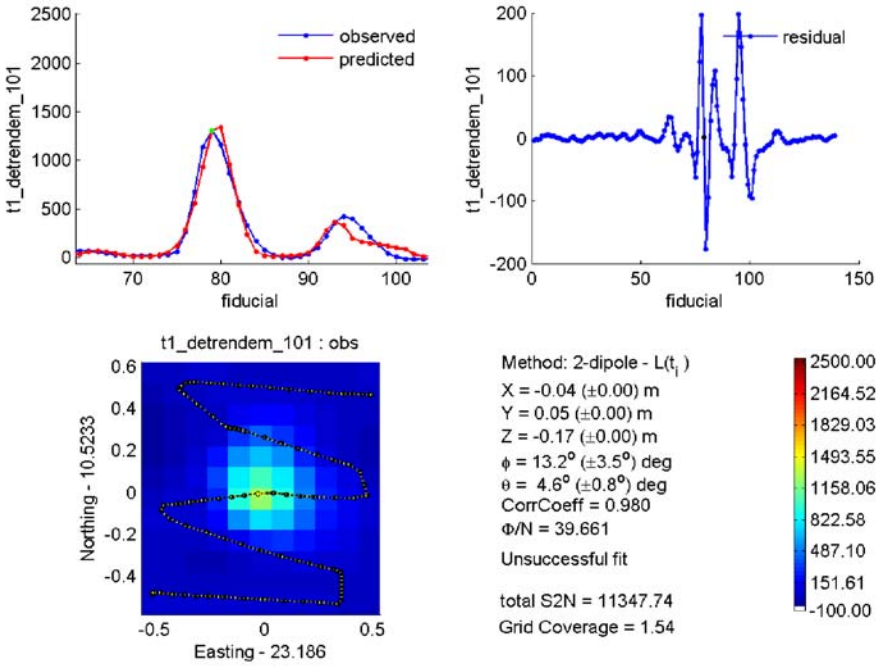

Figure 50. Inversion result for fast survey. Inversion fails, the spatial sampling is too coarse and the amplitude of the anomaly is not captured because of the dynamic mode acquisition, therefore the recorded amplitude of the anomaly is reduced and the polarization parameters derived from the inversion are invalid. Same legend as Figure 46.

Results of the inversions for all surveys and targets are gathered in Figure 51. The data are collected over a 2.125-inch steel ball by following the fixed zigzag and a free-form zigzag and over a 37-mm projectile on a fixed zigzag with the target at a horizontal and vertical orientation. The results are presented in terms of the depth-polarization relationship to illustrate the ambiguity between the two parameters. We find that the best results are achieved for the slow surveys because that mode brings the highest spatial sampling. There remain, however, failures even at slow pace because the separation between lines is too wide. Static test failed because stations are located too far apart.

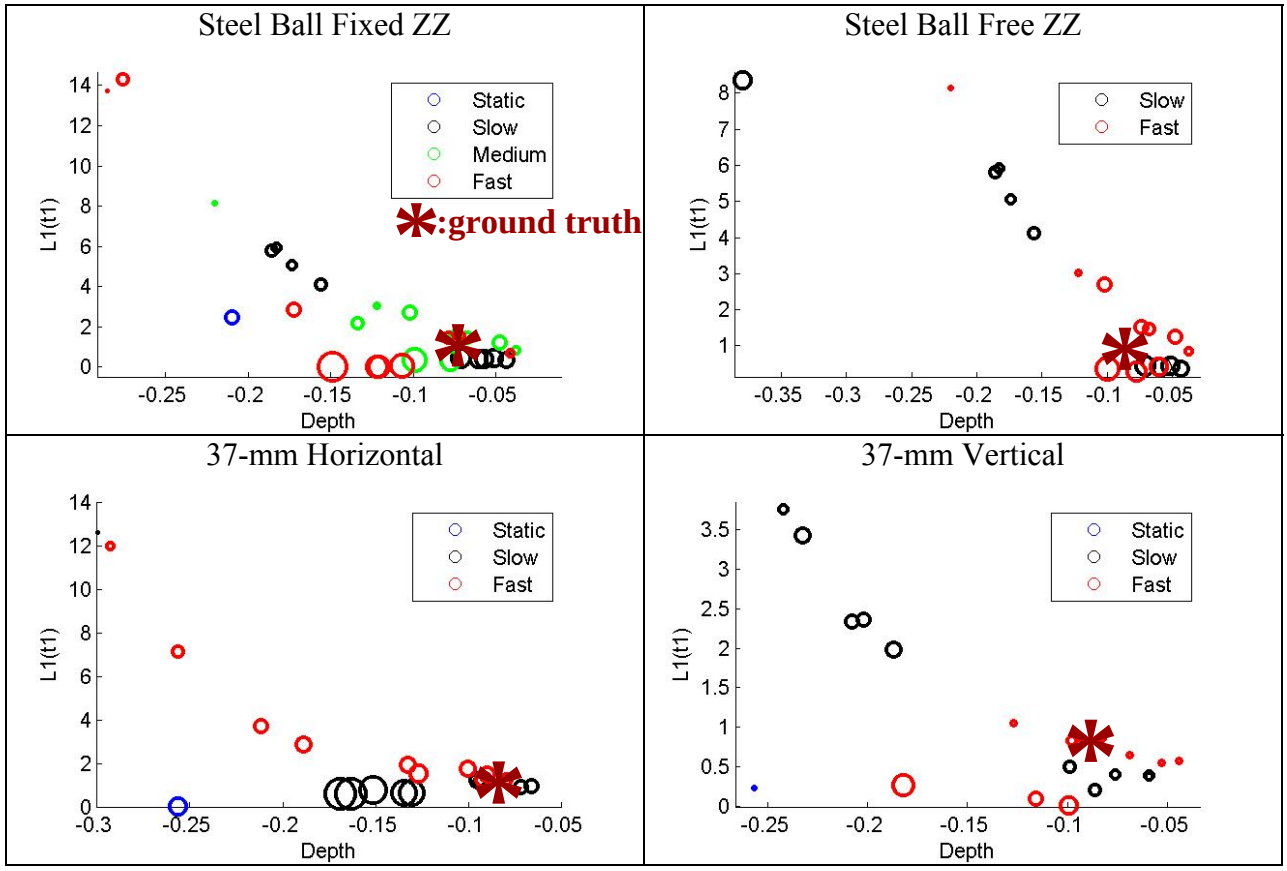

Figure 51. Results for all inversions. Colored circles indicate the survey mode: blue for static, black for slow, green for medium and red for fast. Radius of circle is proportional to amplitude of L2(t1). Targets that are predicted too deep have too large polarization (L1 or L2).

3.5.5. Inversion of EM Data with Trimble Laser Positioning System

New data were collected in Fall 2007 with the Trimble laser positioning system. For integration tests with the Geonics EM61HH-MK2 sensor, a survey guide with a new zigzag pattern was carved in a wood panel with tighter line spacing, following recommendations from the synthetic

tests (Figure 52). Data were collected over a 2.125-inch steel ball and a 37-mm projectile (horizontal and vertical orientation), both items buried at 0.15 m and 0.30 m below the surface. The effective depth below the EM sensor is approximately 0.10 m deeper. For these tests the IMU data are not available. However, the operator took care of pointing the EM sensor always in the same direction (azimuth); we assume therefore that the azimuth is constant and that its value is that of the general direction of the survey (near perpendicular to lines). From the synthetic tests shown in the previous sections we know that that assumption may cause large errors in the predicted depth.

a. New fixed zigzag guide for survey.

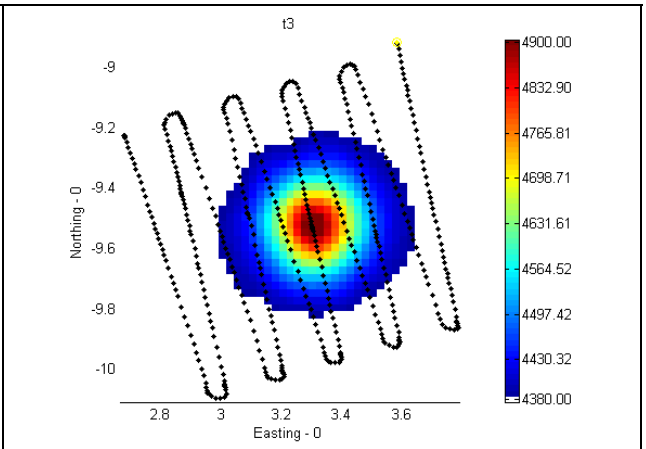

b. Example of EM data collected on new guide (1st time channel)

Figure 52. Zigzag guide for tests with Trimble unit.

Figure 53 summarizes the inversion results for all configurations. Results are presented in terms of classes corresponding to each combination of a target, depth and orientation.

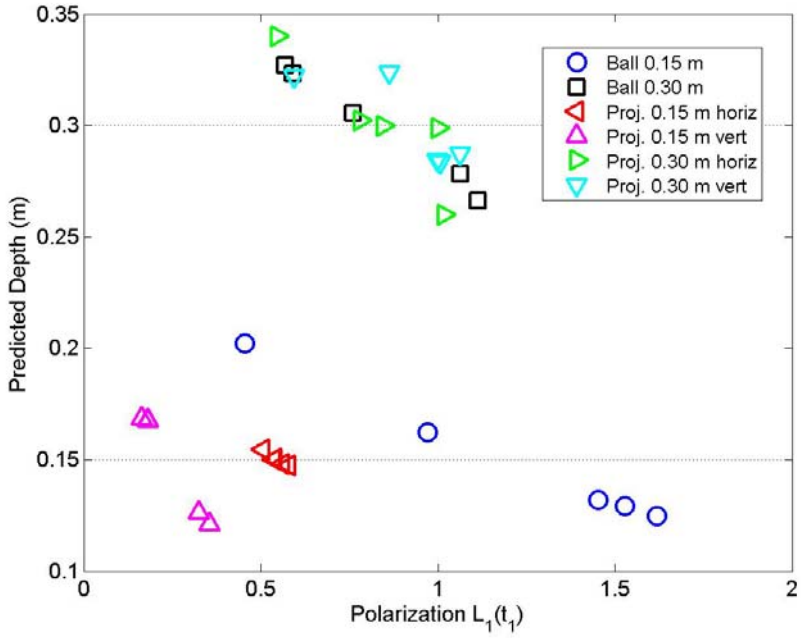

Figure 53. Inversion result for all field data collected with the Trimble system.

Results for the 37-mm projectile are generally stable, with a maximum depth error of 0.02 m at shallow depth and 0.04 m at greater depth, which corresponds to a two-fold variation of the largest component of the polarization tensor. Results for the steel balls are less reliable, with depth errors up to 0.06 m in the shallow case and 0.04 m in the deep case, with corresponding three-fold and two-fold variations in polarizations, respectively.

Figures 54 and 55 show results from the inversion above the steel ball buried at 0.15 m and 0.30 m, respectively, for the worst inversion (in terms of predicting the depth of the buried item) at each depth.

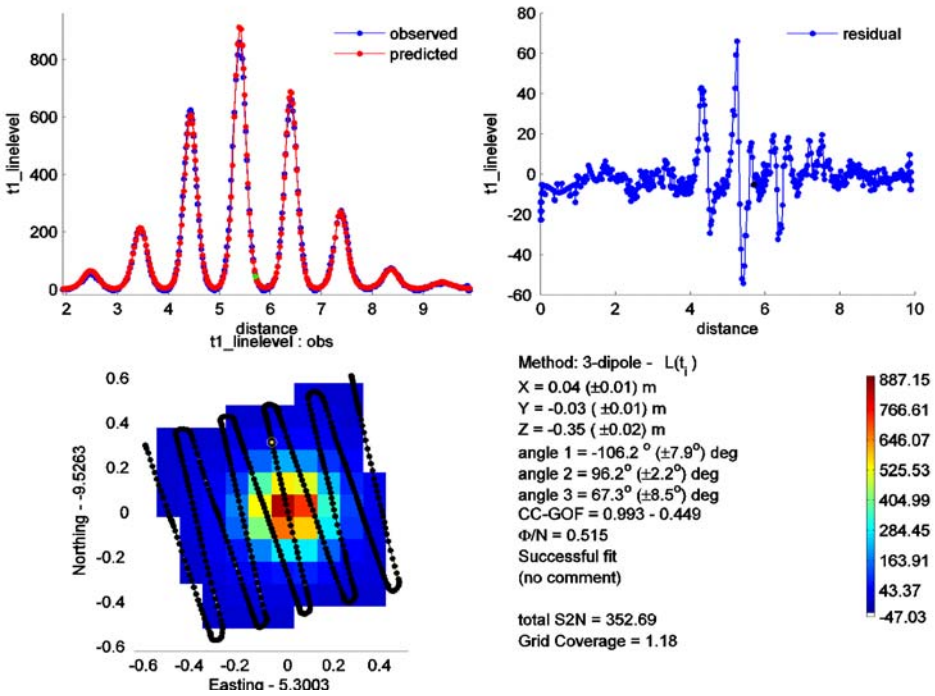

Figure 54. Inversion result for a steel ball at 0.15 m depth, effectively 0.30 m below the sensor. Although the fit is successful, the recovered depth is exaggerated by 0.06 m.

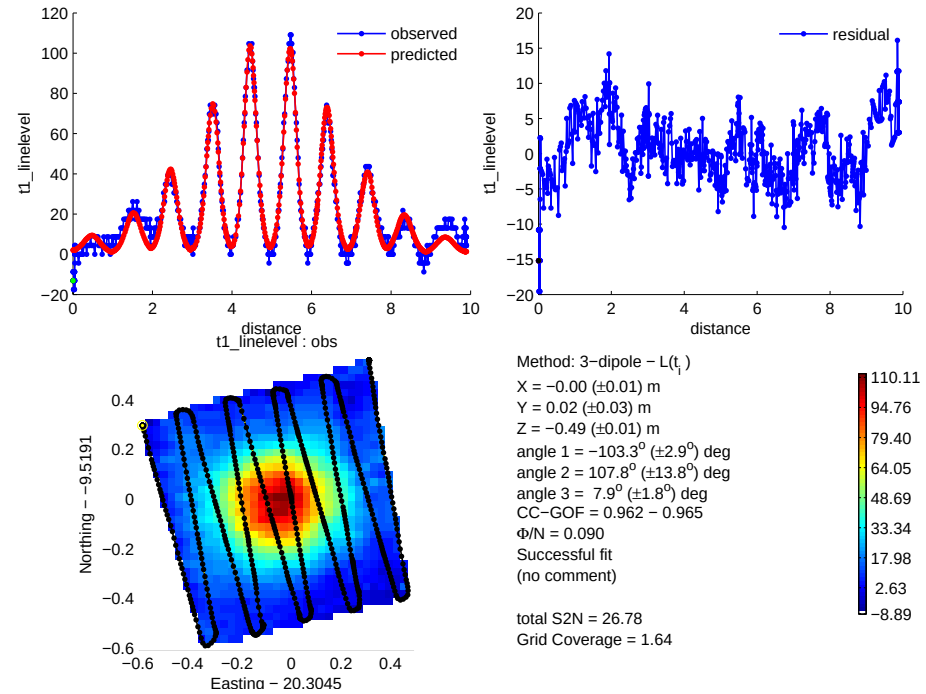

Figure 55. Inversion result for a steel ball at 0.45 m below the sensor. The fit is successful but the recovered depth is exaggerated by 0.04 m.

In both cases the predicted data closely fit the observed data. The inability to recover the accurate depth may be due to the orientation error, which has more affect on the shallow steel ball because its anomaly is comparatively the smallest and therefore is most sensitive to orientation errors on few data points. The worst errors correspond to the earliest surveys, for which we could also assume that the operator was not completely at ease with the survey protocol and might have allowed the sensor azimuth to shift.

Overall this last set of inversions proves to be successful, as depth and polarizations are recovered within a tight range that would allow reliable classification. The success, relative to the first survey campaign, can be attributed to a more accurate positioning system, tighter line spacing and a slow survey pace. Finally, although the tests for deep burial place the target at 0.45 m depth and thus approach the theoretical detection limit for EM61HH (11x diameter of 37 mm projectile), inversions remain successful.

3.6. Discussion

Hand-held sensor data can be used to identify a buried 37 mm projectile at a one foot depth. To achieve this result a survey requires accurate positioning, controlled orientation and high sampling rate along tightly spaced lines.

In this study we showed that the Leica RTS has too large a jitter in the latency for reliable target discrimination using handheld sensor deployment. An algorithm was developed to identify and correct - at first order - the latency issues. We tested the algorithm to combine positional and attitude data from an IMU and showed its potential on synthetic data. Application to improve a field survey was not possible due to the poor quality of the data. Through simulations we illustrated the requirements for accurate positioning and orientation of an EM sensor and the trade-off between a high spatial coverage and near-perfect knowledge of the orientation of a sensor.

Field data from two different experiments were inverted. The first effort showed limited success mostly due to poor spatial coverage, but also to noisy IMU data and residual positional errors with the Leica system (1st order corrected). The second trial used a higher spatial sampling, the Trimble positioning system, and no attitude sensor. In most cases this second campaign provided acceptable results.

Additional work is warranted to thoroughly demonstrate the capability of the system and identify its limits. Data could be collected at a broader range of depths, using at least a tilt meter and digital compass or an IMU to provide better control on the attitude of the sensor, which is a critical variable because the EM sensor is not symmetric. Survey speed could be increased provided that the EM modeling incorporated movement of the sensor head during measurement.

4. MULTI-GUN LASER POSITIONING SYSTEM

Using laser positioning technology requires an unobstructed line-of-sight between the gun and prism to measure positions. This limitation can be overcome by using more than one gun to maintain line-of-sight between the gun and prism; however, there are instances where both guns will lose lock. Therefore, one of the fundamental goals of this project is to develop a multi-gun technology for data collection in wooded environments.

To determine the performance characteristics of the gun and software, tests were conducted in which parameters such as width of screen, distance between screens, and prism velocity were varied. The screens force the interruption of line-of-sight and allowed the internal algorithms of the gun or software to assume control and position the gun to the prism's location.

4.1. Materials

4.1.1. Leica TPS 1203, Trimble ATS600 and SPS930

As described in a previous section.

4.1.2. ActionTarget System

The ActionTarget PT-Runner system consists of a main cable, drive cable, electric motor, idler pulley, control panel, and trolley. The main cable attaches to secure mounting points, the trolley rides on the main cable, and the drive cable attaches to each end of the trolley. The drive cable loops around the idler pulley on one end and the electric motor drive pulley on the other. A toggle switch and rheostat in the control box controls the direction and speed of the trolley. The trolley assembly is non-stabilized, meaning the prism can wobble 1-3 cm side-to-side as it traverses down the cable as the trolley tries to conserve energy and/or is wind blown.

4.1.3. Prism Tracker Software

All the total stations offer commands to control the gun's operation through a communication port. Using this interface Stratton Park Engineering Company Inc. (SPEC) of Boulder, Colorado, a project teammate, developed a software program to control multiple units and establish prism lock after the gun's internal search mechanisms failed to lock onto the prism (Figure 56).

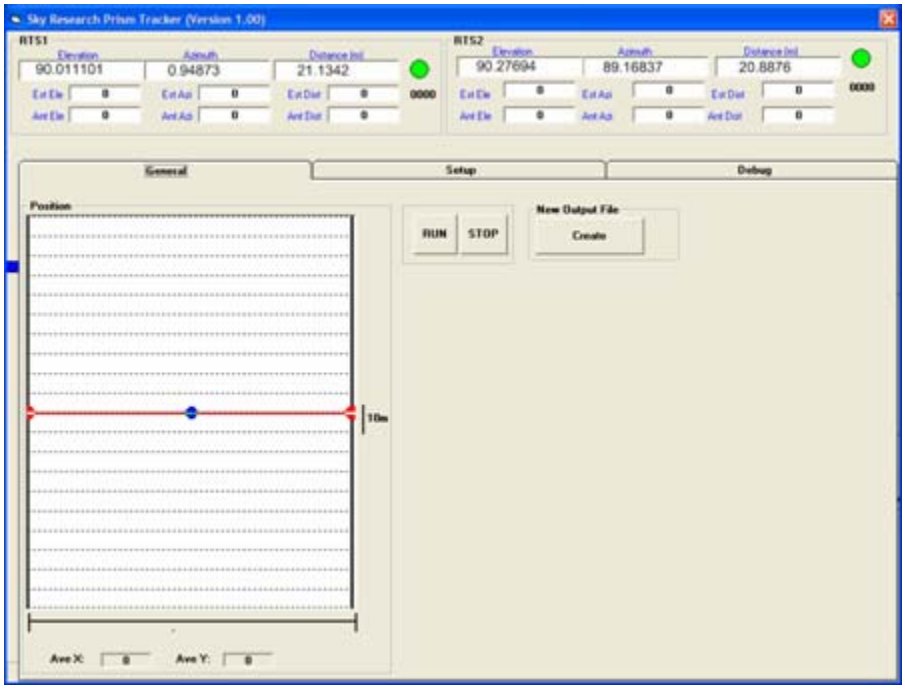

Figure 56. Prism Tracker software display gun information and positions gun to future prism location using information from another gun.

After initial setup of the stations and system initialization/calibration, the software measures the gun angles and displays the prism location on a position map. The software sets up a local coordinate system with the first gun location described as (0, 0) pointing north and the second location described as (0, Y) pointing south, with Y designated as the distance between the guns. The software displays the location of the prism in relation to the guns and some instrument state information. The software also provides audio feedback when the prism is lost and some navigation clues when trying to establish lock.

4.2. Leica 2005 Tests and Results

4.2.1. Controller Software Test 2005

SPEC developed a software program to control multiple RTS and reestablish prism lock after obscured line-of-sight. The program utilizes remote procedure calls (RPC) to issue commands to and receive command replies from the gun. RPC are comma delimited ASCII commands consisting of a command header, command number, and optional command parameters. For example, %R1Q, 9073 is the RPC to toggle prism tracking; when the gun completes this command it sends the reply %R1P, 0, 0:1 when tracking is true and %R1P, 0, 0:0 when tracking is false. The program issues RPC commands over RS232 serial ports. The initial software development was completed in September 2005.

SPEC demonstrated operation of the system in mid-October at the Sky Research project office located outside of Denver, Colorado. The system consisted of two RTS, one prism, one controlling laptop computer, and two cables connecting the RTS guns and the laptop. The guns

were positioned 60 m apart with the laptop located between them. After following a configuration procedure (establishing a local coordinate system), the system was ready for prism tracking.

As the prism moved around the demonstration area, the software displayed the prism's position from both guns and the anticipated position. When one gun loses locks, the anticipated position tells the unlocked gun where the prism can be found. To test the system's ability to reestablish lock after an obscuration, the prism passed on one side of a screen placed 10 m from one gun. The prism velocity stayed constant and when the prism emerged from the screen the unlocked gun locked on after two seconds (Figures 57-59). Subsequent tests had the prism moving on the other side of the screen and in another test the prism reversed direction. The software was able to reestablish lock within 2 to 3 seconds after coming into view.

Figure 57. The RTS unit tracks the prism unit obscured by an obstruction.

Figure 58. The prism is blocked by the plywood obstruction.

Figure 59. The RTS unit regains lock on the prism.

The demonstration revealed some limitations of the system that required modification to increase relock performance. After talking with system technicians and programmers at Leica GeoSystems, Leica proposed the newly issued firmware that may resolve some of the issues and provide more control to the basic operations of the gun. They also recommended changing the order of the issued commands to increase performance. Other limitations of the system are as follows:

- No solution when both guns lose lock;
- Slower prism speed when locked with one gun, speed increases after both RTS units lock onto the prism;

- Unknown accuracy of position data, this requires a test over a known repeatable path to measure the multiple gun system;
- Using projected coordinate system is untested;
- Gun separation fixed to the length of the serial cables (Leica RTS units typically use 2.4 GHz radio communication for remote operations); and
- The system does not store data.

4.2.2. Moving Target Test

The moving target test quantifies the recovery time of a laser-based positioning system by systematically performing tests changing one parameter at a time to measure the response of the instrument. These tests measure the response time of the gun and the controller software as a function of screen width and survey speed. The tests used the ActionTarget moving target system which could move the prism 20 m at 0.5 and 3 m/s. The tests are designed to answer the following questions:

- How wide can an obstruction (e.g., a tree) be while prism lock is maintained?
- What minimum distance between obstructions will cause loss of prism lock?
- How fast can the prism move during a survey traverse with LOS obscuration while still maintaining prism lock?
- What is the system response time when the software needs to re-direct the guns?

All laser positioning systems executed this test in three stages; see Figure 60 for a schematic of the test layout. The three stages of the test are:

1. Single Screens. Single obstruction screens used to block LOS of a single gun.
2. Double Screens. Two obstruction screens used to block LOS of a single gun.
3. Alternating Screen: Two obstruction screens used to block LOS of both guns.

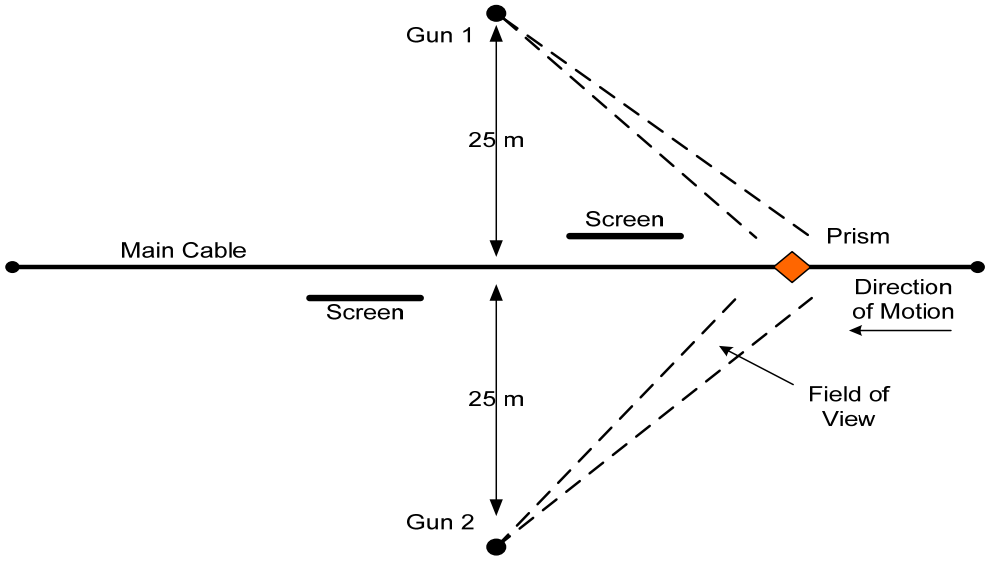

Figure 60. Schematic layout of the moving target test. Two tracking guns were positioned on either side of a test line. Line-of-sight is blocked by screens placed adjacent to the track.

Screens were built using 2" × 4" wooden supports with black plastic stretched between the supports (Figure 61). The plastic allowed the screen width to vary by simply rolling up the plastic onto one of the supports.

Figure 61. Equipment layout for the LOS tests conducted for performance assessment of the multi-gun positioning technology.

The PT-Runner system was set up with a total distance between the ends of the system of 20 m (Figure 61). The guns were placed on either side of the PT-Runner, at a distance of approximately 25 m and centered on the main cable. Test operators sat off to one side to ensure no other obstructions occurred as the prism was moved down the line. The distances from each gun to the main cable were held constant for all tests. The PT-Runner control box did not directly specify trolley speed, so a couple of test runs without the screen in place provided the survey speed.

4.2.3. Single Screen Test

This test measures the distance a moving prism travels before lock is obtained after emerging from behind a screen. The relock is controlled by either the gun's internal search algorithm or the SPEC controller software. This is the simplest case with one screen set midway down the travel line and a gun positioned approximately 20 m away; see Figure 62 for a schematic. By changing the prism speed and screen width, the relock capabilities of the gun and software can be assessed to see how it fluctuates with changing conditions. Table 6 provides a list of the different parameters used for these tests. Not all the instruments used the same parameters because they all perform a little differently compared to each other. For example, the ATS600 has a definable search parameter that was disabled to force the ATS600 to use the controller software to relock onto the prism.

Table 6. Test parameters for Trimble SPS930 Single Screen Test

Test Number	Survey Speed (m/s)	Screen Width (m)
1	0.50	1
2	0.75	1
3	1.00	1
4	1.25	1
5	0.50	2
6	0.75	2
7	1.00	2
8	1.25	2
9	0.50	3
10	0.75	3
11	1.00	3
12	1.25	3

4.2.4. Double Screen Test

This test uses knowledge from the single screen test to determine the minimum distance between two screens the prism can pass and still be tracked by the gun. As was seen in the 2005 Laser Assessment Wooded Test, the distance between trees affected the performance of the gun. With the Leica and Trimble systems, the appearance of the prism allows the gun a chance to update velocity information which helps in tracking. Though the gun may not capture any positions before being obscured, this brief period of prism visibility is crucial to successfully tracking the prism. The double screen also helps the line-of-sight model in predicting the system state and identifying trouble areas. For these tests, in addition to varying the survey speed and screen width, the screen separation distance varied from 0.5 to 1 m (Table 7). The definition for failure is the gun's inability to establish lock and measure positions consistently between the screens.

Table 7. Test parameters for Trimble SPS930 Double Screen Test

Test Number	Survey Speed (m/s)	Screen Width (m)	Separation Width (m)
1	0.50	2	1
2	0.75	2	1
3	1.00	2	1
4	1.25	2	1
5	0.50	2	0.5
6	0.75	2	0.5
7	1.00	2	0.5
8	1.25	2	0.5
9	0.50	2	0.25

Test Number	Survey Speed (m/s)	Screen Width (m)	Separation Width (m)
10	0.75	2	0.25
11	1.00	2	0.25
12	1.25	2	0.25
13	0.50	2	0.15
14	0.75	2	0.15
15	1.00	2	0.15
16	1.25	2	0.15

4.2.5. Alternating Screen Test

The alternating screen test setup is similar to the double screen test except one screen is positioned on the other side of the cable; see Figure 62. Moving the screen to that side obscures the prism from the other gun. Just like with the double screen test, the screens are positioned at some offset and moved closer together or farther apart to find the failure point. This test is designed to measure the efficiency of the controller software when alternating the line-of-sight between the guns. Understanding how the system works in this test environment will help adjust the controller's algorithm to optimize performance. Also, the line-of-sight model will use these test results to better predict the system state and identify trouble areas.

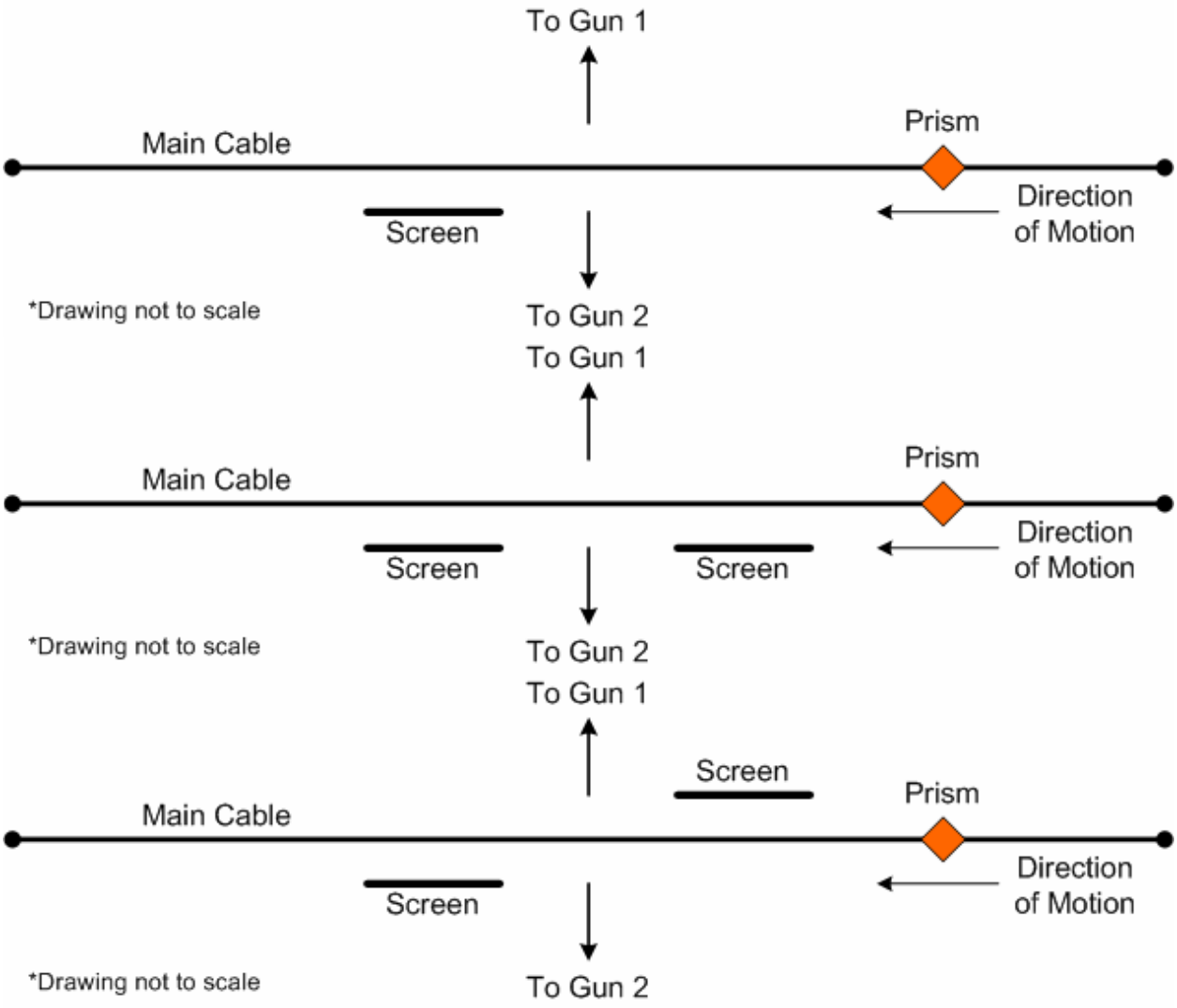

Figure 62. These three images illustrate the equipment setup for the Single Screen (top), Double Screen (middle) and Alternating Screen (bottom) tests.

4.3. Leica 2006 Tests and Results

4.3.1. Single Screen

The Leica used either the internal algorithm to find the prism or the controller software, both of which produce different results. When using the internal algorithm, the Leica regained lock on its own within 0.4 s from the time it reappeared from the screen. With a prism speed around 1.0 m/s, prism lock occurred within 0.5 m. The Leica reliably spotted the moving prism after becoming

visible 95% of the time. The cluster of blue and red points in Figure 63 shows the relock distance for those survey speeds and screen widths.

As the screen width increases to 0.7 m the dynamics of the system changes. The software begins to take control of the relocking procedures and the relock times increase 4 to 5 times more than the internal algorithm times. All the green points in Figure 63 show the relock times as survey speed changes. Two things can be concluded from the 0.7 m screen width data: 1) as the survey speed increases the relock distance increases (easily fit with a line); 2) as the survey speed increases the number of times the prism lock fails increases. All the points with relock distance of zero are tests where the gun failed to lock onto the moving prism. At times the Leica was tracking the prism but could not fine tune the lock at that survey speed to measure a position and other times the prism passed so quickly through the field-of-view of the gun that it started to track but quickly lost the prism.

The success and failure rates summarize the test. At a survey speed of 0.6 m/s, the gun locks onto the prism 90% of the time using the controller software and one test failed to lock. At the approximate survey speed of 0.9 m/s the prism is locked on by the gun 45% of the time and lock completely fail at a rate of 55%. Increasing the speed to 1.1 m/s the prism lock falls to 30% and 60% for no lock at all. There was one test where the internal algorithm actually worked to add the missing 10%, but this was likely a fluke.

There is an optimal location for the Leica instrument where the relock successes of the controller software and survey speed are at a maximum. Though not tested, 0.75 m/s is the likely location of this optimal location. This survey speed or something less is the likely speed for wooded surveys because of obstacle avoidance.

It may appear that the controller software too long to relock onto the prism, this is not the case. The software is operating as designed and it is the summation of the times of each operation in the algorithm that dictates the relock time of the controller software. These operations and their times are as follows:

- Poll the Leica state to see when lock is lost ~ 0.25 seconds
- Calculate future position of prism using velocity information from other gun < 0.01 seconds
- Orient the gun to point to the future location of prism – 1.5 seconds
- Lay in waiting for prism to pass through field-of-view – 1 second

A limitation of the Leica is the instrument cannot lock onto a moving target once it is controlled by 3rd party software. To overcome this limitation the gun points to a location ahead of the prism, is instructed to look for the prism and starts to track once the prism comes into view. There is a 3 second timeout window as the gun is waiting for the prism to enter the field-of-view. When this time expires the operation is repeated again until lock is gained. There was one case, not shown in the figure, where the gun made two attempts to track the prism. This position was about 8 m away from the screen where tracking resumed.

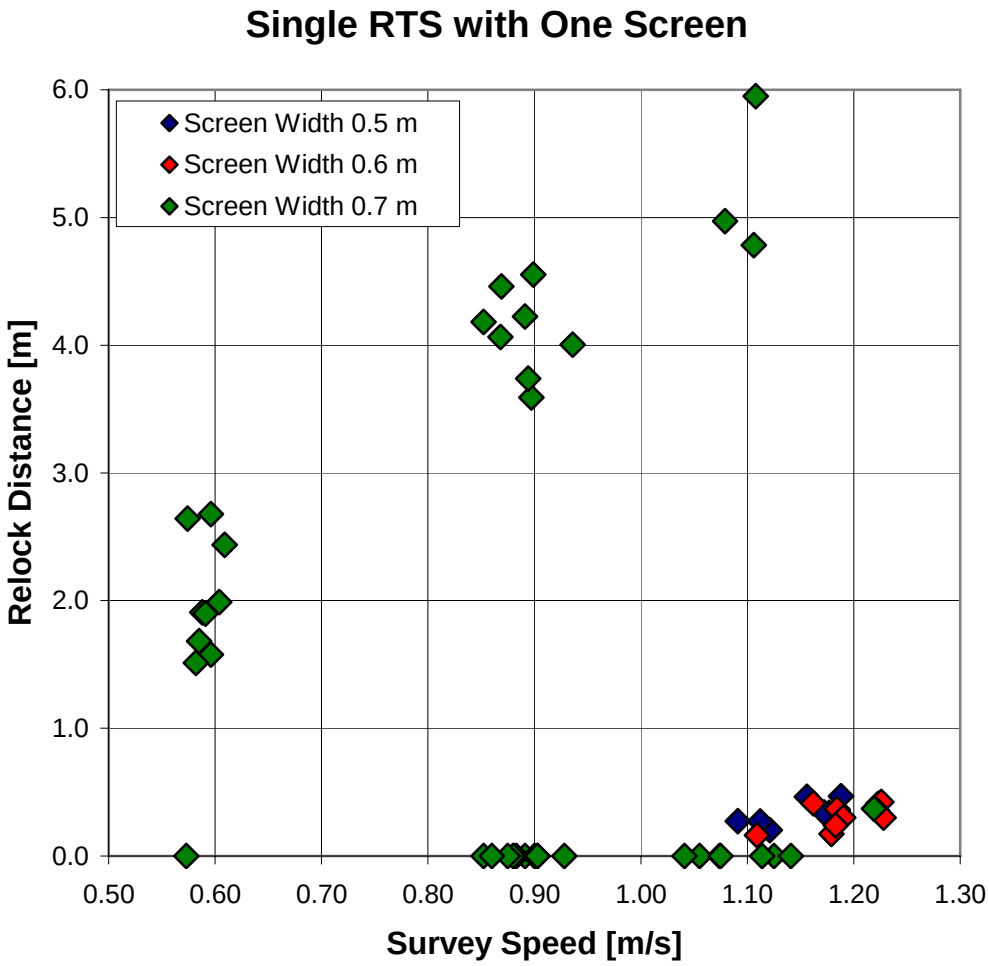

Figure 63. Relock distances for the single screen test reveals as the survey speed increase the relock distance and failure to relock rate increase. The red and blue points show the internal algorithm of the gun relocking on the prism shortly after the prism becomes visible.

4.3.2. Double Screen

Using the results from the single screen test, the screen width and survey speed were set to 0.7 m and 0.5 m/s. This would force the controller software to orient the gun while the speed would let the gun track the prism as it passed through the field-of-view. The distance between the two screens was set to 2.0, 2.5 and 3.0 m. The rational for the 2 m gap was derived from the single screen test where the RTS would typically recover the prism in 2.0 ± 0.4 m.

Figure 64 and Table 8 display the results from the double screen test. The definition of a "complete success" is where the prism moves down the line, obscured by screen 1, emerges and relocked, obscured by screen 2, emerges and relocked. The definition of "missed the gap" is where the prism moves down the line, obscured by screen 1, emerges, obscured by screen 2, emerges and relocked. There the gun did not have enough time to track the prism before being

obscured by screen 2. The definition of "no relock after 2nd screen" is where the prism moves down the line, obscured by screen 1, emerges and relocked, obscured by screen 2, emerges but never relocked. The definition of "complete failure" is where the prism moves down the line, obscured by screen 1, emerges and never locked on again.

Table 8. Results of the Double Screen Test

Test Parameters						
Shadow Size	**Gap Size**	**Survey Speed**	**Complete Success**	**Missed the Gap**	**No Relock After 2nd Screen**	**Complete Failure**
0.7	2.0	0.58	10%	70%	0%	20%
0.7	2.5	0.56	80%	10%	10%	10%
0.7	3.0	0.53	90%	0%	10%	0%
		Totals	50%	38%	5%	13%

From Figure 64, there are three distinct clusters of points. The first cluster at relock distance = 0 is the combination of "missed the gap", "no relock after 2nd screen" and "complete failure". Graphically it is difficult to see which data belong to which category but the complete failures have the diamonds and circles. The second cluster is the middle cluster of points. These points represent a successful completion of the test. The last cluster is made up of points from the "missed the gap" group. These points are primarily diamonds meaning they relate back to the screen 1 relock distances.

The "missed the gap" category is the most significant result from this test. We used the results from the single screen test to set the parameters of the double screen test. Recall from the single screen test, at survey speed 0.59 ± 0.01 m/s the relock distance was 2.04 ± 0.45 m, with 6 of the relock distances falling below 2 m. For the double screen test, 2 of 20 worked correctly, 14 of 20 missed the gap and 4 of 20 failed completely. These results really do not support the single screen test results as we had hoped but provide some insight into the deployment strategy for the Leica instrument in forested environments.

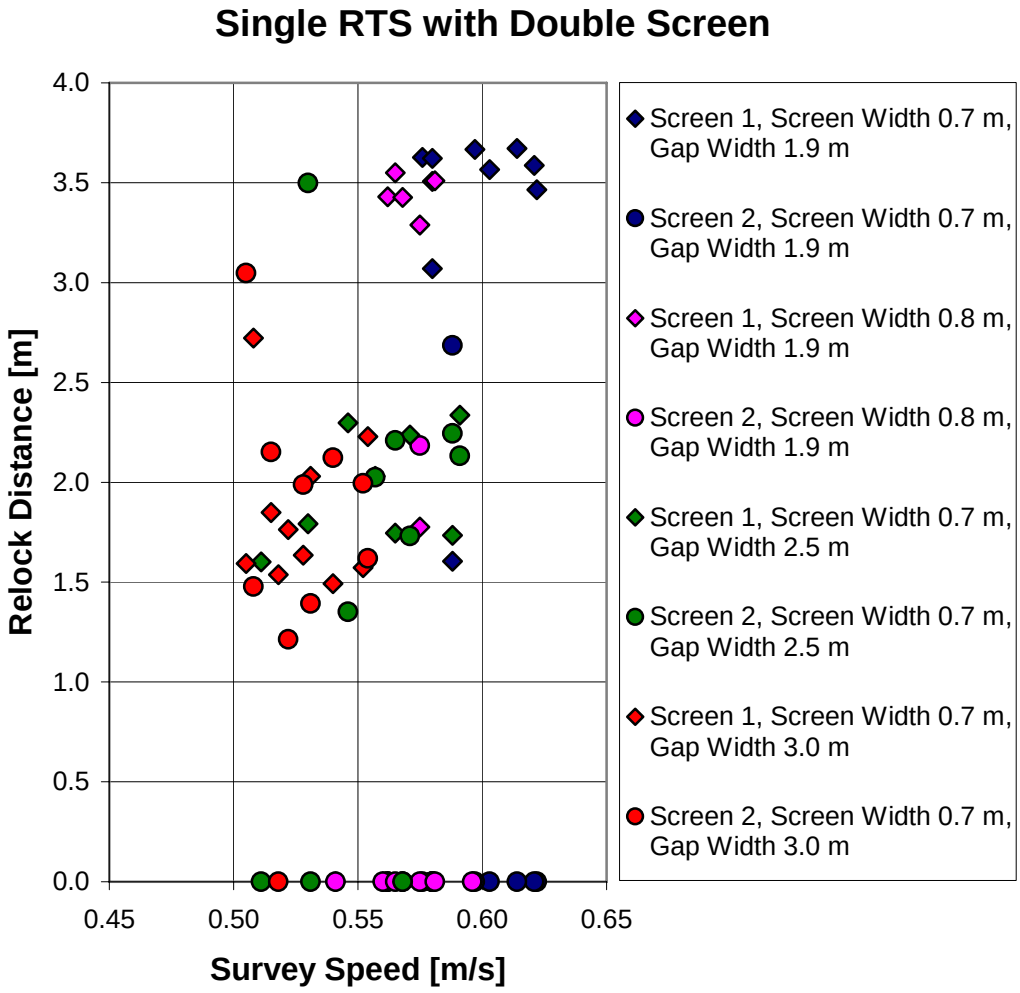

Figure 64. The relock distances for the double screen test. Three point clusters are evident and make up the 4 categories of results.

4.3.3. Alternating Screens

The alternating screen test measures system performance during intermittent line-of-sight for both guns. Two screens were placed 3.0 m apart and located on either side of the main cable. During the test, the prism was traveling at 0.55 m/s, this speed was found from the single screen test to provide the most number of dynamic relocks. The guns encountered the screens 20 times. For half of these encounters, manual pointing of the guns was required to reestablish prism lock. Only during one run did the system perform as expected. Both guns performed equally well regardless of distance to main cable. When prism speed increased to 0.80 m/s, the system achieved 75% reliability for relocking. At this speed the gun is able to predict the position of the gun without assistance from the other gun. As shown in Figure 65, the distance to relock is a function of prism speed; however, for real-world surveys using man-portable platforms higher survey speeds may not be practical. See Appendix A for the tabular results.

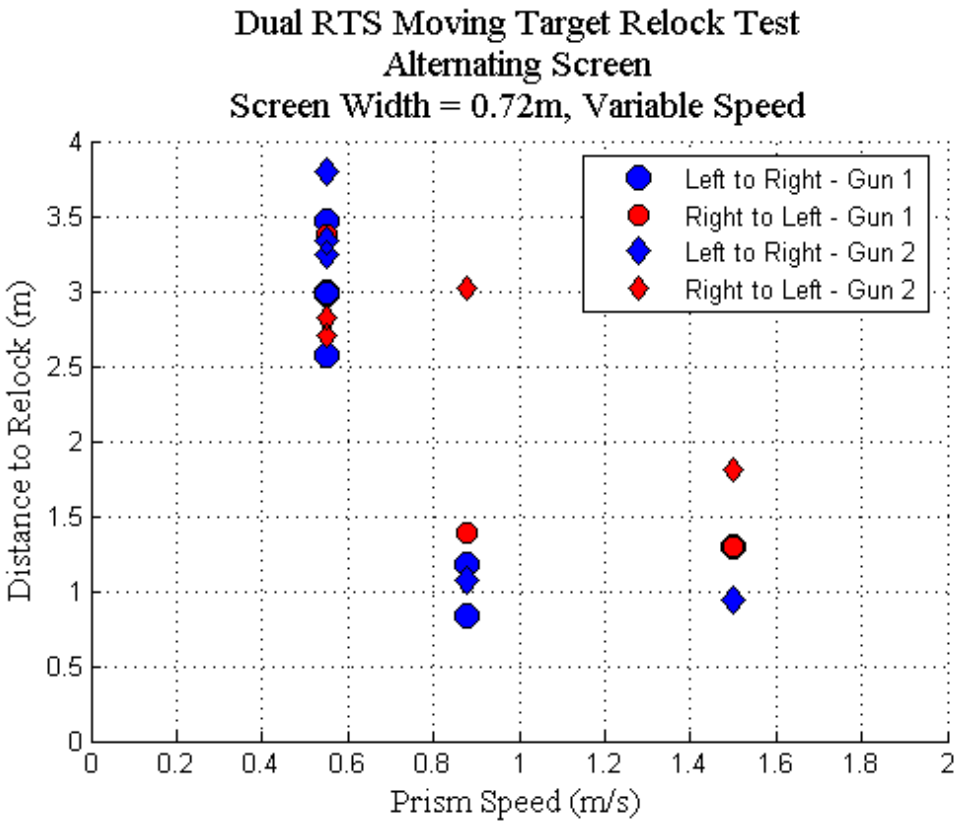

Figure 65. Relock distance for the alternating screen tests. There are two distinct grouping of points. The first grouping is where the gun uses the built-in prediction method to relock. The second group is where the gun uses the system's prediction to relock onto the prism.

These results are disconcerting. The prism was traveling slow enough so the gun could lock onto the moving prism and the distance between the screens was large enough to give the gun ample tracking time between the next to screen to establish lock. Using successful testing conditions from one test did not provide the expected outcome for this test. Only when the prism speed was increased to over 1.0 m/s, an unrealistic survey speed in the woods, did the Leica perform properly. The operation of the Leica appears too unpredictable for use in the field under 3rd party software control.

4.4. Trimble 2007 Tests and Results

When lock is lost due to a line-of-sight obstruction to one of the guns, relock times in the range of 0 to 3 seconds are favorable though the ability to lock onto a moving prism is far more important. In 2007, we shifted from the Leica instrument to the Trimble instrument. The moving target test results of the Leica were the reason for shifting instruments. The Trimble instruments use an active prism as a means of searching for and tracking the prism. The active prism consists of a ring of mirrors and LED. The LED flashes infrared light that the Trimble sees.

The relock tests are conducted using one or two screens. The general methodology for setting up the screens for both the single and double screen tests are as follows: two guns will be set up 30 m away from either end of a survey line and screens will be set up 1 to 2 m from the survey line midpoint. Each test using a prescribed screen width and survey speed repeated 5 times in both directions resulting 10 passes.

4.4.1. Trimble ATS600 Results

4.4.1.1. Single Screen

Figure 66 shows the relock times for the Trimble ATS600 single screen test. Each colored marker represents the 4 different survey speeds while the X-axis displays the different screen widths used. Most noticeable from the plot is the 3 distinct zones of times. The most surprising cluster is the data right above 0 s. This cluster represents a unique condition where the gun locked onto the prism right after it emerged from the screen. The second cluster, around 0.6 s, is the typical operation of the gun. This is the typical response time for the gun to realign the lock on the prism after emerging from behind the screen. The third cluster, around 3.0 s, shows the operation of the gun under control of the controller software. These data are inline with the performance of the software. There are no lock failures in these tests; this means the gun is locking onto the prism on the first try. The tabular test data are summarized in Appendix A.

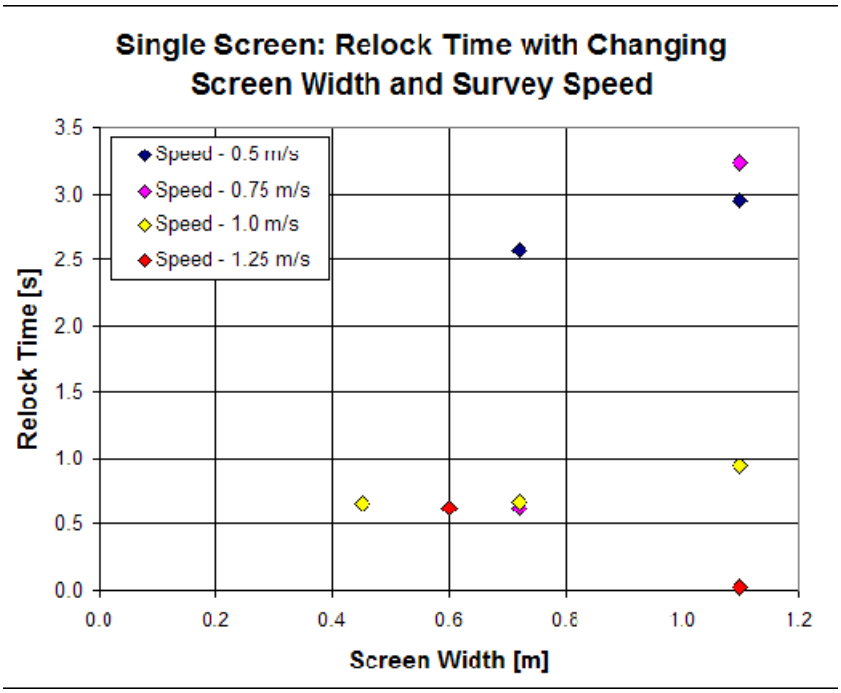

Figure 66. Results of Trimble ATS600 single screen test.

4.4.1.2. Double Screen

Figure 67 show the results of the double screen test with the X-axis displaying the survey speed, the Y-axis showing the relock time and the different markers showing the screen number. The width of the screen and the survey speed forces the ATS600 to use the multi-gun control software to locate the prism. The gun needs approximately 2.7 seconds to locate, track and measure prism locations. The single screen test supports the results from this double screen test. Tabular test data are summarized in Appendix A.

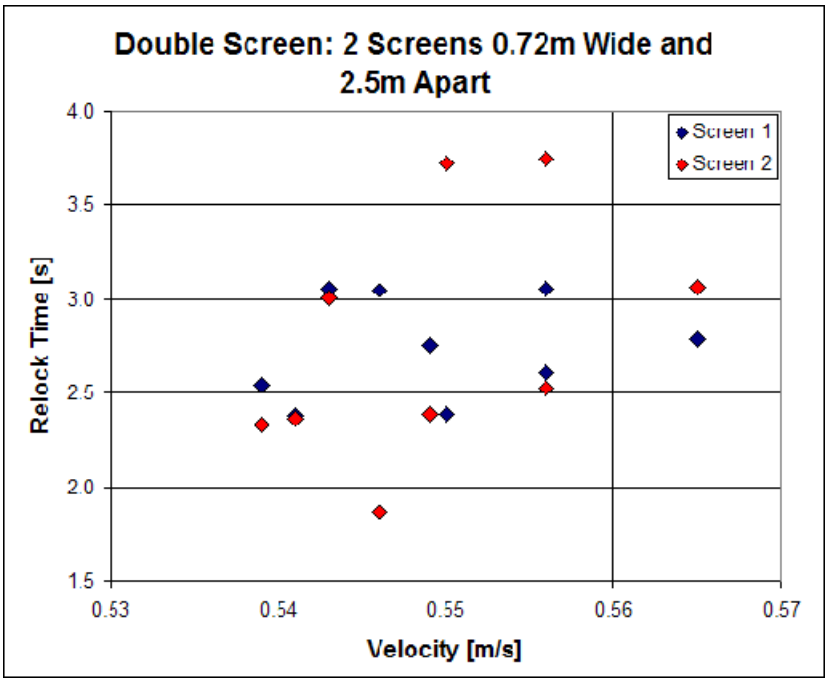

Figure 67. Results of Trimble ATS600 double screen test.

4.4.1.3. Alternating Screen

Figure 68 shows the results of the relock test for the Trimble ATS600. It is clear from the figure that there are 2 clusters of data. The first cluster represents the gun controlling itself with the internal algorithm and the relock times are around 0.6 s. The second cluster, around 2.5 s, is when the multi-gun control software assumes control of the gun to find the prism. The 2.5 s range is typical control software operation time. Tabular test data are summarized in Appendix A.

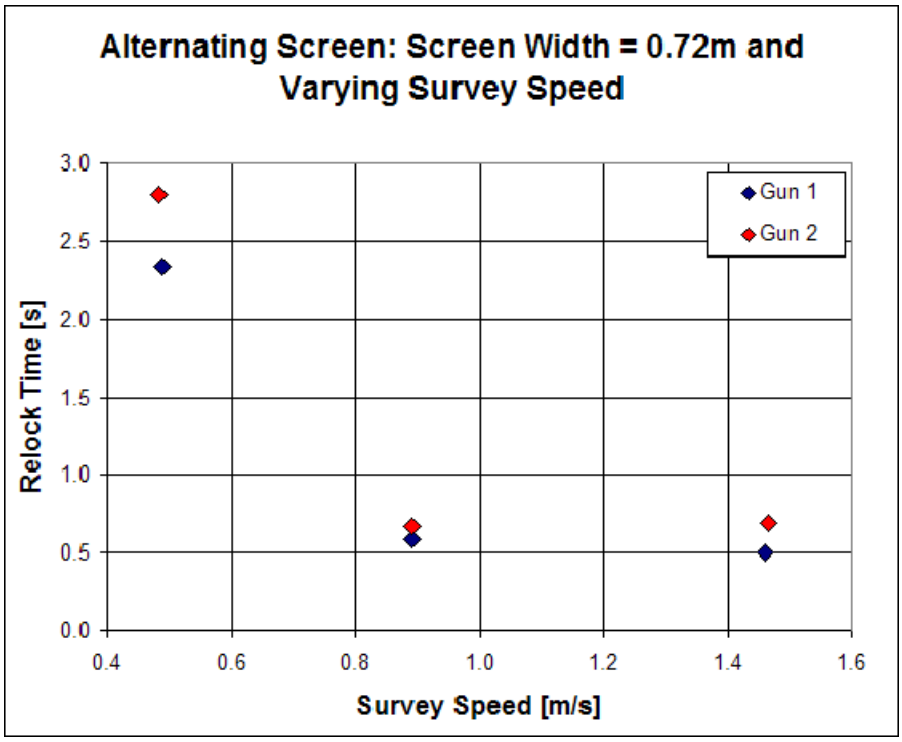

Figure 68. Results of Trimble ATS600 alternating screen test.

4.4.2. Trimble SPS930 Results

4.4.2.1. Single Screen

Figure 69 shows the relock times for the Trimble SPS930 single screen test. Each colored marker represents the 4 different survey speeds while the X-axis displays the 3 different screen widths used. There is an increasing linear trend of the relock time as the screen width increases. According to the data, for every 1 m of increased screen width the gun takes approximately 0.1 second longer to establish lock. At the 3 m screen width, the relock times become highly variable. The standard deviation of the relock time is slightly more than double that for the other tests and appears to be a hardware limitation. As the prism speed increases, the gun is turning faster angles and the subtle adjustments to fine tune the lock takes just a little bit longer. Tabular test data are summarized in Appendix A.

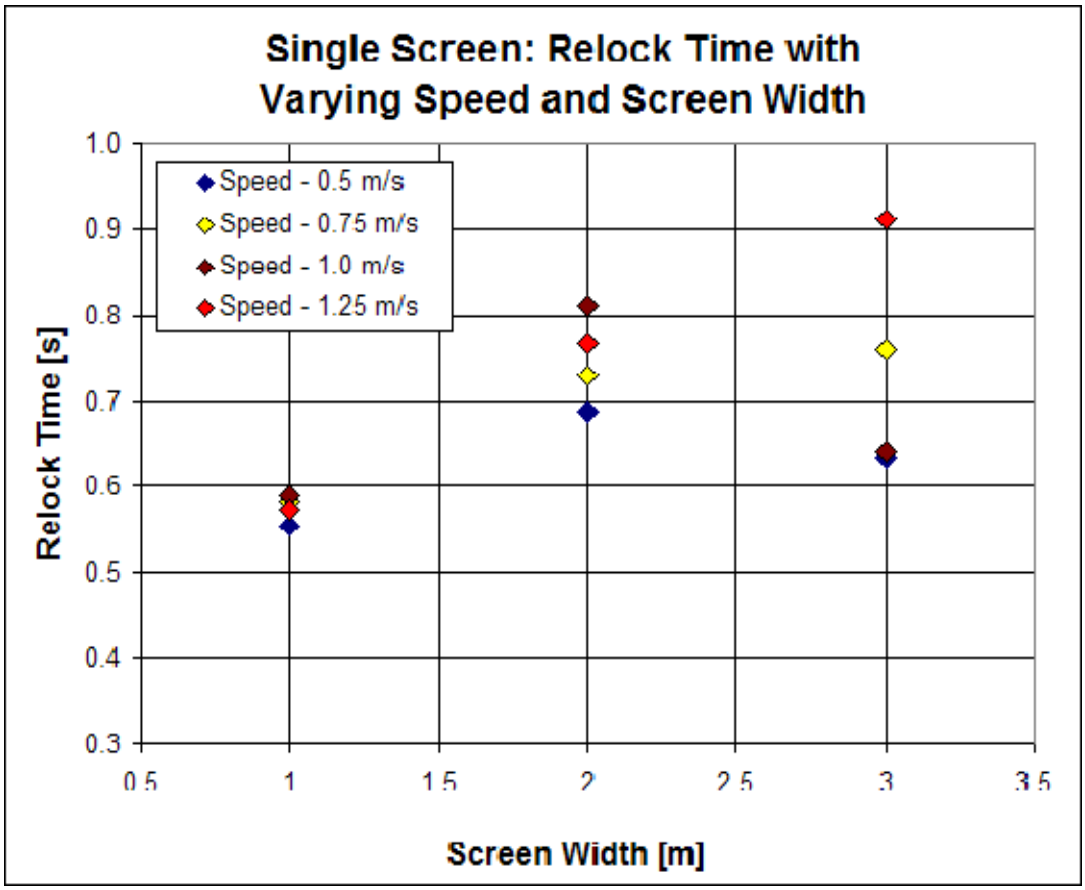

Figure 69. Results of Trimble SPS930 single screen test.

4.4.2.2. Double Screen

Figure 70 shows the relock times for the Trimble SPS930 double screen test. The relock times for these tests cluster around 0.75 second regardless of speed. When the width between the screens decreases and the survey speed increases, the amount of time the prism spends in the gap area decreases and the gun cannot fine tune the lock onto the prism. This explains the 0.0 and 0.1 second relock time for the 0.5 m gap width. The prism traversed the gap so quickly the gun could not fine tune the prism lock enough to measure the position before the prism moved behind the other screen, this is the cause for the 0.0 second relock time for screen one. When the prism emerged from the second screen, the relock is 0.1 second. At this speed and with this gap size this survey configuration shows a complete failure of the system to effectively operate. Staying with this configuration, it is clear that surveying slower is better. The Trimble SPS930 - Double Screen Summary table in Appendix A shows that with the prism moving at 0.75 and 1.0 m/s the gap was missed 5 of 10 times and 6 of 10 times, respectively. These test parameters result in less than optimal site conditions. Tabular test data are summarized in Appendix A.

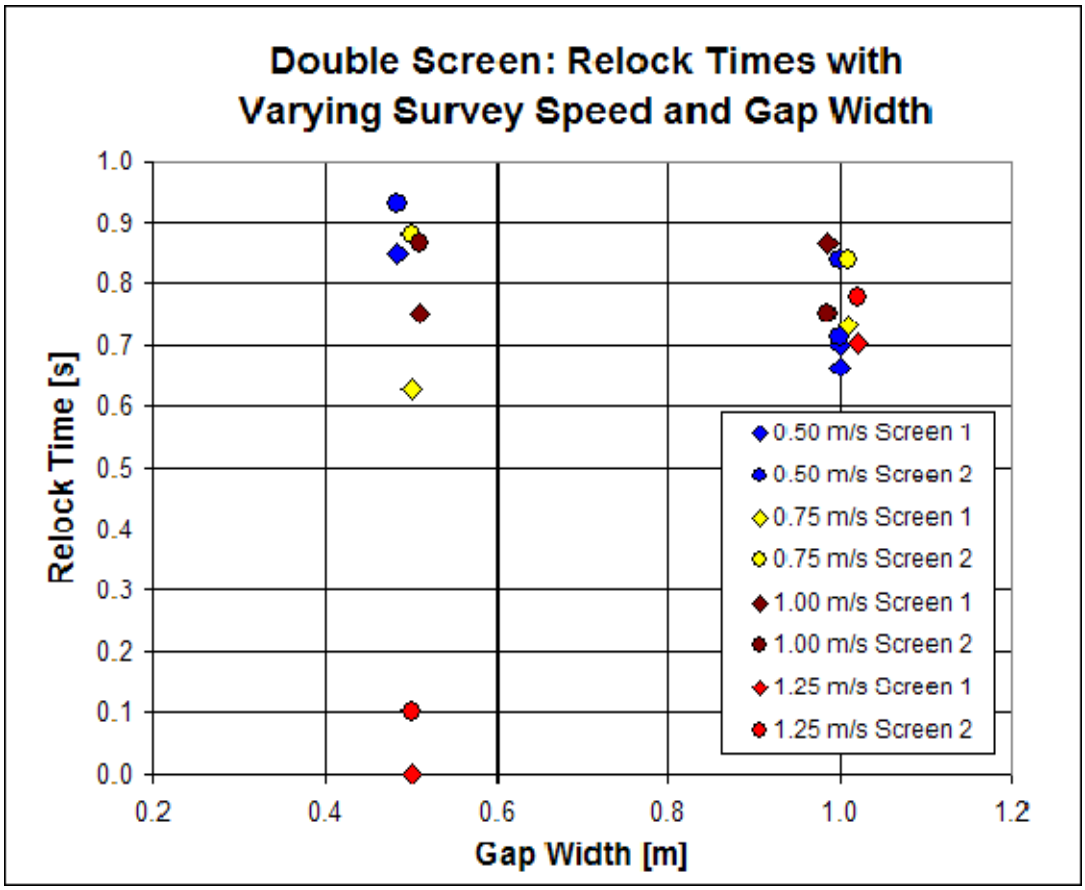

Figure 70. Results of Trimble SPS930 double screen test.

4.5. Discussion

The built-in tracking capabilities of the Leica have been investigated and found to be remarkable. However, programmatic control of the Leica proved problematic and inconsistent. Initial tests of the system identified several limitations including issues related to relock.

Additional testing of the firmware resulted in a greater understanding of the commands controlling critical functions of the system. These tests also provided more information on the working of the Leica system, including the need to access the Leica firmware to further develop the dual gun system sufficiently to meet the project objectives.

Additionally, discussions were initiated with Leica to gain access to the firmware involved with the commands in order to correct the problems that are resulting in the system reliability issues. However, Leica support staff were unable to provide access to the firmware in a timeframe suitable for the project.

Therefore, to address the possible barrier to successful Leica technology modification, a discussion was initiated with Trimble regarding their RTS technology. While both Trimble and Leica are making continual improvements with the RTS technology, as demands for precision

tracking are emerging in several construction applications, Trimble was more supportive and available to work with us on this project.

The Trimble unit represents the latest advancement in RTS technology, and presented a superior capability – relative to the present Leica system. In particular, two aspects of the newest Trimble technology are relevant to the multiple-gun tracking problem. First, Trimble employed innovative motor-control technology that allows for more precise timing of position solutions. The specification of the variability of the delay-time of the receipt of the solution is approximately 1 ms, a significant improvement to the Leica. Second, the Trimble system provided positioning solutions at a stable 10 Hz.

The relock time measures the hardware's ability to establish lock on the prism after it emerges from behind a screen. The moving target test measures this crucial time using very repeatable methods. All the guns are able to anticipate the prism's location for a given length of time after obscuring the line-of-sight. The guns perform this by using the prism's velocity just before the obstruction to maintain the gun's angular velocity while looking for the prism. The ActionTarget system moves the prism with a very consistent velocity down the cable. During a real world survey, ground coupling through wheels or body movements will create small velocity changes making it harder for the gun to anticipate where the prism will be n-seconds after losing lock.

The internal searching algorithm works well for these tests but the practicality of the algorithm has yet to be proven in the forested domain. The shadows zones of trees close to the gun become large the farther away from the gun. It is here where the internal algorithm may fail and the controller software will prove its usefulness. Currently, the software points the gun to some location n-seconds ahead of the prism. In the forest environment, this may not work effectively since the gun could be pointing to another shadow zone. To mitigate this effect, there has been a discussion about integrating the line-of-sight model into the controller software. This integration will allow the software to find the optimal spot to point the gun to track the prism as it emerges from the shadow zone.

From all the testing performed on the dual gun system, several conclusions were drawn:

- Multiple guns can track a single prism, which provide the basis of more robust digital geophysical mapping in wooded environments.
- Multiple-gun tracking can be performed using both internal tracking functions on the Leica and Trimble units and using Prism Tracker software developed under this project. The Prism Tracker software extends the functionality of the internal search function by using the prism location derived from the other gun.
- When LOS is lost by gun 1, prism location information from gun 2 can be used to point gun 1 and relock onto the prism.
- The time to reacquire lock on an obscured prism is based on the speed of prism, firmware command response times, and user set search parameters for the internal algorithms.
- Relock after the prism is obscured is immediate if the prism remains in the field of view of the gun. The field of view is dependent on the distance between the gun and prism.
- Average relock times of must be less than 5 seconds to make the system usable for real-world surveying deployments.

4.6. Forest Testing 2008

One of the main objectives of this project is to improve sensor positioning capabilities during wooded surveys. To achieve this objective, the Trimble SPS930 and Prism Tracker software were deployed to a wooded site in Kerby, OR. Kerby was chosen because of site access and the forest was primarily comprised of ponderosa pine with few or no branches up to 2 m. The Prism Tracker software, designed by SPEC, was updated to interface with the new Trimble hardware.

4.6.1. Methods

The purpose of this test was to assess the ability of the two SPS930 guns to track a prism as it moves through a forested site. The intermittent line-of-sight between the gun and prism makes positioning difficult. The site measured about 33 m × 33 m and contained 125 trees (Figure 71). The different tree densities made some areas more difficult to survey than other areas, which is typical of wooded environments.

The tree positions were surveyed using a Leica TPS1200 and radii were measured with a measuring tape were entered into the LOS model (see section 5 for LOS model discussion). The LOS model calculated the optimal positions for two opposed guns on the edge of a site by minimizing the shadow areas. Shadow areas are areas where the gun cannot see the prism because a tree trunk blocks the line-of-sight. The LOS model calculates the shadow areas for each tree by calculating the two tangent points between the gun and tree trunk then extending a line to the edge of the model's domain. The optimal locations were (26, 0) and (33, 36). Other positions were slightly better but one condition for the Prism Tracker software is both guns need to see each other.

As the guns tracked and measured prism positions this information was recorded by the Prism Tracker software and displayed on the screen. The software monitored the status of the gun by checking the status field in the data stream. When either gun lost sight of the prism the software would alert which gun lost sight and what the software was doing to regain lock. The software has a predetermined time-out period before assuming control of the gun. The gun's internal algorithm was found to be very quick in determining the prism location so this time-out period allowed the gun to perform its searching before the software assumed control.

To test the performance of the SPS930 and the Prism Tracker software, the prism started at one end of the site, where both guns had lock and then was moved across the site to the other end. Walking speed was kept between 0.5 and 0.75 m/s and the prism was held still to make the movement across the site as smooth as possible. The entire site was not traversed because tree density was higher at one end of the site compared to the other and tracking would be next to impossible. We had intended to traverse the entire site but after observing the behavior of the system in the more densely treed areas it was decided to stick to the less dense areas. Also the survey lines were kept in the middle of the site to give both guns equal opportunity to track the prism.

4.6.2. Results

Figure 71 shows the results of the first survey transect overlaid with the LOS model results. There is a good correlation to the shadows areas calculated by the model and the gaps in the survey positions. There are some places where there are points inside of a shadow area. This is caused by the discrete boxes of the model space. Also the rotations and translations performed to move the data into the model's local coordinate systems are not exact. Again this is caused by the discrete nature of the model. The survey transect start point is on the east side.

During testing, it was noticed that the Prism Tracker software did not take control of gun 1 but allowed the gun's internal search algorithm to control the gun. However, Prism Tracker assumed control of gun 2 at position (23, 10) and lock was regained at position (16, 10). The reason for the large gap in positioning was the software pointed gun 2 to a location where the prism was in a gun 2 shadow and needed to recalculate a new position and point the gun to the new location. Between (15, 10) and (7, 10), gun 2 travels through an intermittent line-of-sight area and while gun 2 is tracking the glow of the active prism the gun is unable to find tune the lock and measure the distance.

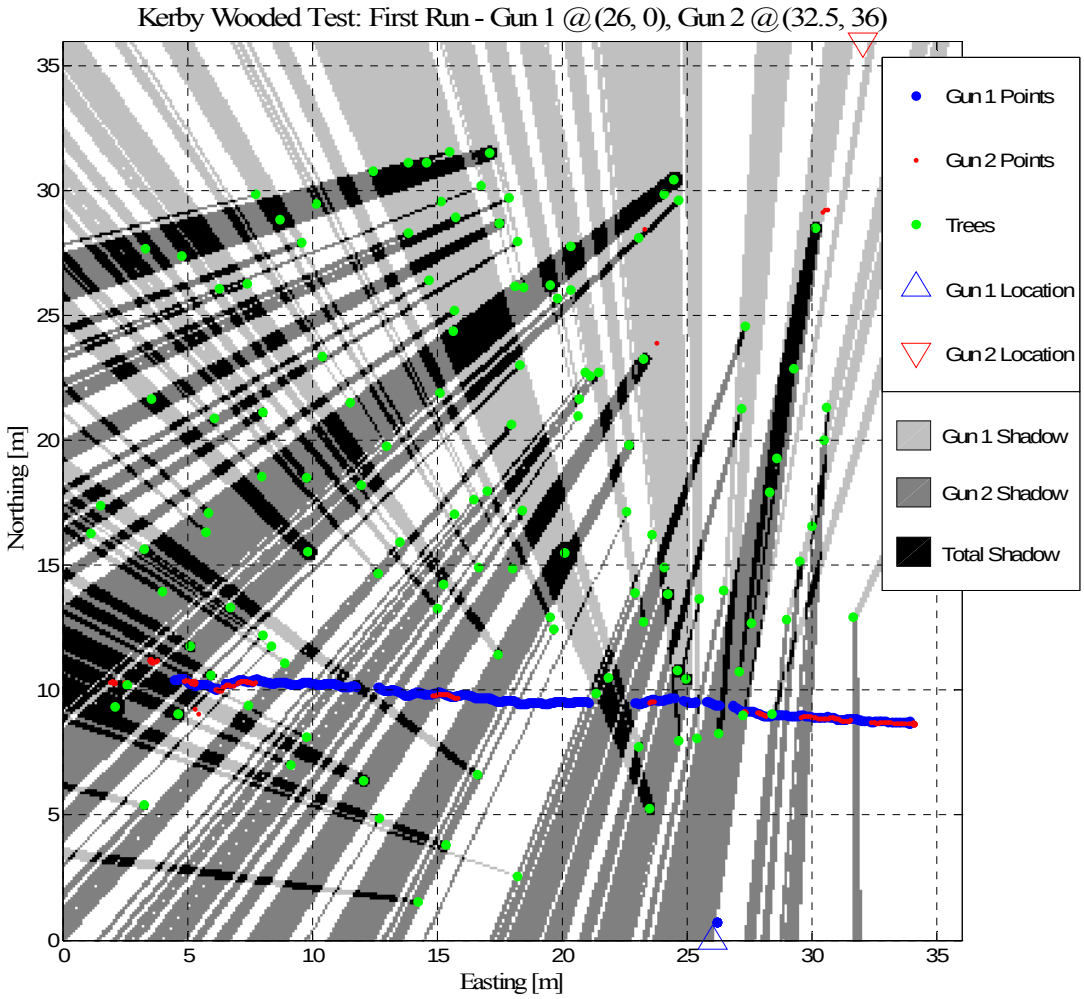

Figure 71. The results from the first survey with the shadow zones as calculated from the LOS model.

Under some conditions both guns would lose lock. When this happens the prism must be moved to a location where one or both guns can see the prism and lock can be reestablished. This occurrence can be seen at position (17, 17). Here the prism travels through a large flip-flop of gun 1 and gun 2 shadows and neither gun is able to effectively track the prism. The prism was stopped near (17, 17) and lock established. From there, the prism continued to travel to the west and gun 2 loses lock after the prism moves through a series of shadows. Even after an extended "open area" gun 2 cannot lock onto the prism. The prism travels through a large gun 2 shadow then stops where lock was manually established.

During the testing the SPS930 would occasionally lock-up and refuse to accept any commands and the system would have to be rebooted. This was either a glitch in the firmware or a programming problem in the tracker software. It is more likely a firmware glitch than a

programming problem because the program sends commands and waits for responses. During the lock-up, the gun would track the prism but would not record positions, even after repeated attempts to start position measurements. These lock-ups occurred on both SPS930 units but more frequently occurred on gun 2. It is our opinion that gun 2 experienced more frequent lock-ups because it was experiencing a more intermittent line-of-sight during the testing.

Table 9 summarizes the percentage of the path that had measured positions with the lower percentages reflecting areas where the gun is unable to record the prism position. Run 1 has the highest percentage for gun 1 and the lowest for gun 2 and the cause for this is the prism was much closer to gun 1 than gun 2. Figure 72 shows the positions for run 2 against the model results and the prism as it traveled from close to gun 1 northward toward gun 2. It is not surprising to see that as the prism paths move farther northward the number of positions from gun 1 start to decrease. The coverage from gun 2 increases slightly but there is a higher density of trees in the northern part of the site than the southern which is responsible for the lopsided results.

Table 9. Percentage of Path Surveyed

Run #	% of Path Surveyed	
	Gun 1	Gun 2
1	88.7	20.9
2	50.7	28.8
3	35.4	32.6
4	60.1	36.5

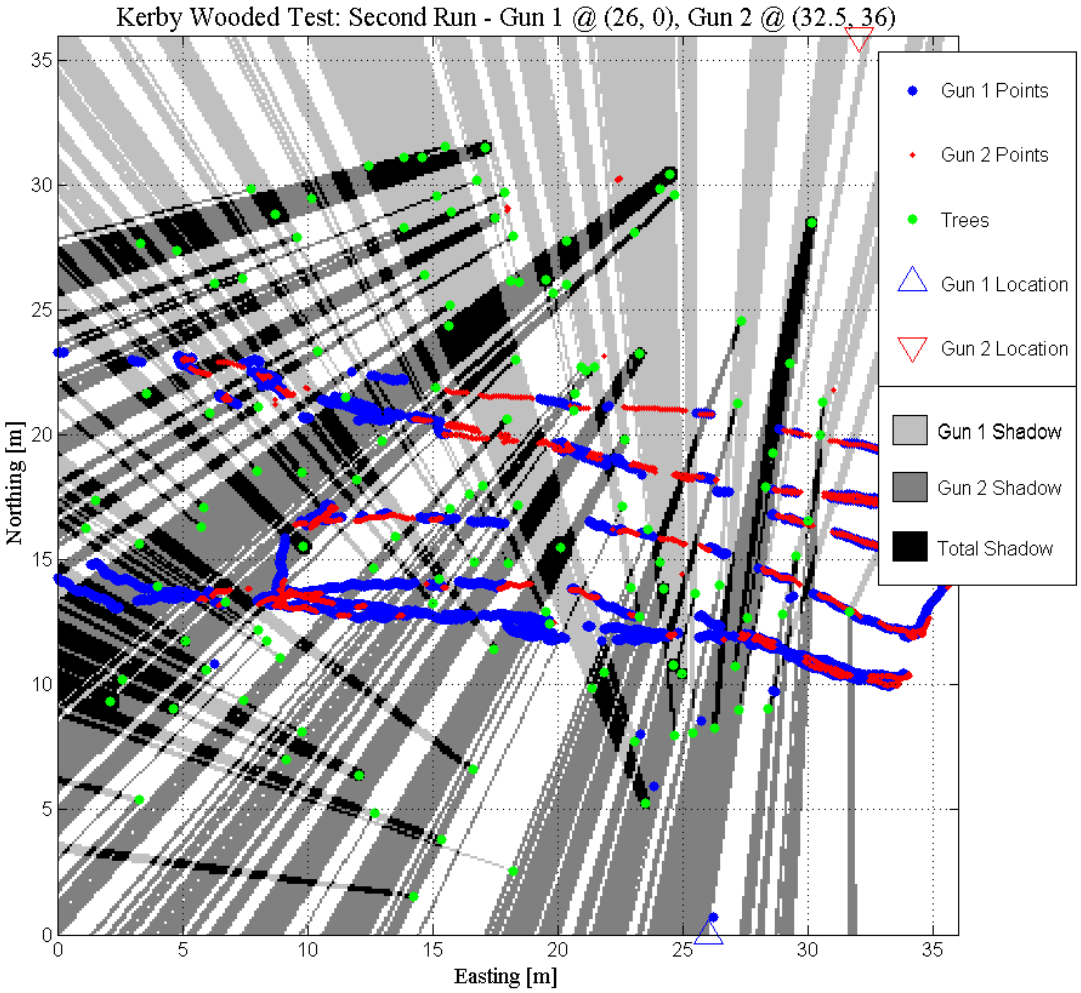

Figure 72. The results from the second survey with the shadow zones as calculated from the LOS model.

Figure 73 shows the results from the third survey. These paths were mostly in the center of the site and the results shown in Table 9 show a near equal performance of the two guns. When comparing the images from run 2 and 3, which have paths that are close together, it can be seen the gun's performance is nearly the same. The northern track from both runs has very consistent results for gun 2. However, during run three gun 1 tracks the prism as it travels west to east until the prism reaches position (27, 20) and does not recover until the prism stops moving at the end of the line. The results for the southern pass of run 3 for gun one has a consistent result with run 2. Gun 2 results for the southern pass are not all that spectacular and show a bad performance. Gun 2 on the eastern path locked up and required a reboot.

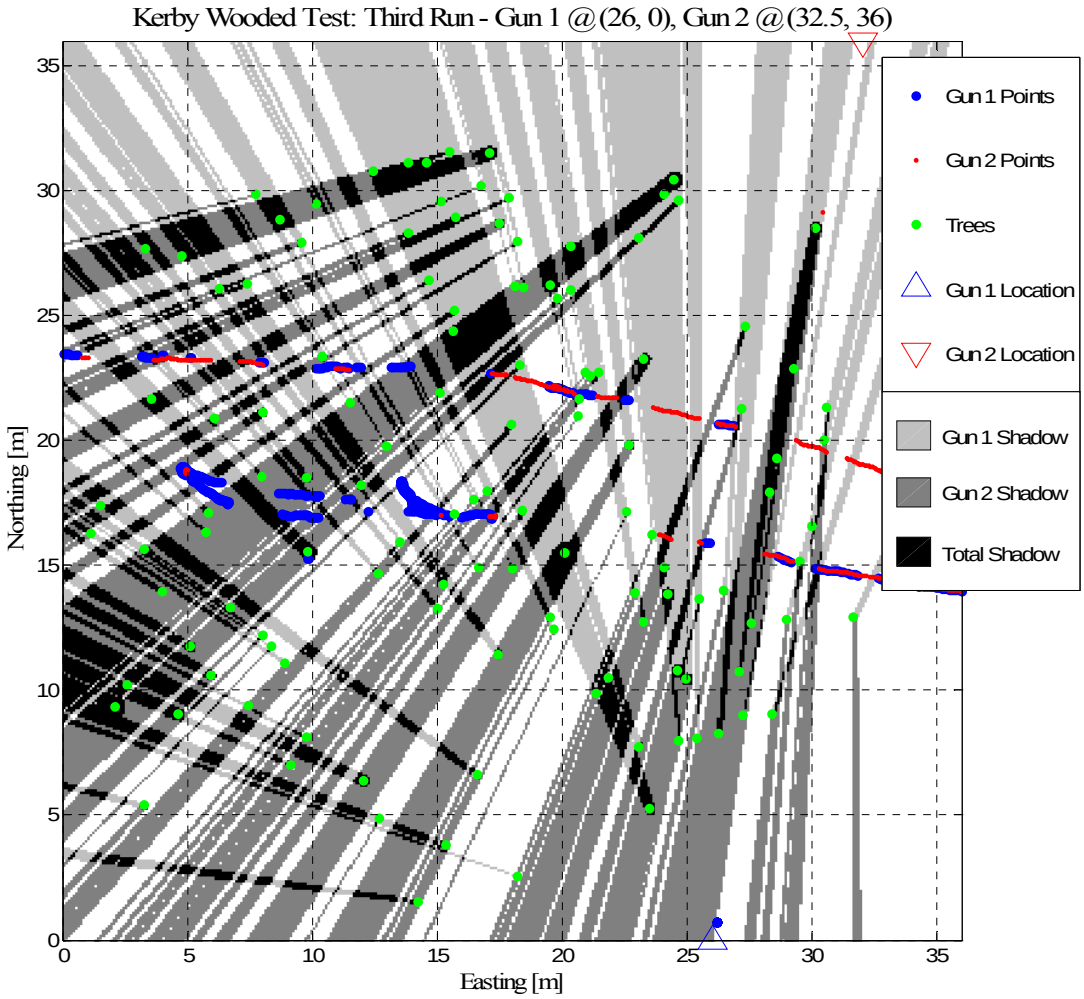

Figure 73. The results from the third survey with the shadow zones as calculated from the LOS model.

Figure 74 shows the results from the fourth survey. The southern passes for gun 2 had degraded performance because of the number of shadow areas. During the last pass, which travels from west to east, gun 2 loses the prism at (11, 14) and never recovers because it locked up and required a reboot.

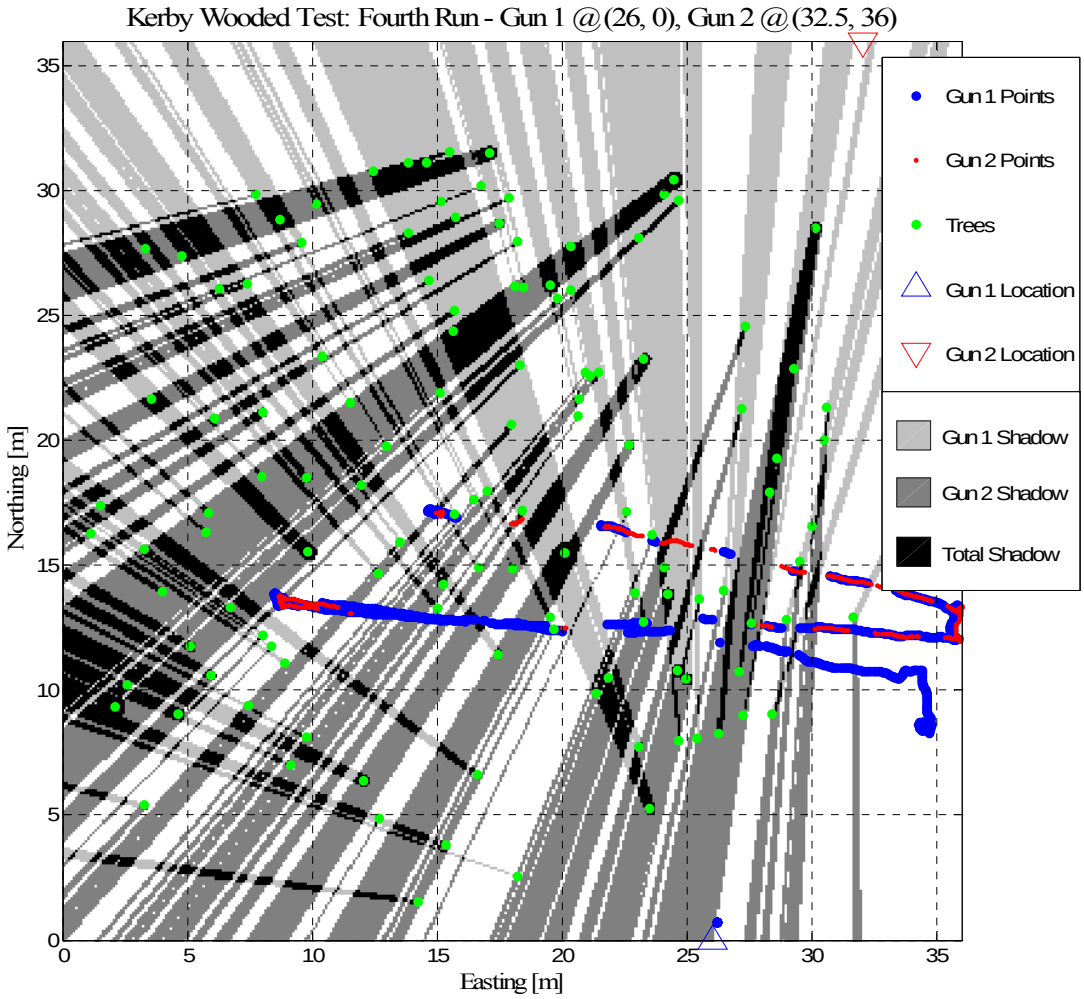

Figure 74. The results from the fourth survey with the shadow zones as calculated from the LOS model.

4.6.3. Discussion

After reviewing all the data from these tests, there is something very important to learn about the limitations of the system and the types of environments in which the system will work. Looking back at all the results it is clear that gun 1 performed the best. This is mostly because the tree density was higher to the north. In the midsection of the site the performance of each gun was nearly equal. As illustrated in Table 10, as the distance between gun and prism increases, the percentage of the site seen decreases. At around 20 m in northing, the percentage of the 'seen' site is nearly equal for both guns. Here with 60% of the site 'seen', the guns had a 50% effective positioning capability. This number may seem a little low, but when considering all the small trees and gaps, the gun is able to track the prism through the trees but not able to measure distances because the lock on prism is not fine-tuned enough for EDM operations. During the

first run, when the prism was closest to gun 1, the percentage of the site surveyed was 88% with 76% of the site 'seen' by gun 1. The percent of the path surveyed is higher than the site seen because the entire site was not surveyed. Between (0, 10) and (5, 10) the site is for the most part a shadow. After adjusting the percentage of site seen for along the path, the numbers fall in line with 90% of the site seen and 88% of the path surveyed. Comparing with the numbers from gun 2, the system is on target with 50% effectiveness.

Table 10. Percentage of Site Seen By Each Gun at Different Northing

Y Distance	% of Site Seen	
	Gun 1	Gun 2
5	96.1	47.4
10	76.2	46.8
15	71.1	54.1
20	59.4	61.4
25	47.6	70.3
30	39.1	83.5

Some work can be done to increase the effectiveness of the system. By using the model results to aid in the positioning when the line-of-sight is obscured, the Prism Tracker software can better select an orientation to point the gun to wait for the prism to emerge from the shadow. This would eliminate the need for the software to blindly point the gun to a position where there is a shadow. However, this would not correct the problem when many small shadows exist, making tracking possible but distance measurements impossible.

The site was extremely challenging for a first time run. The system performed quite well given the number of trees. It is recommended that the system not be deployed to a site with more than 6 trees per 25 m^2 area (2400 trees/hectare) at a distance of no more than 30 m between gun and tree and tree diameter should not exceed 8 inches in radius. This appears to be the maximum tree density the system can handle because the shadow zone becomes too large for the system to work optimally (Figure 75).

The software for Prism Tracker and the SPS930 were both essentially beta-versions. The Prism Tracker could have more robust error and status checking subroutines to deal with problems in communication with the SPS930. The SPS930 could have firmware glitches that the hardware engineers did not anticipate. The SPS930 is not designed to work in an environment like the one to which we surveyed. It is designed to work on a construction site where the line-of-sight is obscured for a couple of seconds as a piece of heavy machinery passes by.

The Prism Tracker software has a number of limitations that prevented it from being ready for true field deployments, but it is a good first round piece of software. The biggest issue is the software records all the data in local coordinates and lacks projected coordinates support. In this test, the guns were offset by 10° in azimuth but the software collected the data as if the guns were on the north-south line (0° offset). It would have been beneficial if the guns could have been setup on a known point then back-sighted to another known point to establish the correct coordinate system. The voiced feedback from the software was a nice addition and could be

easily amplified to allow the person at the prism to move in the correct direction to reestablish lock after an extended LOS interruption.

Even with the occasional lock-up, the SPS930 performed very well. With the faster sampling rate and more stable sample timing, the active prism and SPS930 are a significant improvement over the passive prism and the Leica TPS series.

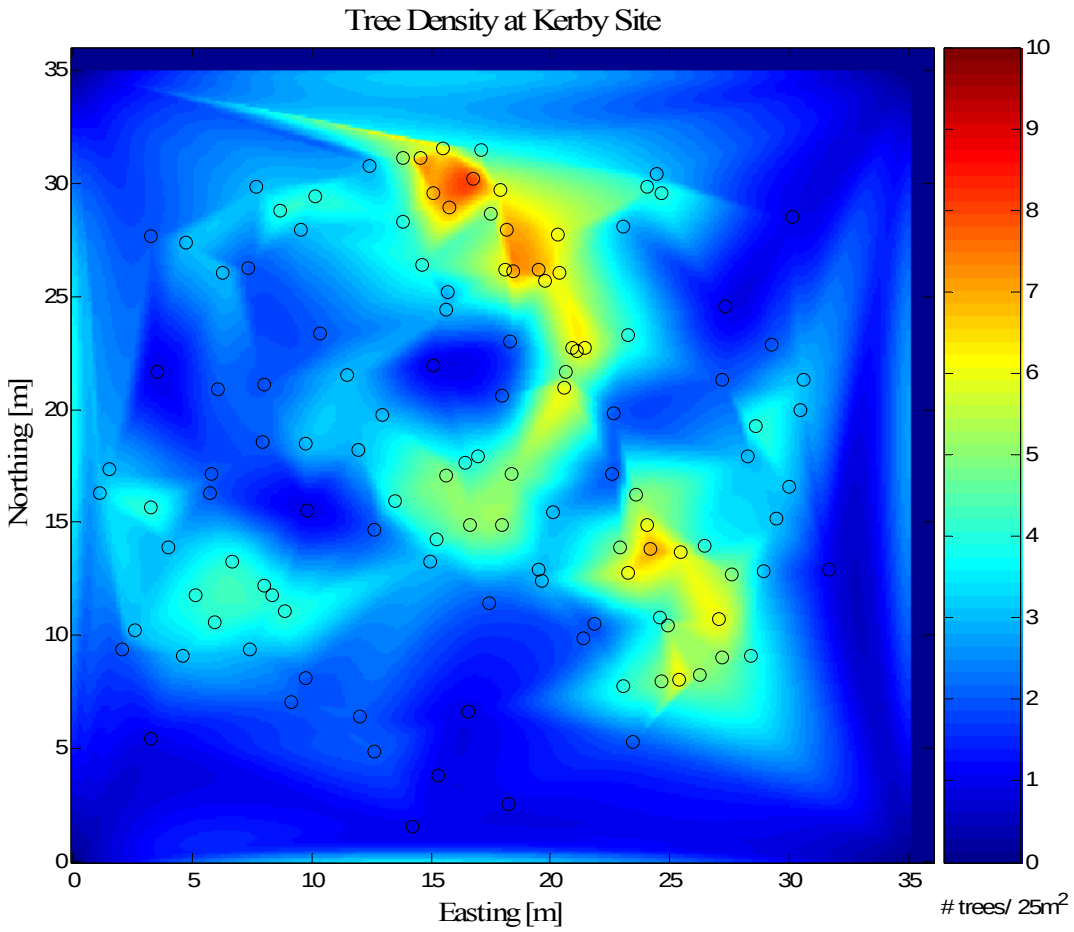

Figure 75. Tree density at the Kerby site. The ideal tree density should be no more than 6 trees/25 m^2.

5. LINE OF SIGHT MODELING

There are many challenges to surveying a wooded environment with a line-of-sight instrument; the most important one can be stated in a question. "Where does line-of-sight exist?" The LOS answers that question. The LOS model finds the optimal location for two guns on the parallel sides of a survey area and can predict the areas where the surveyor will expect to find problems. The LOS model uses instrument parameters (e.g., relock time), survey speed, tree locations and tree size to find the best gun locations to optimize instrument line-of-sight.

5.1. Methods

The model calculates the shadow zones using the locations, angles and distances between the gun and tree edges. Using the survey speed and survey direction, the one-dimensional shadow distance, typically across the shadow in the survey direction, are converted to time. Many of the gun's parameter use a time unit so it makes sense to convert the model to a time base. The model accepts gun specific parameters such as lose lock and relock time to calculate the trouble spots. Laser-based positioning systems account for intermittent prism loss by guessing the prism location based on the last couple seconds of velocity information. The gun will continue "tracking" for some user definable length of time in the hope that the prism will reappear. This time is called the Lose Lock Time. The range of the Leica's Lose Lock Time was between 0 and 3 seconds, ATS600 is around 1 second and the Trimble SPS930 is user defined between 0 to 10 seconds. Relock Time has two definitions:

1. The time used by the multi-gun control software to assume control of the gun, position the gun, regain prism lock, and make the first good position measurement.
2. The time when the prism emerges from the screen to the time of the first good measurement.

With the parameters listed above the model is able to calculate regions of prism state. The model has 6 prism lock states which are described below:

1. Seen by Both – All guns see the prism
2. Not Seen by Gun 1 – Prism is in a shadow zone for gun-1
3. Not Seen by Gun 2 – Prism is in a shadow zone for gun-2
4. Not Seen by Both – Prism is in a shadow zone for all guns
5. Gun Relocking Mode – One of the guns is relocking onto the prism
6. Manual Relock Mode – A condition exists where both guns lost lock and manual intervention is needed to establish lock.

Manual Relock Mode occurs when the prism is obscured from both guns for longer than the Lose Lock Time or when the prism travels from a gun-1 shadow zone into a gun-2 shadow zone without sufficient time for gun-1 to lock onto the prism.

5.2. Results

Figure 76 shows the results of the model for an arbitrarily wooded site with inputs of 5 seconds, 0.5 m/s and 3 seconds for the relock time, survey speed and lose lock time, respectively. For this tree configuration the optimal location for gun-1 is (52, 0) and for gun-2 is (27, 60). Initially, both guns see 47% of the site with 20% of the site in the gun-1 shadow zone and 27% of the site in the gun-2 shadow zone while 3% of the site is a combination of trees and complete shadow areas. After using the hardware parameters the area seen by both guns is reduced to 35% with a 2 second relock time and 14% with an 8 second relock time. The shorter the relock time the more stable the system. The manual relock area comprises 2% of the site. This number is misleading because the model assumes straight line paths instead of preferred pathways. For example, the model surveys through a tree where in real-life the preferred pathway would be around a tree and decided in the field and based on gun location.

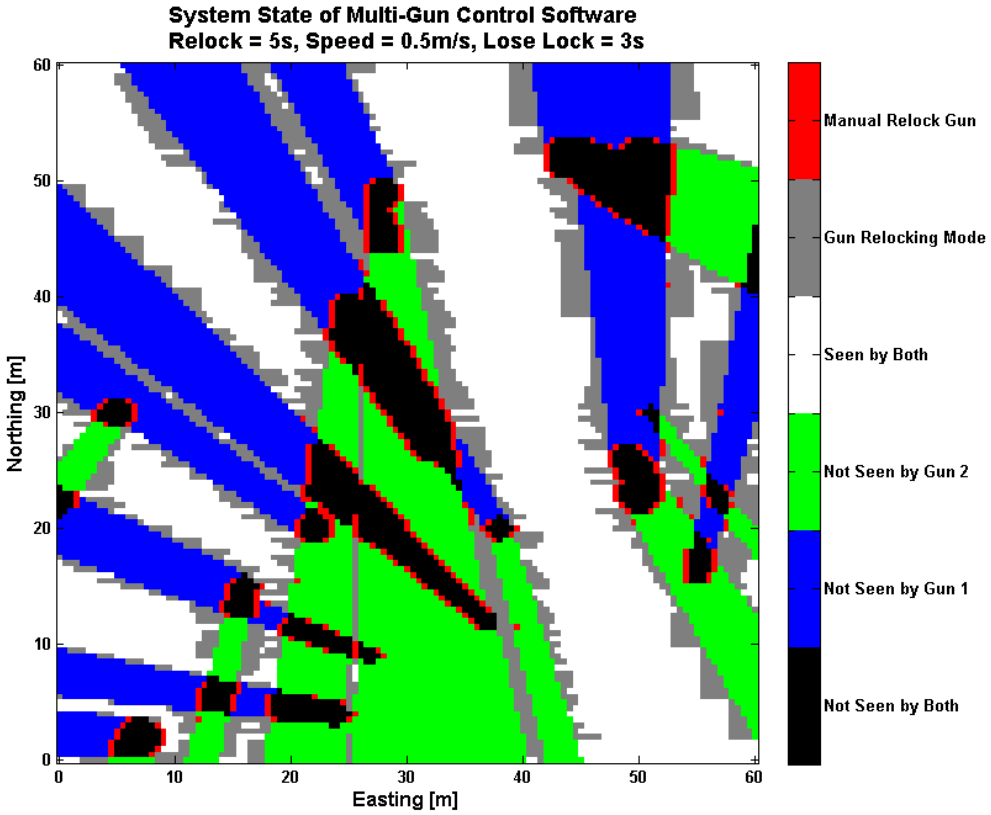

Figure 76. Results from the LOS model showing the predicted gun state for a 5 second relock time, 3 second lose lock time and a 0.5 m/s prism speed.

5.3. Discussion

Figure 77 shows how the relock mode area changes with changing survey speed and relock mode. The SPS930 performed with a 1% to 10% relock mode area depending on survey speed

and shadow distance traversed. The Leica has a 4 to 8 second relock time and the relock area is between 15% and 35%. Trimble's active prism and better performing hardware is a significant improvement over the older Leica technology.

To reduce the manual relock areas the multi-gun controller software could use the LOS model results to orient the gun in such a direction to establish lock on the edge of a shadow zone. The testing of this integration is beyond the scope of the project, but could greater increase system performance in wooded or limited line-of-sight environments.

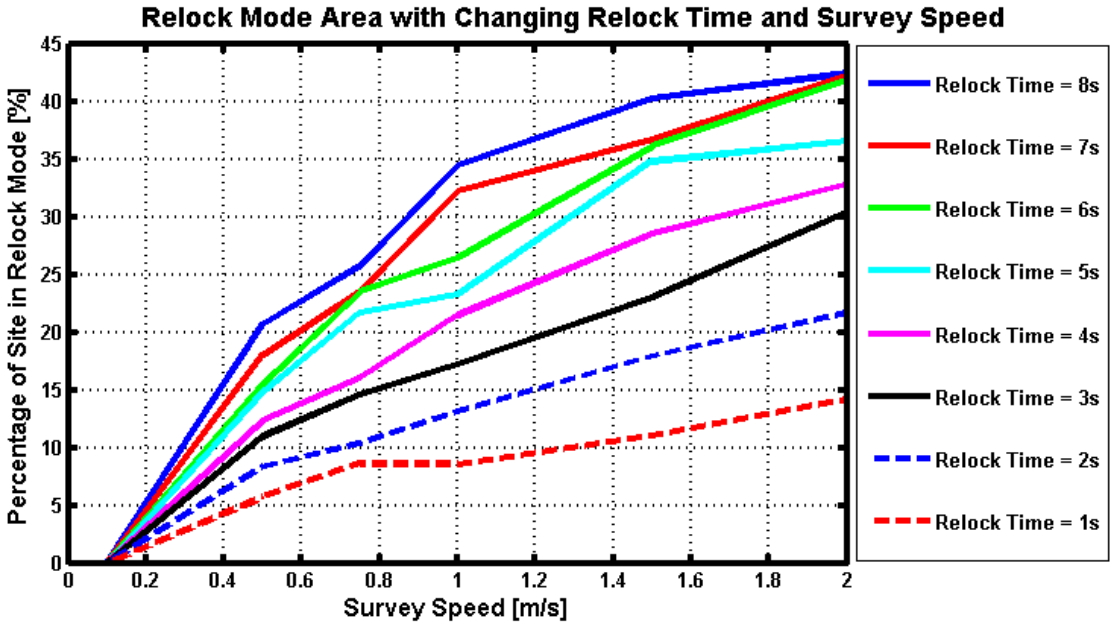

Figure 77. The percentage of the site where the gun is in relock mode with varying survey speeds and relock times. As the relock time increases, the percentage of the survey site in relock mode increases.

REFERENCES CITED

Barrow, B.J., and Nelson, H., "Effect Of Positioning Measurements On Inverting Electromagnetic Induction Data From Unexploded Ordnance", UXO Forum, April 2001, New Orleans.

Bell, T., 2005 Geo-location Requirements for UXO Discrimination Paper prepared for UXO Location Workshop, Annapolis, May 2005.

Brandt, A. and Gardner, J. F., 1998. *Constrained Navigation Algorithms for Strapdown Inertial Navigation Systems with Reduced Set of Sensors*. Proceedings of the American Control Conference, Philadelphia, Pennsylvania.

EM61HH-MK2 Product Description, 2005, http://www.geonics.com/html/em61hh-mk2.html.

Foley, J., Sensor Orientation Effects on UXO Geophysical Target Discrimination, SERDP & ESTCP Symposium & Workshop, Washington DC, Dec 2-5, 2003.

Foley, J. and Mehl, R., Increasing UXO Geophysical Survey Capabilities with Flexible, Accurate, and Robust Robotic Total Station Technology, proceedings from the UXO Forum, Orlando, FL, September 2002.

Foley J. and Mehl, R. SERDP MM-1441 2005 Annual Report, December 2005. Prepared by Sky Research, Inc.

Foley, J., Mehl, R., and Miele, M., Advancements in UXO Detection and Discrimination through Robotic Total Station Mapping Technology, Proceedings from the Society of American Military Engineers, Seattle, WA, May 27-30, 2003.

Innovative Navigation Systems to Support Digital Geophysical Mapping, ESTCP #200129, Phase II Demonstrations. Revised Report, September 24, 2004. Prepared by US Army Corps of Engineers, U.S. Army Corps of Engineers-Huntsville Center.

Julier , S. J., and Uhlmann, J. K., 2004. *Unscented Filtering and nonlinear estimation*. IEEE Proc., Vol. 92 (3), 401-422.

Kalman, R. E., 1960. *A New Approach to Linear Filtering and Prediction Problems*. Transaction of the ASME—Journal of Basic Engineering, *82* (D), 35-45.

Maybeck, P. S., 1979. *Stochastic models, estimation, and control* (Vol. 141).

Pasion, L. R., 2007. *Inversion of Time Domain Electromagnetic Data for the Detection of Unexploded Ordnance*. Ph.D. Thesis, The University of British Columbia.

Pasion, L. R., Oldenburg, D. W., 2001. *A Discrimination Algorithm for UXO Using Time Domain Electromagnetics.* Journal of Engineering and Environmental Geophysics 6 (2), 91–102.

Rios, J. A., and White, E., 2001. *Fusion Filter Algorithm Enhancements For a MEMS GPS/IMU*. Technical report, Crossbow.

Sensor Orientation Effects on UXO Geophysical Target Discrimination, SERDP MM-1310, Draft Final Report, November, 2006. Prepared by Sky Research, Inc.

Trimble SPS930 and SPS930 Universal Total Stations Datasheet, 2007, http://trl.trimble.com/docushare/dsweb/Get/Document-390940/Datasheet%20-%20S6730%20and%20S6%20Universal%20Total%20Stations.pdf.

Welch, G., and Bishop, G., 1997. *SCAAT: Incremental Tracking with Incomplete Information*. In T. Whitted (Ed.), Computer Graphics (SIGGRAPH 97 Conference Proc., 333-344). Los Angeles, CA, USA (August): ACM Press, Addison-Wesley.

APPENDIX A

This appendix contains the entire moving target data reduced to tabular form. The summary table contains all of the average values from the File Result tables. The File Results tables contain all the reduced data from the test files. The data images show the raw position data in a graphical format.

Column Description
Filename – Data File Name
Left or Right – Direction of prism travel
Shadow Size – Width of the Screen in meters
Average Speed – Average speed of the prism as it travels down the line in m/s
Gap Size/Gap Between Screens – Distance in meters between the screens.
Gap Length – Distance of the data gap in meters
Gap Time – Length of time of the gap in seconds
Shadow Time – Length of time of the prism behind the screen in seconds
Relock Time – Difference between Gap Time and Shadow Time in seconds. This is the length of time the gun takes to relock onto the prism.
Relock Distance – Distance of the relock in meters

Trimble 5600 – Single Screen Summary

Filename	Shadow Size	Average Speed	Gap Length	Gap Time	Shadow Time	Relock Time	Relock Distance
SS45S.txt	0.45	1.100	1.173	1.065	0.409	0.656	0.723
SS06S2.txt	0.60	1.130	1.300	1.150	0.531	0.619	0.700
SS72S.txt	0.72	0.883	1.309	1.484	0.816	0.667	0.589
SS72S2.txt	0.72	0.777	1.204	1.552	0.928	0.624	0.484
SS72S3.txt	0.72	1.028	1.411	1.372	0.700	0.672	0.691
SS72S_internal.txt	0.72	0.503	2.015	4.012	1.435	2.577	1.295
SS11S3.txt	1.10	0.496	2.565	5.172	2.218	2.954	1.465
SS11S5.txt	1.10	1.123	1.126	1.000	0.976	0.024	0.026
SS11S_internal.txt	1.10	1.029	2.064	2.007	1.070	0.937	0.964
SS11S2_internal.txt	1.10	0.775	3.603	4.649	1.419	3.230	2.503

Trimble 5600 – Single Screen File Results

Left or Right	Line Number	Shadow Size	Average Speed	Gap Length	Gap Time	Shadow Time	Relock Time	Relock Distance
SS45S.txt								
R2L	1	0.45	1.027	1.029	1.002	0.438	0.564	0.579
R2L	2	0.45	1.117	1.119	1.002	0.403	0.599	0.669
R2L	3	0.45	1.107	1.036	0.936	0.407	0.529	0.586
R2L	4	0.45	1.094	1.123	1.027	0.411	0.615	0.673
R2L	5	0.45	1.127	1.864	1.654	0.399	1.255	1.414
L2R	1	0.45	1.083	1.104	1.019	0.416	0.604	0.654
L2R	2	0.45	1.095	1.108	1.012	0.411	0.601	0.658
L2R	3	0.45	1.109	1.111	1.002	0.406	0.596	0.661
L2R	4	0.45	1.116	1.115	0.999	0.403	0.596	0.665
L2R	5	0.45	1.124	1.125	1.001	0.400	0.601	0.675
Averages			**1.100**	**1.173**	**1.065**	**0.409**	**0.656**	**0.723**
Standard Deviations			**0.029**	**0.245**	**0.208**	**0.011**	**0.212**	**0.245**

Left or Right	Line Number	Shadow Size	Average Speed	Gap Length	Gap Time	Shadow Time	Relock Time	Relock Distance
SS06S1.txt								
R2L	1	0.60	1.119	1.314	1.174	0.536	0.638	0.714
R2L	2	0.60	1.131	1.324	1.171	0.531	0.640	0.724
R2L	3	0.60	1.123	1.324	1.179	0.534	0.645	0.724
R2L	4	0.60	1.139	1.328	1.166	0.527	0.639	0.728
R2L	5	0.60	1.152	1.339	1.162	0.521	0.641	0.739
L2R	1	0.60	1.122	1.306	1.164	0.535	0.629	0.706
L2R	2	0.60	1.129	1.305	1.156	0.531	0.624	0.705
L2R	3	0.60	1.111	1.305	1.175	0.540	0.635	0.705
L2R	4	0.60	1.134	1.306	1.152	0.529	0.623	0.706
L2R	5	0.60	1.134	1.140	1.005	0.529	0.476	0.540
SS06S2.txt								
R2L	1	0.60	1.145	1.329	1.161	0.524	0.637	0.729
R2L	2	0.60	1.147	1.331	1.160	0.523	0.637	0.731
R2L	3	0.60	1.142	1.349	1.181	0.525	0.656	0.749
R2L	4	0.60	1.138	1.337	1.175	0.527	0.648	0.737
R2L	5	0.60	1.075	1.255	1.167	0.558	0.609	0.655
L2R	1	0.60	1.118	1.120	1.002	0.537	0.465	0.520
L2R	2	0.60	1.130	1.313	1.162	0.531	0.631	0.713
L2R	3	0.60	1.143	1.320	1.155	0.525	0.630	0.720
L2R	4	0.60	1.150	1.321	1.149	0.522	0.627	0.721
L2R	5	0.60	1.124	1.332	1.185	0.534	0.651	0.732
Averages			**1.130**	**1.300**	**1.150**	**0.531**	**0.619**	**0.700**
Standard Deviations			**0.022**	**0.068**	**0.053**	**0.011**	**0.056**	**0.068**

SS72S.txt								
R2L	1	0.72	0.892	1.348	1.511	0.807	0.704	0.628
R2L	2	0.72	0.828	1.205	1.455	0.870	0.586	0.485
R2L	3	0.72	0.828	1.371	1.656	0.870	0.786	0.651
R2L	4	0.72	0.899	1.338	1.488	0.801	0.687	0.618
R2L	5	0.72	0.895	1.339	1.496	0.804	0.692	0.619
L2R	1	0.72	0.895	1.203	1.344	0.804	0.540	0.483
L2R	2	0.72	0.902	1.369	1.518	0.798	0.720	0.649
L2R	3	0.72	0.900	1.358	1.509	0.800	0.709	0.638
L2R	4	0.72	0.902	1.353	1.500	0.798	0.702	0.633
L2R	5	0.72	0.891	1.210	1.358	0.808	0.550	0.490
Averages			**0.883**	**1.309**	**1.484**	**0.816**	**0.667**	**0.589**
Standard Deviations			**0.029**	**0.072**	**0.087**	**0.028**	**0.081**	**0.072**

Left or Right	Line Number	Shadow Size	Average Speed	Gap Length	Gap Time	Shadow Time	Relock Time	Relock Distance
SS72S2.txt								
R2L	1	0.72	0.790	1.173	1.485	0.911	0.573	0.453
R2L	2	0.72	0.790	1.177	1.490	0.911	0.578	0.457
R2L	3	0.72	0.721	1.302	1.806	0.999	0.807	0.582
R2L	4	0.72	0.789	1.180	1.496	0.913	0.583	0.460
R2L	5	0.72	0.722	1.190	1.648	0.997	0.651	0.470
L2R	1	0.72	0.788	1.209	1.534	0.914	0.621	0.489
L2R	2	0.72	0.793	1.204	1.518	0.908	0.610	0.484
L2R	3	0.72	0.791	1.207	1.526	0.910	0.616	0.487
L2R	4	0.72	0.784	1.192	1.520	0.918	0.602	0.472
L2R	5	0.72	0.801	1.201	1.499	0.899	0.600	0.481
Averages			**0.777**	**1.204**	**1.552**	**0.928**	**0.624**	**0.484**
Standard Deviations			**0.030**	**0.037**	**0.101**	**0.037**	**0.068**	**0.037**

SS72S3.txt								
R2L	1	0.72	1.027	1.359	1.323	0.701	0.622	0.639
R2L	2	0.72	1.027	1.353	1.317	0.701	0.616	0.633
R2L	3	0.72	1.023	1.346	1.316	0.704	0.612	0.626
R2L	4	0.72	1.025	1.703	1.661	0.702	0.959	0.983
L2R	1	0.72	1.024	1.362	1.330	0.703	0.627	0.642
L2R	3	0.72	1.031	1.380	1.339	0.698	0.640	0.660
L2R	4	0.72	1.035	1.391	1.344	0.696	0.648	0.671
L2R	5	0.72	1.032	1.391	1.348	0.698	0.650	0.671
Averages			**1.028**	**1.411**	**1.372**	**0.700**	**0.672**	**0.691**
Standard Deviations			**0.004**	**0.119**	**0.117**	**0.003**	**0.117**	**0.119**

SS72S_internal.txt								
R2L	1	0.72	0.504	2.023	4.014	1.429	2.585	1.303
R2L	2	0.72	0.505	2.020	4.000	1.426	2.574	1.300
R2L	3	0.72	0.499	1.921	3.850	1.443	2.407	1.201
R2L	4	0.72	0.501	2.094	4.180	1.437	2.743	1.374
R2L	5	0.72	0.436	1.937	4.443	1.651	2.791	1.217
L2R	1	0.72	0.516	2.594	5.027	1.395	3.632	1.874
L2R	2	0.72	0.518	2.000	3.861	1.390	2.471	1.280
L2R	3	0.72	0.518	1.828	3.529	1.390	2.139	1.108
L2R	4	0.72	0.519	1.914	3.688	1.387	2.301	1.194
L2R	5	0.72	0.515	1.818	3.530	1.398	2.132	1.098
Averages			**0.503**	**2.015**	**4.012**	**1.435**	**2.577**	**1.295**
Standard Deviations			**0.025**	**0.221**	**0.455**	**0.079**	**0.434**	**0.221**

Left or Righ	Line Number	Shadow Size	Average Speed	Gap Length	Gap Time	Shadow Time	Relock Time	Relock Distance
SS11S3.txt								
R2L	1	1.10	0.492	2.514	5.110	2.236	2.874	1.414
R2L	3	1.10	0.487	2.483	5.099	2.259	2.840	1.383
L2R	1	1.10	0.503	2.460	4.891	2.187	2.704	1.360
L2R	2	1.10	0.502	2.574	5.127	2.191	2.936	1.474
SS11S4.txt								
R2L	1	1.10	0.485	2.363	4.872	2.268	2.604	1.263
R2L	2	1.10	0.489	2.890	5.910	2.249	3.661	1.790
R2L	4	1.10	0.500	2.502	5.004	2.200	2.804	1.402
L2R	1	1.10	0.508	2.609	5.136	2.165	2.970	1.509
L2R	3	1.10	0.496	2.474	4.988	2.218	2.770	1.374
L2R	4	1.10	0.498	2.780	5.582	2.209	3.373	1.680
Averages			**0.496**	**2.565**	**5.172**	**2.218**	**2.954**	**1.465**
Standard Deviations			**0.008**	**0.159**	**0.326**	**0.034**	**0.323**	**0.159**

SS11S5.txt								
R2L	1	1.10	1.105	1.130	1.000	0.995	0.005	0.030
R2L	2	1.10	1.140	1.131	1.000	0.965	0.035	0.031
R2L	3	1.10	1.065	1.042	1.000	1.032	-0.032	-0.058
R2L	4	1.10	1.139	1.133	1.000	0.966	0.034	0.033
R2L	5	1.10	1.135	1.143	1.000	0.969	0.031	0.043
R2L	6	1.10	1.135	0.000	0.000	0.000	0.000	0.000
L2R	1	1.10	1.132	1.104	1.000	0.972	0.028	0.004
L2R	2	1.10	1.123	1.119	1.000	0.979	0.021	0.019
L2R	3	1.10	1.121	1.123	1.000	0.981	0.019	0.023
L2R	4	1.10	1.112	1.121	1.000	0.990	0.010	0.021
L2R	5	1.10	1.136	1.128	1.000	0.968	0.032	0.028
L2R	6	1.10	1.133	1.124	1.000	0.971	0.029	0.024
Averages			**1.123**	**1.126**	**1.000**	**0.976**	**0.024**	**0.026**
Standard Deviations			**0.012**	**0.340**	**0.302**	**0.294**	**0.012**	**0.012**

SS11S_internal.txt								
R2L	1	1.10	1.026	2.204	2.148	1.072	1.076	1.104
R2L	2	1.10	1.029	2.038	1.981	1.069	0.912	0.938
R2L	3	1.10	1.025	2.041	1.991	1.073	0.918	0.941
R2L	4	1.10	1.037	1.875	1.808	1.061	0.747	0.775
R2L	5	1.10	1.031	2.217	2.150	1.067	1.083	1.117
L2R	2	1.10	1.032	2.042	1.979	1.066	0.913	0.942
L2R	3	1.10	1.027	2.216	2.158	1.071	1.087	1.116
L2R	4	1.10	1.021	1.879	1.840	1.077	0.763	0.779
Averages			**1.029**	**2.064**	**2.007**	**1.070**	**0.937**	**0.964**
Standard Deviations			**0.005**	**0.140**	**0.137**	**0.005**	**0.137**	**0.140**

Left or Right	Line Number	Shadow Size	Average Speed	Gap Length	Gap Time	Shadow Time	Relock Time	Relock Distance
SS11S2_internal.txt								
R2L	1	1.10	0.771	3.676	4.768	1.427	3.341	2.576
R2L	2	1.10	0.773					
R2L	4	1.10	0.774	3.560	4.599	1.421	3.178	2.460
R2L	5	1.10	0.777	3.821	4.918	1.416	3.502	2.721
R2L	6	1.10	0.779	3.330	4.275	1.412	2.863	2.230
L2R	1	1.10	0.775	3.463	4.468	1.419	3.049	2.363
L2R	2	1.10	0.777	3.359	4.323	1.416	2.907	2.259
L2R	3	1.10	0.772	3.871	5.014	1.425	3.589	2.771
L2R	4	1.10	0.776	3.744	4.825	1.418	3.407	2.644
L2R	5	1.10	0.779					
Averages			**0.775**	**3.603**	**4.649**	**1.419**	**3.230**	**2.503**
Standard Deviations			**0.003**	**0.207**	**0.276**	**0.005**	**0.273**	**0.207**

Trimble 5600 – Single Screen Data Images

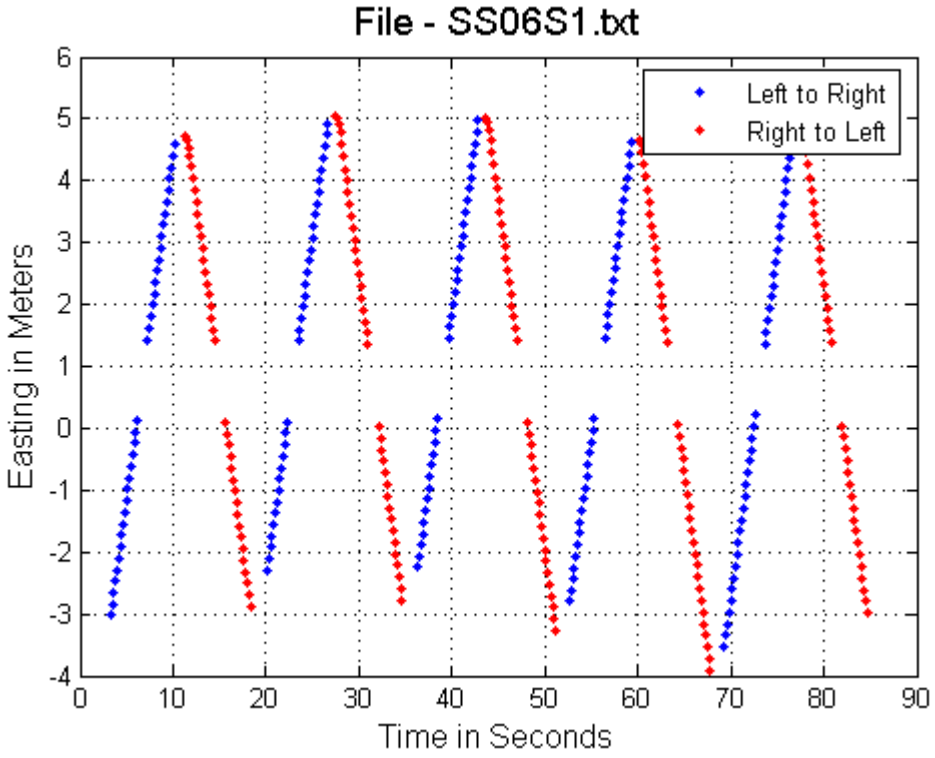

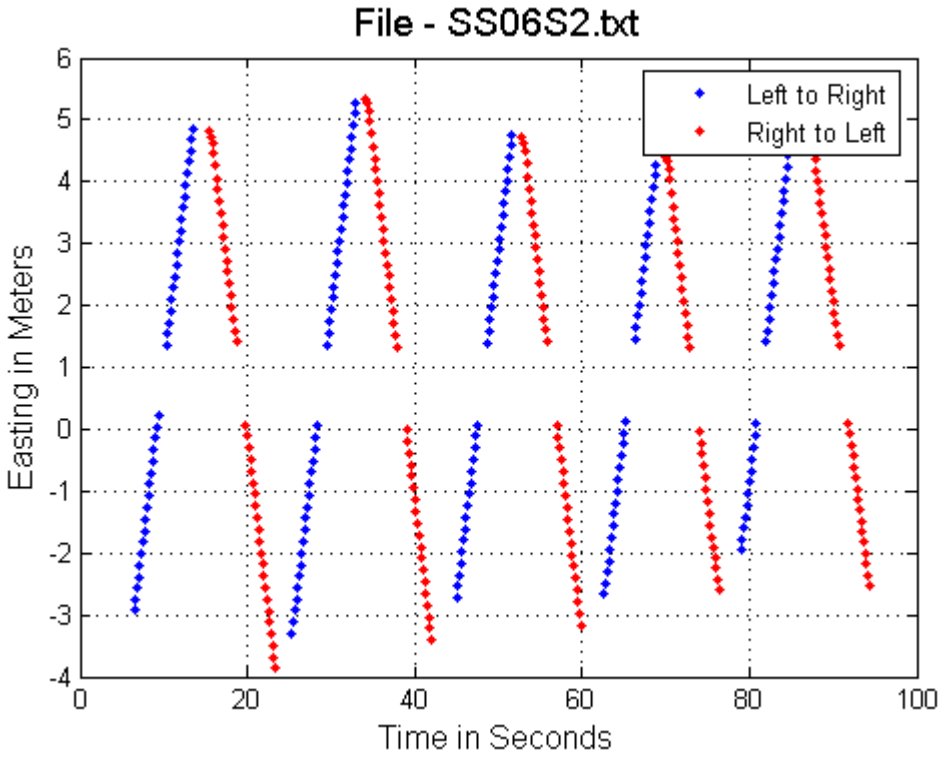

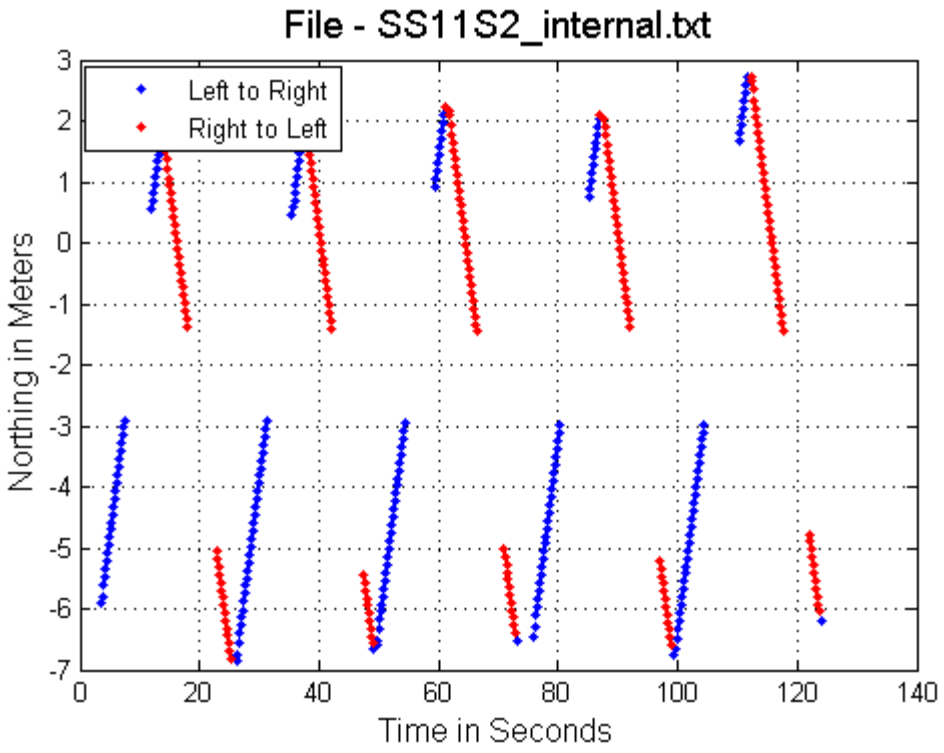
File - SS11S2_internal.txt
Left to Right
Right to Left
Northing in Meters
Time in Seconds
3
2
1
0
-1
-2
-3
-4
-5
-6
-7
0
20
40
60
80
100
120
140

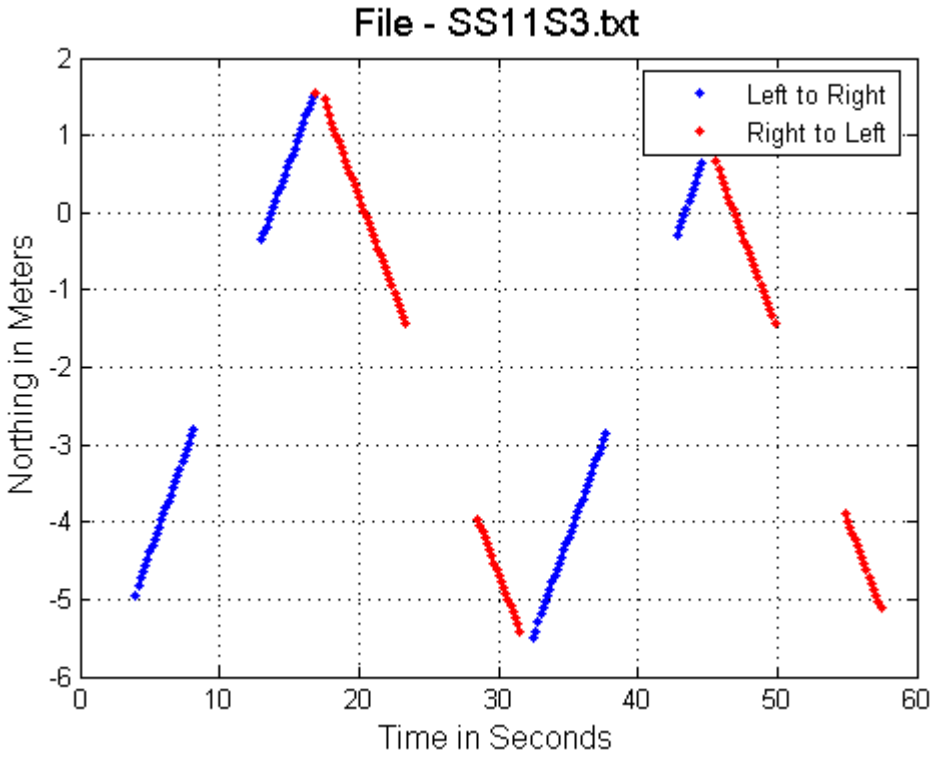
File - SS11S3.txt
Left to Right
Right to Left
Northing in Meters
Time in Seconds
2
1
0
-1
-2
-3
-4
-5
-6
0
10
20
30
40
50
60

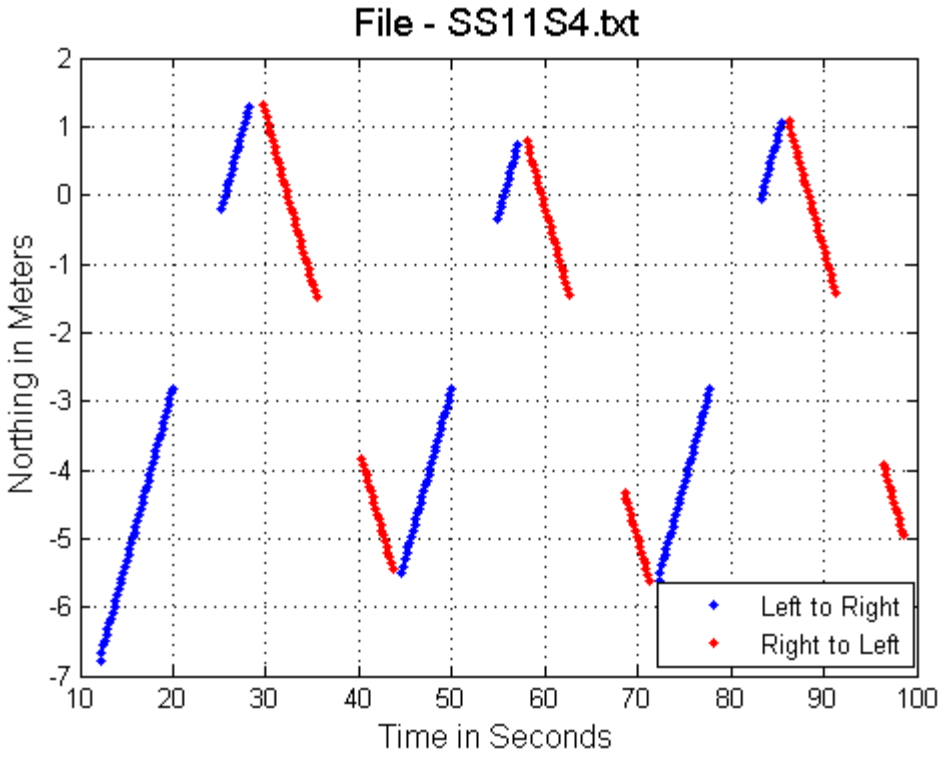
File - SS11S4.txt
Northing in Meters
Time in Seconds
Left to Right
Right to Left

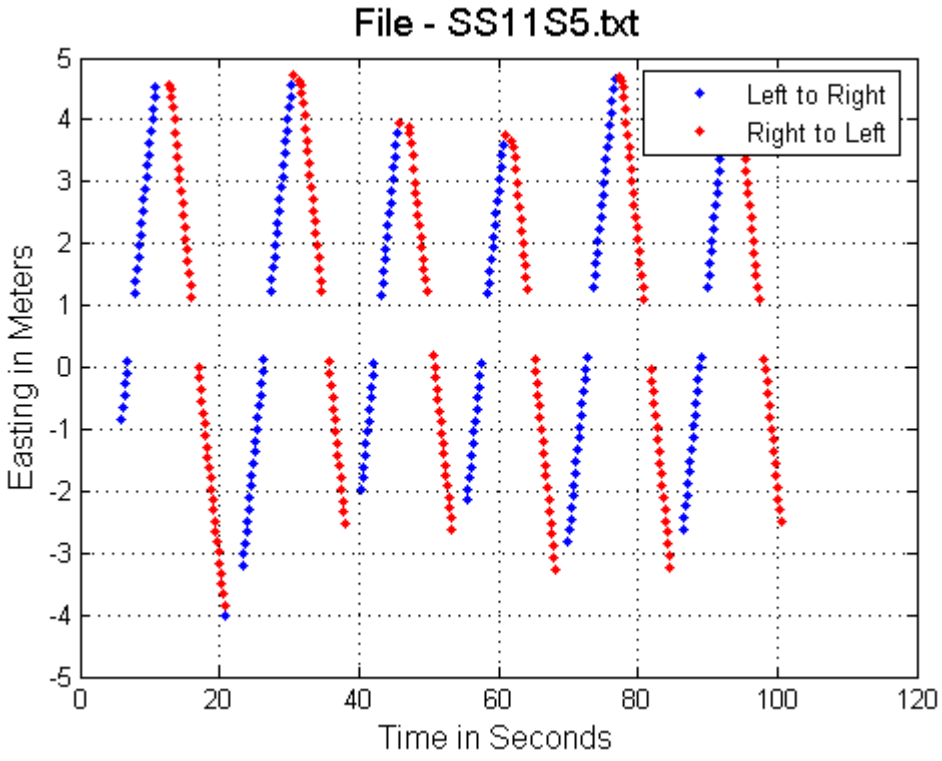
File - SS11S5.txt
Easting in Meters
Time in Seconds
Left to Right
Right to Left

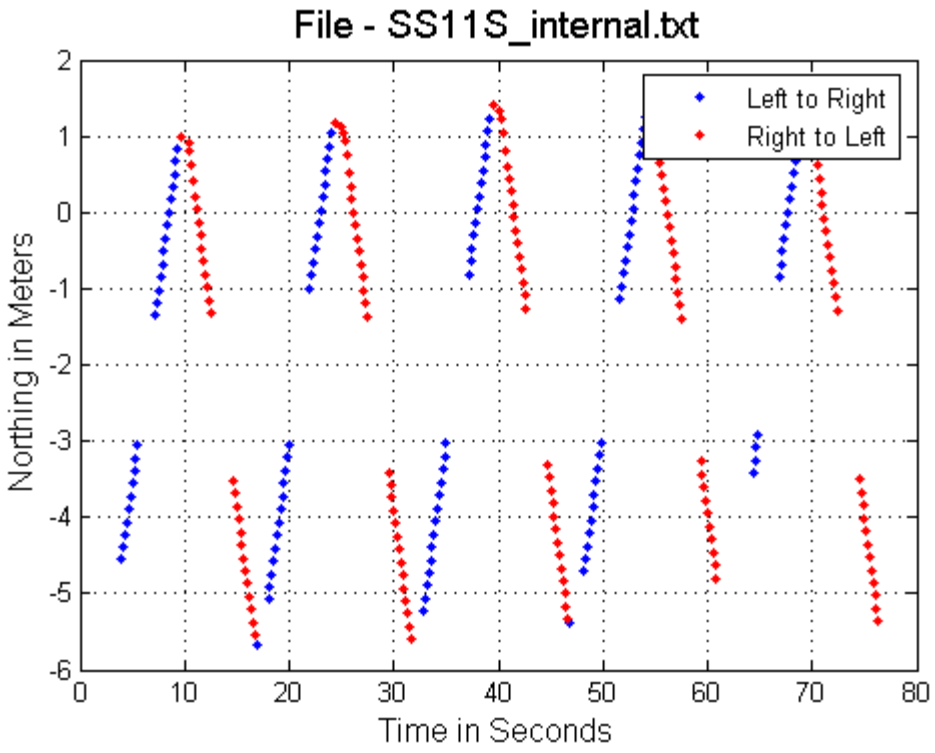
File - SS11S_internal.txt
Left to Right
Right to Left
Northing in Meters
Time in Seconds
2
1
0
-1
-2
-3
-4
-5
-6
0
10
20
30
40
50
60
70
80

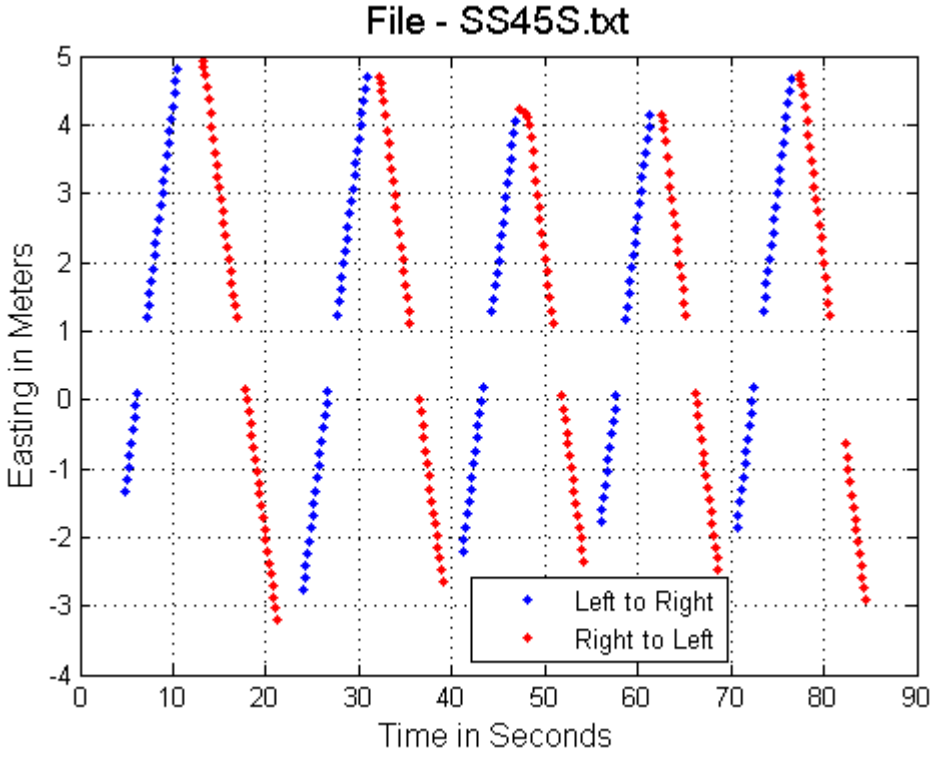
File - SS45S.txt
Left to Right
Right to Left
Easting in Meters
Time in Seconds
5
4
3
2
1
0
-1
-2
-3
-4
0
10
20
30
40
50
60
70
80
90

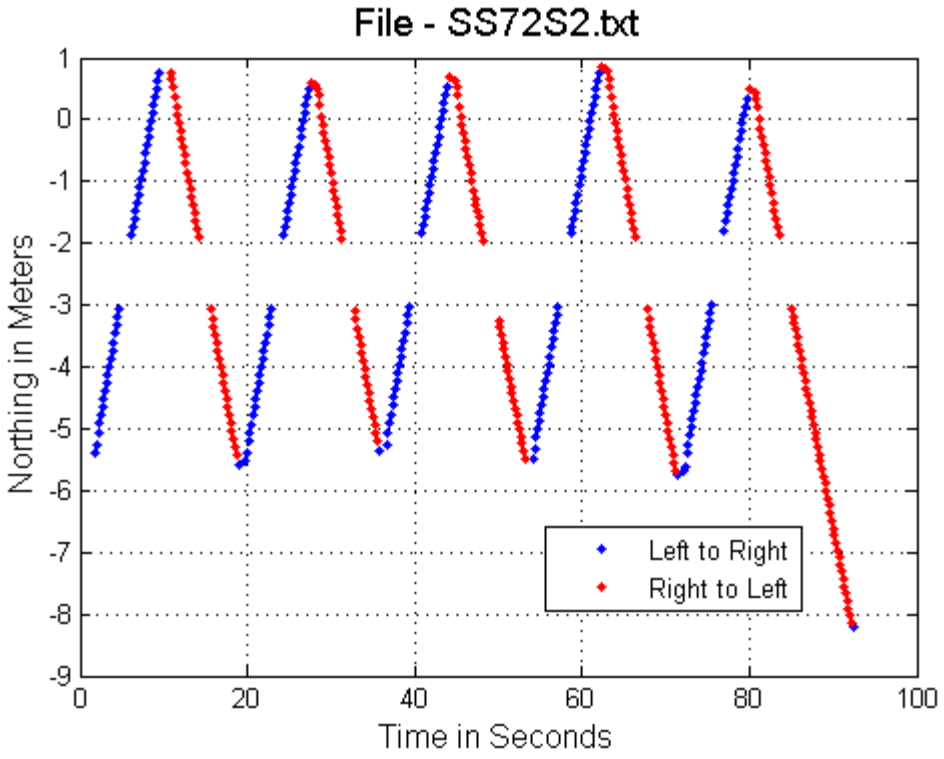
File - SS72S2.txt
Northing in Meters
Time in Seconds
Left to Right
Right to Left
1
0
-1
-2
-3
-4
-5
-6
-7
-8
-9
0
20
40
60
80
100

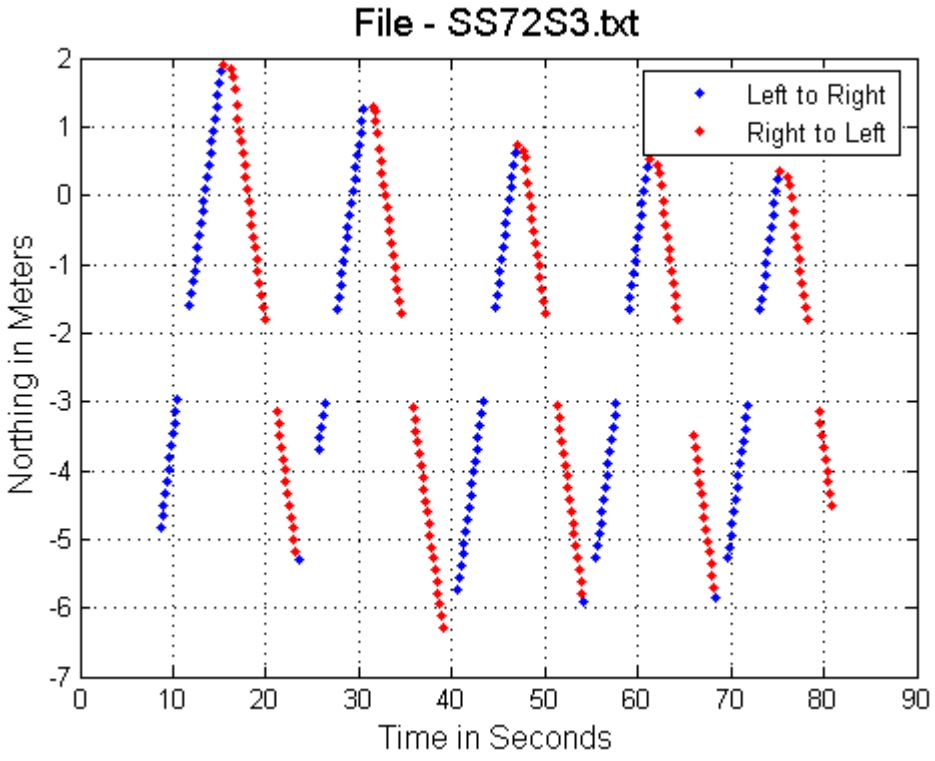
File - SS72S3.txt
Northing in Meters
Time in Seconds
Left to Right
Right to Left
2
1
0
-1
-2
-3
-4
-5
-6
-7
0
10
20
30
40
50
60
70
80
90

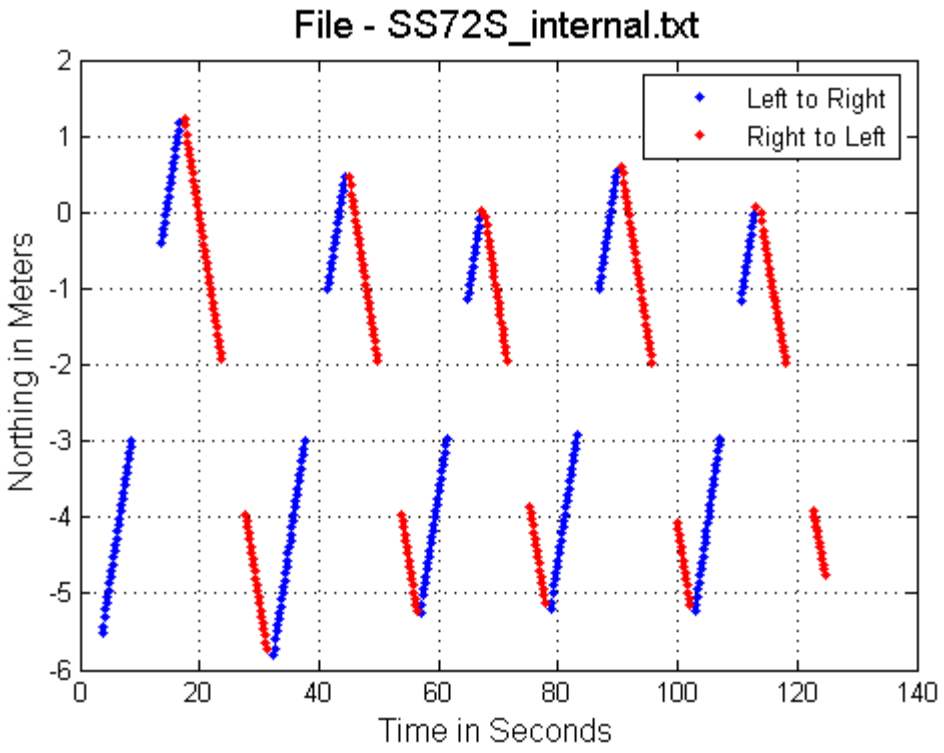
File - SS72S_internal.txt
Left to Right
Right to Left
Northing in Meters
Time in Seconds
2
1
0
-1
-2
-3
-4
-5
-6
0
20
40
60
80
100
120
140

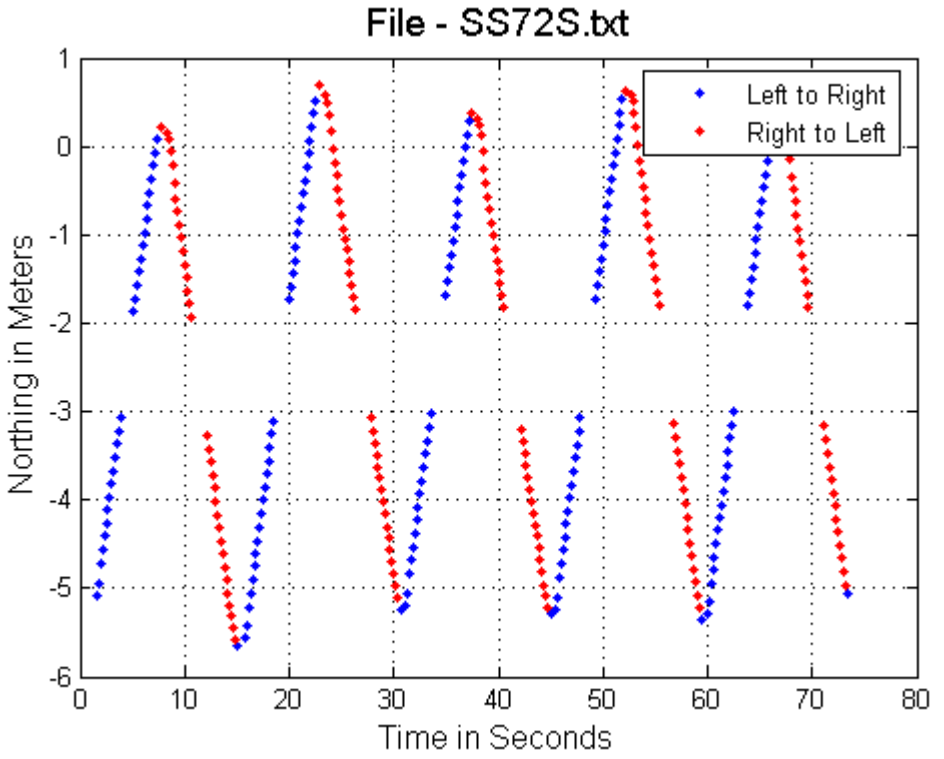
File - SS72S.txt
Left to Right
Right to Left
Northing in Meters
Time in Seconds
1
0
-1
-2
-3
-4
-5
-6
0
10
20
30
40
50
60
70
80

Trimble 5600 – Double Screen Summary

Left or Right	Line Number	Shadow Size	Gap Between Screens	Average Speed	Screen 1				
					Gap Length	Gap Time	Shadow Time	Relock Time	Relock Distance
DS25S.txt									
R2L	1	0.7	2.0	0.539	2.071	3.842	1.299	2.544	1.371
R2L	2	0.7	2.0	0.543	2.357	4.341	1.289	3.052	1.657
R2L	3	0.7	2.0	0.546	2.366	4.333	1.282	3.051	1.666
R2L	4	0.7	2.0	0.556	2.399	4.315	1.259	3.056	1.699
R2L	5	0.7	2.0	0.550	2.013	3.660	1.273	2.387	1.313
L2R	1	0.7	2.0	0.541	1.988	3.675	1.294	2.381	1.288
L2R	2	0.7	2.0	0.549	2.211	4.027	1.275	2.752	1.511
L2R	3	0.7	2.0	0.556	2.152	3.871	1.259	2.612	1.452
L2R	4	0.7	2.0	0.565	2.273	4.023	1.239	2.784	1.573
Averages				**0.549**	**2.203**	**4.010**	**1.274**	**2.735**	**1.503**
Standard Deviations				**0.008**	**0.157**	**0.272**	**0.019**	**0.275**	**0.157**

Left or Right	Line Number	Shadow Size	Gap Between Screens	Average Speed	Screen 2				
					Gap Length	Gap Time	Shadow Time	Relock Time	Relock Distance
DS25S.txt									
R2L	1	0.7	2.0	0.539	1.958	3.633	1.299	2.334	1.258
R2L	2	0.7	2.0	0.543	2.331	4.293	1.289	3.004	1.631
R2L	3	0.7	2.0	0.546	1.720	3.150	1.282	1.868	1.020
R2L	4	0.7	2.0	0.556	2.106	3.788	1.259	2.529	1.406
R2L	5	0.7	2.0	0.550	2.748	4.996	1.273	3.724	2.048
L2R	1	0.7	2.0	0.541	1.980	3.660	1.294	2.366	1.280
L2R	2	0.7	2.0	0.549	2.010	3.661	1.275	2.386	1.310
L2R	3	0.7	2.0	0.556	2.783	5.005	1.259	3.746	2.083
L2R	4	0.7	2.0	0.565	2.433	4.306	1.239	3.067	1.733
Averages				**0.549**	**2.230**	**4.055**	**1.274**	**2.780**	**1.530**
Standard Deviations				**0.008**	**0.368**	**0.641**	**0.019**	**0.650**	**0.368**

Trimble 5600 – Double Screen Data Images

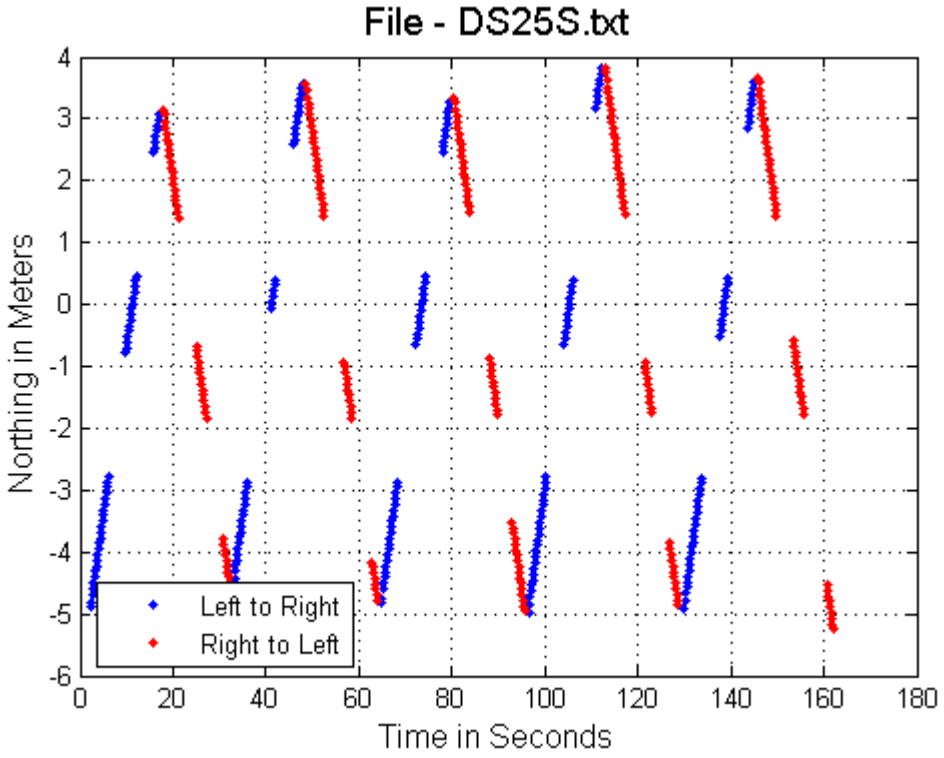

Trimble 5600 – Alternating Screen Summary

Filename	Shadow Size	Average Speed	Gap Length	Gap Time	Shadow Time	Relock Time	Relock Distance
AS_1g1.txt	0.72	1.461	1.456	1.000	0.494	0.506	0.736
AS_1g2.txt	0.72	1.465	1.735	1.184	0.492	0.692	1.015
AS_0g1.txt	0.72	0.488	1.851	3.829	1.492	2.338	1.131
AS_0g2.txt	0.72	0.483	2.105	4.305	1.506	2.799	1.385
AS_3g1.txt	0.72	0.891	1.246	1.399	0.808	0.592	0.526
AS_3g2.txt	0.72	0.891	1.320	1.482	0.809	0.673	0.600

Trimble 5600 – Alternating Screen File Results

Left or Right	Line Number	Shadow Size	Average Speed	Gap Length	Gap Time	Shadow Time	Relock Time	Relock Distance
AS_1g1.txt		Gun 1						
R2L	1	0.72	1.384	1.413	1.021	0.520	0.501	0.693
R2L	2	0.72	1.388	1.634	1.177	0.519	0.659	0.914
R2L	3	0.72	1.398	1.419	1.015	0.515	0.500	0.699
R2L	4	0.72	1.395	1.646	1.180	0.516	0.664	0.926
R2L	5	0.72	1.190	3.458	2.906	0.605	2.301	2.738
L2R	1	0.72	1.526	1.498	0.982	0.472	0.510	0.778
L2R	2	0.72	1.512	1.493	0.987	0.476	0.511	0.773
L2R	3	0.72	1.512	1.490	0.985	0.476	0.509	0.770
L2R	4	0.72	1.530	1.498	0.979	0.471	0.508	0.778
L2R	5	0.72	1.500	1.011	0.674	0.480	0.194	0.291
Averages			**1.461**	**1.456**	**1.000**	**0.494**	**0.506**	**0.736**
Standard Deviations			**0.066**	**0.185**	**0.147**	**0.023**	**0.135**	**0.185**

AS_1g2.txt		Gun 2						
R2L	1	0.72	1.394	1.607	1.153	0.516	0.636	0.887
R2L	2	0.72	1.400	1.614	1.153	0.514	0.639	0.894
R2L	3	0.72	1.403	1.613	1.150	0.513	0.636	0.893
R2L	4	0.72	1.407	1.589	1.129	0.512	0.618	0.869
R2L	5	0.72	1.577	1.598	1.013	0.457	0.557	0.878
L2R	1	0.72	1.504	1.783	1.186	0.479	0.707	1.063
L2R	2	0.72	1.512	2.014	1.332	0.476	0.856	1.294
L2R	3	0.72	1.499	0.000	0.000	0.480	-0.480	-0.720
L2R	4	0.72	1.497	1.796	1.200	0.481	0.719	1.076
L2R	5	0.72	1.490	2.004	1.345	0.483	0.862	1.284
Averages			**1.465**	**1.735**	**1.184**	**0.492**	**0.692**	**1.015**
Standard Deviations			**0.063**	**0.573**	**0.387**	**0.021**	**0.384**	**0.573**

Left or Right	Line Number	Shadow Size	Average Speed	Gap Length	Gap Time	Shadow Time	Relock Time	Relock Distance
AS_2g1.txt		Gun 1						
R2L	1	0.72	0.495	2.141	4.350	1.456	2.894	1.421
L2R	1	0.72	0.580	1.121	2.000	1.240	0.760	0.401
Averages			**0.538**	**1.631**	**3.175**	**1.348**	**1.827**	**0.911**
Standard Deviations			**0.060**	**0.721**	**1.662**	**0.153**	**1.509**	**0.721**

AS_2g2.txt		Gun 2						
R2L	1	0.72	0.493	2.344	4.840	1.459	3.381	1.624
L2R	1	0.72	0.571	2.793	4.830	1.262	3.568	2.073
Averages			**0.532**	**2.569**	**4.835**	**1.361**	**3.475**	**1.849**
Standard Deviations			**0.055**	**0.317**	**0.007**	**0.139**	**0.132**	**0.317**

AS_0g1.txt		Gun 1						
R2L	1	0.72	0.437	1.944	4.449	1.648	2.801	1.224
R2L	2	0.72	0.438	1.883	4.299	1.644	2.655	1.163
R2L	3	0.72	0.434	1.739	4.007	1.659	2.348	1.019
R2L	4	0.72	0.438	1.948	4.447	1.644	2.804	1.228
R2L	5	0.72	0.435	1.647	3.786	1.655	2.131	0.927
L2R	1	0.72	0.541	1.857	3.433	1.331	2.102	1.137
L2R	2	0.72	0.540	1.848	3.422	1.333	2.089	1.128
L2R	4	0.72	0.538	1.841	3.422	1.338	2.084	1.121
L2R	6	0.72	0.540	1.849	3.424	1.333	2.091	1.129
L2R	8	0.72	0.541	1.949	3.603	1.331	2.272	1.229
Averages			**0.488**	**1.851**	**3.829**	**1.492**	**2.338**	**1.131**
Standard Deviations			**0.055**	**0.096**	**0.438**	**0.167**	**0.302**	**0.096**

AS_0g2.txt		Gun 2						
R2L	1	0.72	0.433	1.948	4.499	1.663	2.836	1.228
R2L	2	0.72	0.433	1.464	3.381	1.663	1.718	0.744
R2L	4	0.72	0.437	1.590	3.638	1.648	1.991	0.870
R2L	5	0.72	0.431	1.590	3.689	1.671	2.019	0.870
L2R	1	0.72	0.534	2.700	5.056	1.348	3.708	1.980
L2R	2	0.72	0.533	2.674	5.017	1.351	3.666	1.954
L2R	4	0.72	0.532	2.522	4.741	1.353	3.387	1.802
L2R	6	0.72	0.532	2.352	4.421	1.353	3.068	1.632
Averages			**0.483**	**2.105**	**4.305**	**1.506**	**2.799**	**1.385**
Standard Deviations			**0.053**	**0.518**	**0.653**	**0.166**	**0.795**	**0.518**

Left or Right	Line Number	Shadow Size	Average Speed	Gap Length	Gap Time	Shadow Time	Relock Time	Relock Distance
AS_3g1.txt		Gun 1						
R2L	1	0.72	0.868	1.294	1.491	0.829	0.661	0.574
R2L	2	0.72	0.877	1.614	1.840	0.821	1.019	0.894
R2L	3	0.72	0.885	1.187	1.341	0.814	0.528	0.467
R2L	4	0.72	0.891	1.193	1.339	0.808	0.531	0.473
R2L	5	0.72	0.900	1.203	1.337	0.800	0.537	0.483
L2R	1	0.72	0.888	1.175	1.323	0.811	0.512	0.455
L2R	2	0.72	0.896	1.183	1.320	0.804	0.517	0.463
L2R	3	0.72	0.894	1.196	1.338	0.805	0.532	0.476
L2R	4	0.72	0.902	1.203	1.334	0.798	0.535	0.483
L2R	5	0.72	0.913	1.215	1.331	0.789	0.542	0.495
Averages			**0.891**	**1.246**	**1.399**	**0.808**	**0.592**	**0.526**
Standard Deviations			**0.013**	**0.133**	**0.163**	**0.012**	**0.156**	**0.133**

AS_3g2.txt		Gun 2						
R2L	1	0.72	0.866	1.294	1.494	0.831	0.663	0.574
R2L	2	0.72	0.876	1.307	1.492	0.822	0.670	0.587
R2L	3	0.72	0.887	1.318	1.486	0.812	0.674	0.598
R2L	4	0.72	0.897	1.339	1.493	0.803	0.690	0.619
R2L	5	0.72	0.901	1.353	1.502	0.799	0.703	0.633
L2R	1	0.72	0.882	1.329	1.507	0.816	0.690	0.609
L2R	2	0.72	0.886	1.479	1.669	0.813	0.857	0.759
L2R	3	0.72	0.892	1.201	1.346	0.807	0.539	0.481
L2R	4	0.72	0.902	1.211	1.343	0.798	0.544	0.491
L2R	5	0.72	0.917	1.366	1.490	0.785	0.704	0.646
Averages			**0.891**	**1.320**	**1.482**	**0.809**	**0.673**	**0.600**
Standard Deviations			**0.015**	**0.079**	**0.091**	**0.013**	**0.089**	**0.079**

Trimble 5600 – Alternating Screen Data Images

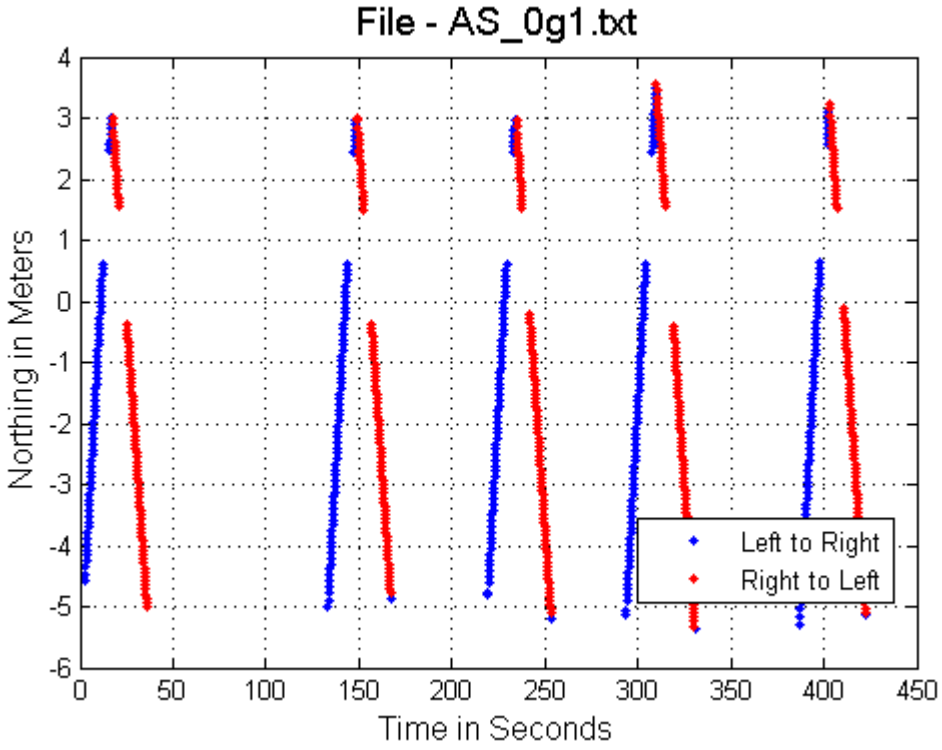

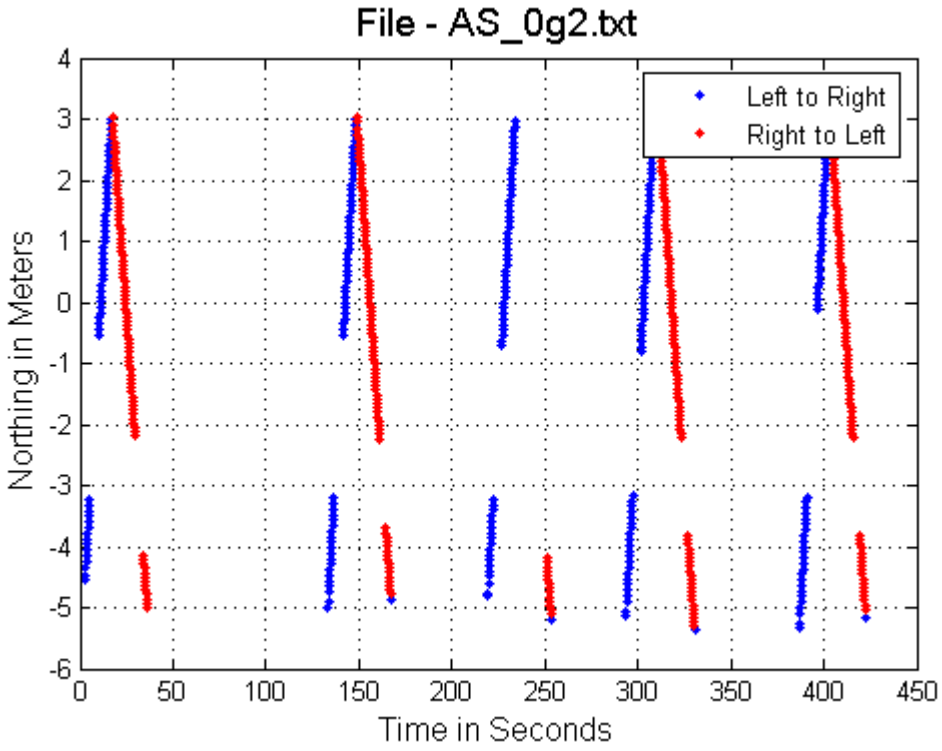

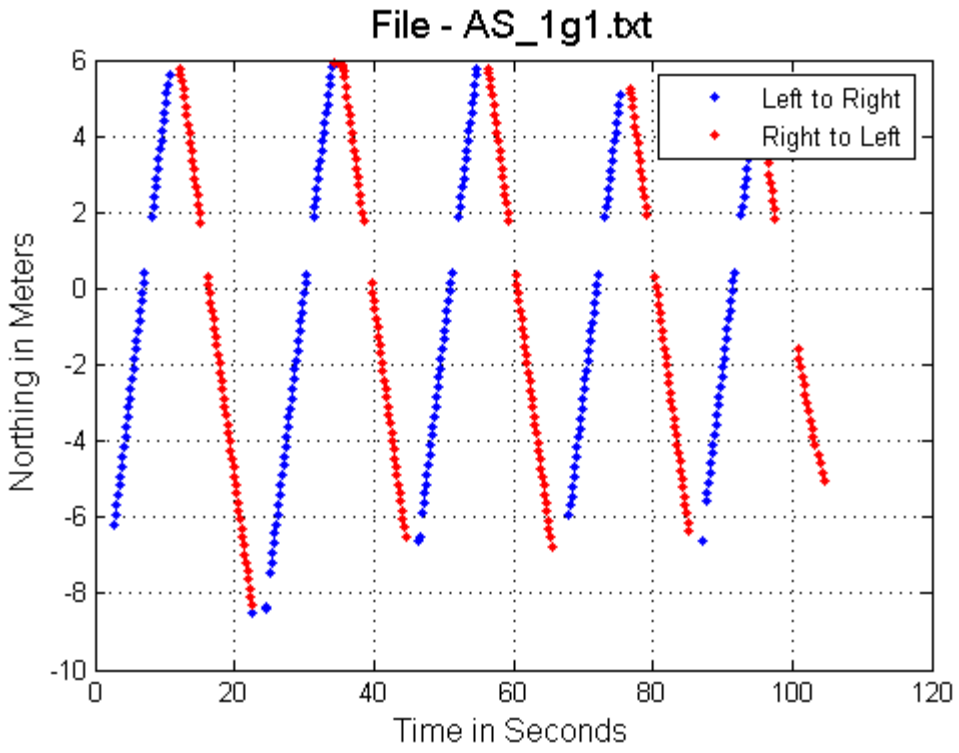
File - AS_1g1.txt
Left to Right
Right to Left
Northing in Meters
Time in Seconds
6
4
2
0
-2
-4
-6
-8
-10
0
20
40
60
80
100
120

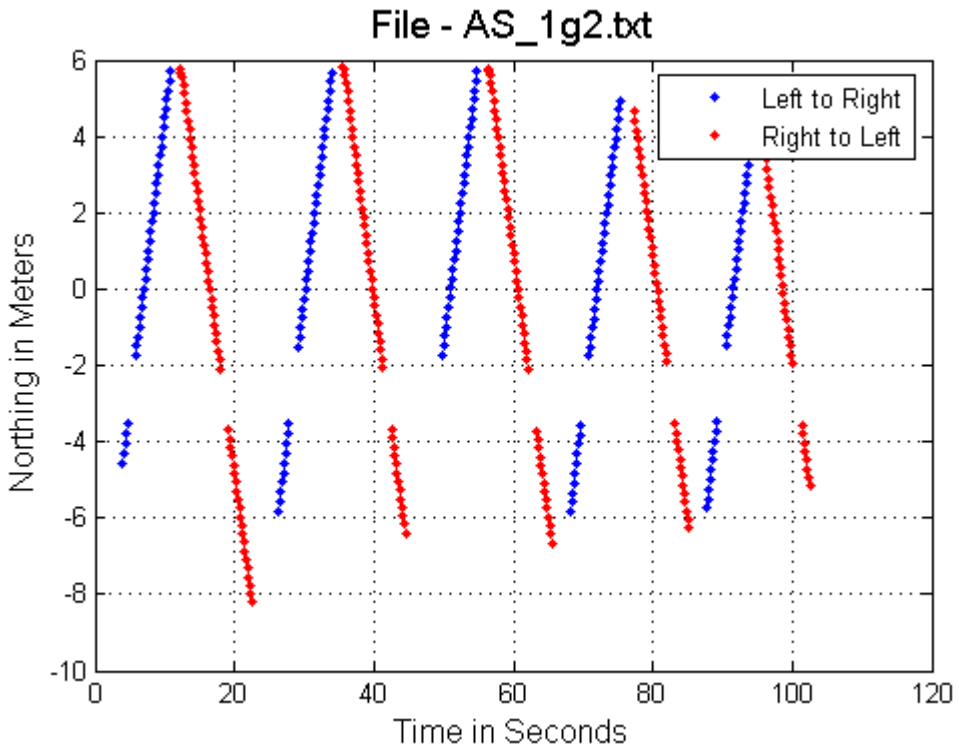
File - AS_1g2.txt
Left to Right
Right to Left
Northing in Meters
Time in Seconds
6
4
2
0
-2
-4
-6
-8
-10
0
20
40
60
80
100
120

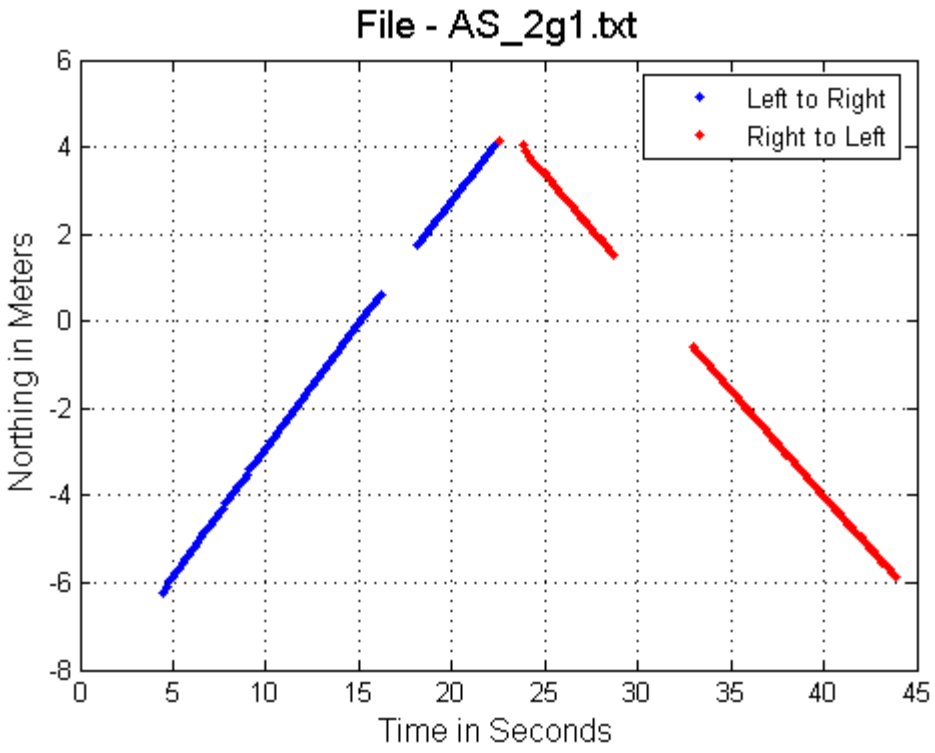
File - AS_2g1.txt
Left to Right
Right to Left
Northing in Meters
Time in Seconds
6
4
2
0
-2
-4
-6
-8
0
5
10
15
20
25
30
35
40
45

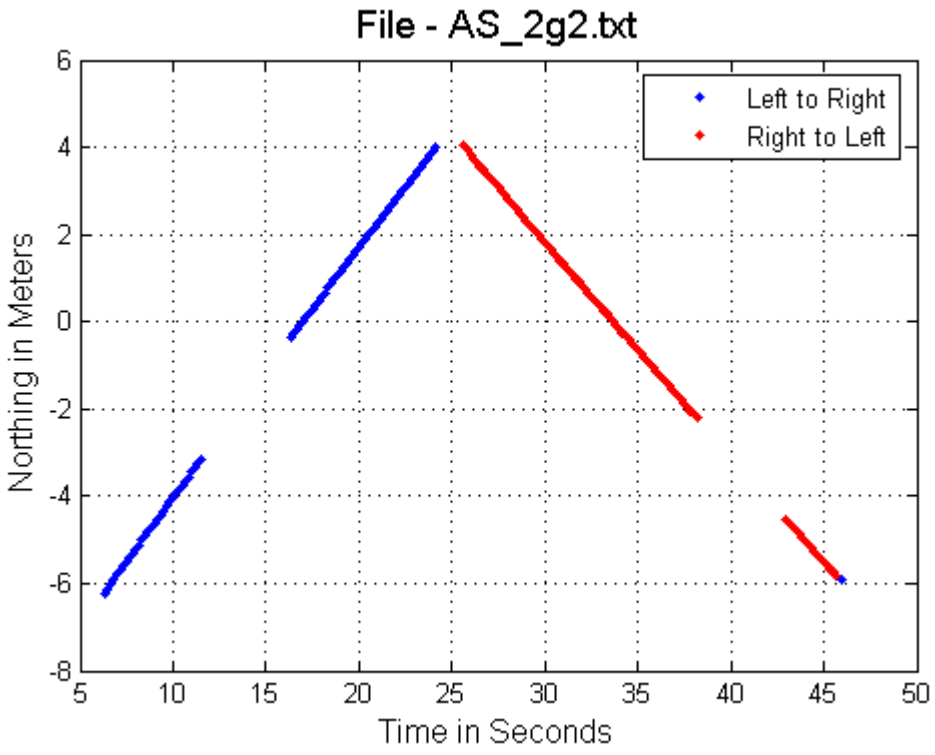
File - AS_2g2.txt
Left to Right
Right to Left
Northing in Meters
Time in Seconds
6
4
2
0
-2
-4
-6
-8
5
10
15
20
25
30
35
40
45
50

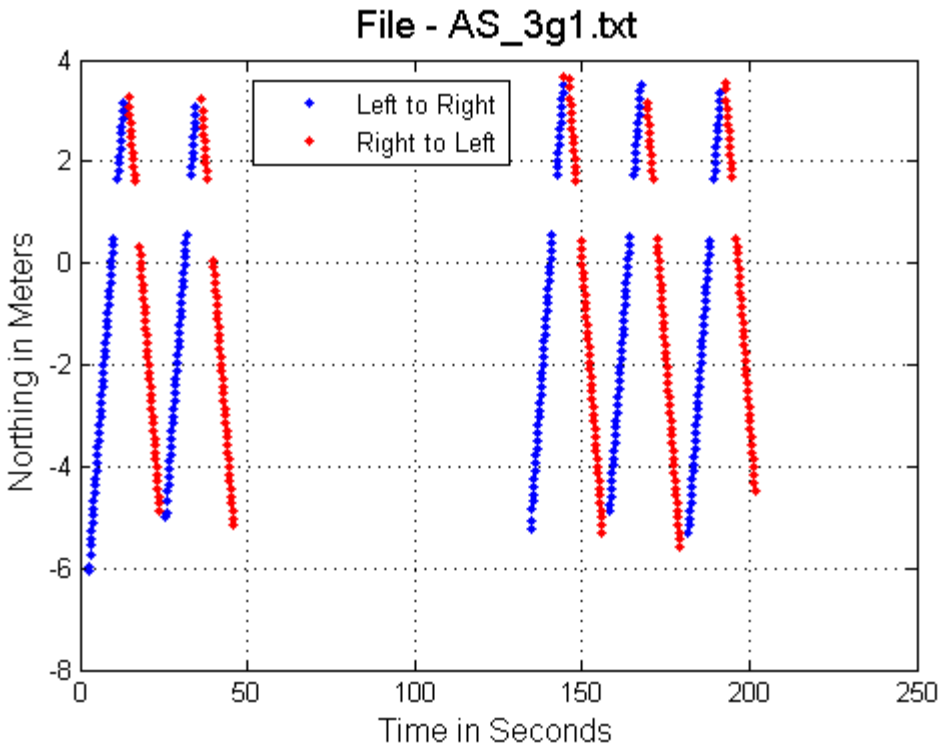
File - AS_3g1.txt
Left to Right
Right to Left
Northing in Meters
Time in Seconds
4
2
0
-2
-4
-6
-8
0
50
100
150
200
250

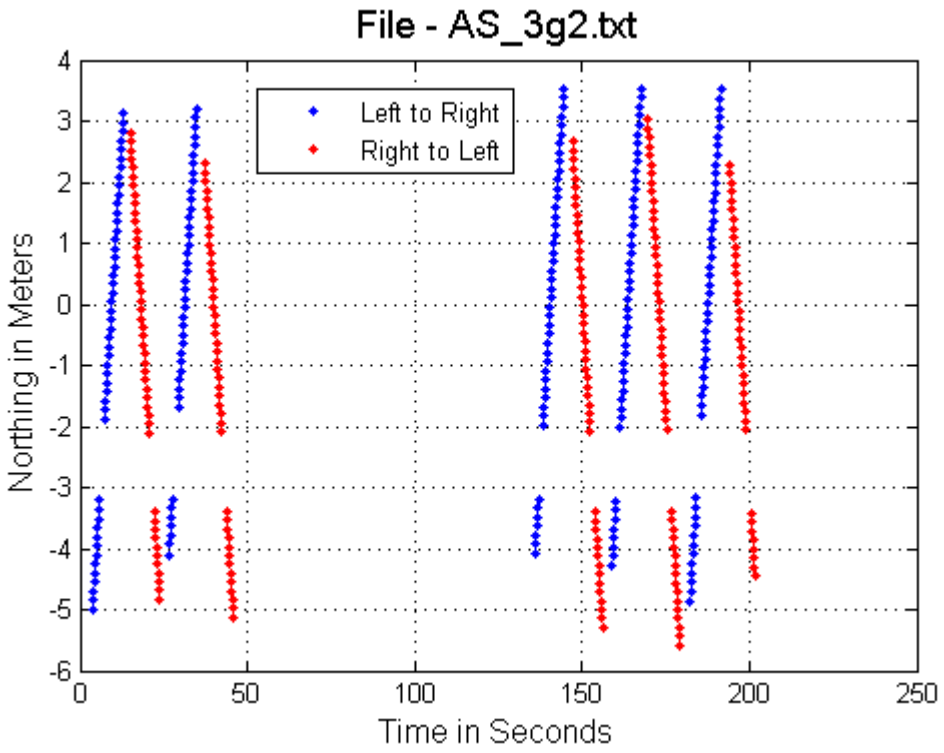
File - AS_3g2.txt
Left to Right
Right to Left
Northing in Meters
Time in Seconds
4
3
2
1
0
-1
-2
-3
-4
-5
-6
0
50
100
150
200
250

Trimble SPS930 – Single Screen Summary

Filename	Screen Width	Average Speed	Gap Length	Gap Time	Shadow Time	Relock Time	Relock Distance
-131751.txt	1	0.500	1.282	2.593	2.039	0.554	0.282
-132832.txt	1	0.718	1.414	1.986	1.404	0.583	0.414
-133345.txt	1	0.937	1.547	1.667	1.077	0.590	0.547
-133730.txt	1	1.112	1.625	1.488	0.915	0.573	0.625
-135404.txt	2	0.483	2.319	4.904	4.216	0.688	0.319
-140232.txt	2	0.740	2.535	3.458	2.728	0.730	0.535
-140810.txt	2	1.023	2.812	2.786	1.976	0.810	0.812
-141338.txt	2	1.119	2.844	2.573	1.805	0.767	0.844
-143017.txt	3	0.505	3.168	6.356	5.998	0.635	0.319
-143839.txt	3	0.767	3.577	4.694	3.935	0.759	0.577
-144230.txt	3	0.944	3.607	3.840	3.200	0.640	0.607
-144837.txt	3	1.076	4.032	4.145	3.074	0.911	1.032

Trimble SPS930 – Single Screen File Results

Direction	Line Number	Shadow Size	Average Speed	Gap Length	Gap Time	Shadow Time	Relock Time	Relock Distance
scs930_9-25-07-131751.txt								
R2L	1	1	0.465	1.414	3.041	2.151	0.890	0.414
R2L	2	1	0.378	1.102	2.915	2.646	0.270	0.102
R2L	3	1	0.447	1.308	2.926	2.237	0.689	0.308
R2L	4	1	0.453	1.302	2.874	2.208	0.667	0.302
R2L	5	1	0.439	1.040	2.369	2.278	0.091	0.040
L2R	1	1	0.563	1.360	2.416	1.776	0.639	0.360
L2R	2	1	0.585	1.299	2.221	1.709	0.511	0.299
L2R	3	1	0.556	1.464	2.633	1.799	0.835	0.464
L2R	4	1	0.559	1.235	2.209	1.789	0.420	0.235
L2R	5	1	0.555	1.293	2.330	1.802	0.528	0.293
Averages			**0.500**	**1.282**	**2.593**	**2.039**	**0.554**	**0.282**
Standard Deviations			**0.071**	**0.130**	**0.322**	**0.309**	**0.246**	**0.130**

scs930_9-25-07-132832.txt								
R2L	1	1	0.613	1.533	2.501	1.631	0.869	0.533
R2L	2	1	0.657	1.399	2.129	1.522	0.607	0.399
R2L	3	1	0.690	1.326	1.922	1.449	0.472	0.326
R2L	4	1	0.661	1.313	1.986	1.513	0.474	0.313
R2L	5	1	0.659	1.457	2.211	1.517	0.693	0.457
L2R	1	1	0.776	1.424	1.835	1.289	0.546	0.424
L2R	2	1	0.789	1.424	1.805	1.267	0.537	0.424
L2R	3	1	0.776	1.421	1.831	1.289	0.543	0.421
L2R	4	1	0.781	1.423	1.822	1.280	0.542	0.423
L2R	5	1	0.781	1.423	1.822	1.280	0.542	0.423
Averages			**0.718**	**1.414**	**1.986**	**1.404**	**0.583**	**0.414**
Standard Deviations			**0.068**	**0.062**	**0.229**	**0.137**	**0.119**	**0.062**

Direction	Line Number	Shadow Size	Average Speed	Gap Length	Gap Time	Shadow Time	Relock Time	Relock Distance
scs930_9-25-07-133345.txt								
R2L	1	1	0.800	1.569	1.961	1.250	0.711	0.569
R2L	2	1	0.887	1.501	1.692	1.127	0.565	0.501
R2L	3	1	0.849	1.592	1.875	1.178	0.697	0.592
R2L	4	1	0.871	1.588	1.823	1.148	0.675	0.588
R2L	5	1	0.859	1.499	1.745	1.164	0.581	0.499
L2R	1	1	1.016	1.665	1.639	0.984	0.655	0.665
L2R	2	1	1.022	1.462	1.431	0.978	0.452	0.462
L2R	3	1	1.023	1.566	1.531	0.978	0.553	0.566
L2R	4	1	1.020	1.464	1.435	0.980	0.455	0.464
L2R	5	1	1.020	1.565	1.534	0.980	0.554	0.565
Averages			**0.937**	**1.547**	**1.667**	**1.077**	**0.590**	**0.547**
Standard Deviations			**0.091**	**0.064**	**0.185**	**0.107**	**0.093**	**0.064**

scs930_9-25-07-133730.txt								
R2L	1	1	0.792	1.861	2.350	1.263	1.087	0.861
R2L	2	1	0.974	1.368	1.405	1.027	0.378	0.368
R2L	3	1	1.042	1.647	1.581	0.960	0.621	0.647
R2L	4	1	1.008	1.644	1.631	0.992	0.639	0.644
R2L	5	1	1.059	1.272	1.201	0.944	0.257	0.272
R2L	6	1	1.083	1.609	1.486	0.923	0.562	0.609
L2R	1	1	1.244	1.668	1.341	0.804	0.537	0.668
L2R	2	1	1.238	1.676	1.354	0.808	0.546	0.676
L2R	3	1	1.233	1.671	1.355	0.811	0.544	0.671
L2R	4	1	1.233	1.670	1.354	0.811	0.543	0.670
L2R	5	1	1.204	1.754	1.457	0.831	0.626	0.754
L2R	6	1	1.231	1.655	1.344	0.812	0.532	0.655
Averages			**1.112**	**1.625**	**1.488**	**0.915**	**0.573**	**0.625**
Standard Deviations			**0.143**	**0.158**	**0.295**	**0.137**	**0.195**	**0.158**

scs930_9-25-07-135404.txt								
R2L	1	2	0.389	2.385	6.131	5.141	0.990	0.385
R2L	2	2	0.430	2.336	5.433	4.651	0.781	0.336
R2L	3	2	0.427	2.397	5.614	4.684	0.930	0.397
R2L	4	2	0.434	2.362	5.442	4.608	0.834	0.362
R2L	5	2	0.428	2.388	5.579	4.673	0.907	0.388
L2R	1	2	0.547	2.305	4.214	3.656	0.558	0.305
L2R	2	2	0.545	2.256	4.139	3.670	0.470	0.256
L2R	3	2	0.545	2.261	4.149	3.670	0.479	0.261
L2R	4	2	0.531	2.246	4.230	3.766	0.463	0.246
L2R	5	2	0.549	2.258	4.113	3.643	0.470	0.258
Averages			**0.483**	**2.319**	**4.904**	**4.216**	**0.688**	**0.319**
Standard Deviations			**0.066**	**0.061**	**0.799**	**0.584**	**0.220**	**0.061**

Direction	Line Number	Shadow Size	Average Speed	Gap Length	Gap Time	Shadow Time	Relock Time	Relock Distance
scs930_9-25-07-140232.txt								
R2L	1	2	0.637	2.649	4.159	3.140	1.019	0.649
R2L	2	2	0.684	2.507	3.665	2.924	0.741	0.507
R2L	3	2	0.654	2.704	4.135	3.058	1.076	0.704
R2L	4	2	0.667	2.559	3.837	2.999	0.838	0.559
R2L	5	2	0.681	2.355	3.458	2.937	0.521	0.355
R2L	6	2	0.679	2.347	3.457	2.946	0.511	0.347
R2L	7	2	0.679	2.570	3.785	2.946	0.839	0.570
L2R	1	2	0.812	2.635	3.245	2.463	0.782	0.635
L2R	2	2	0.812	2.718	3.347	2.463	0.884	0.718
L2R	3	2	0.812	2.385	2.937	2.463	0.474	0.385
L2R	4	2	0.813	2.634	3.240	2.460	0.780	0.634
L2R	5	2	0.810	2.390	2.951	2.469	0.481	0.390
L2R	6	2	0.810	2.397	2.959	2.469	0.490	0.397
L2R	7	2	0.815	2.635	3.233	2.454	0.779	0.635
Averages			**0.740**	**2.535**	**3.458**	**2.728**	**0.730**	**0.535**
Standard Deviations			**0.075**	**0.135**	**0.409**	**0.280**	**0.203**	**0.135**

scs930_9-25-07-140810.txt								
R2L	1	2	0.825	2.800	3.394	2.424	0.970	0.800
R2L	2	2	0.953	2.995	3.143	2.099	1.044	0.995
R2L	3	2	0.940	2.778	2.955	2.128	0.828	0.778
R2L	4	2	0.935	2.973	3.180	2.139	1.041	0.973
R2L	5	2	0.965	2.777	2.878	2.073	0.805	0.777
R2L	6	2	0.964	2.960	3.071	2.075	0.996	0.960
R2L	7	2	0.890	2.975	3.343	2.247	1.096	0.975
L2R	1	2	1.119	2.668	2.384	1.787	0.597	0.668
L2R	2	2	1.128	2.557	2.267	1.773	0.494	0.557
L2R	3	2	1.122	2.673	2.382	1.783	0.600	0.673
L2R	4	2	1.126	2.896	2.572	1.776	0.796	0.896
L2R	5	2	1.127	2.668	2.367	1.775	0.593	0.668
L2R	6	2	1.116	2.763	2.476	1.792	0.684	0.763
L2R	7	2	1.117	2.890	2.587	1.791	0.797	0.890
Averages			**1.023**	**2.812**	**2.786**	**1.976**	**0.810**	**0.812**
Standard Deviations			**0.108**	**0.139**	**0.395**	**0.219**	**0.197**	**0.139**

Direction	Line Number	Shadow Size	Average Speed	Gap Length	Gap Time	Shadow Time	Relock Time	Relock Distance
scs930_9-25-07-141338.txt								
R2L	1	2	0.964	3.036	3.149	2.075	1.075	1.036
R2L	2	2	1.009	2.977	2.950	1.982	0.968	0.977
R2L	3	2	0.940	2.965	3.154	2.128	1.027	0.965
R2L	4	2	1.029	2.971	2.887	1.944	0.944	0.971
R2L	5	2	1.018	2.967	2.915	1.965	0.950	0.967
R2L	6	2	1.047	2.871	2.742	1.910	0.832	0.871
R2L	7	2	1.002	2.521	2.516	1.996	0.520	0.521
R2L	8	2	1.085	2.860	2.636	1.843	0.793	0.860
L2R	1	2	1.229	2.555	2.079	1.627	0.452	0.555
L2R	2	2	1.225	2.677	2.185	1.633	0.553	0.677
L2R	3	2	1.219	3.060	2.510	1.641	0.870	1.060
L2R	4	2	1.221	2.804	2.296	1.638	0.658	0.804
L2R	5	2	1.234	2.689	2.179	1.621	0.558	0.689
L2R	6	2	1.240	2.937	2.369	1.613	0.756	0.937
L2R	7	2	1.225	3.066	2.503	1.633	0.870	1.066
L2R	8	2	1.221	2.553	2.091	1.638	0.453	0.553
Averages			**1.119**	**2.844**	**2.573**	**1.805**	**0.767**	**0.844**
Standard Deviations			**0.087**	**0.197**	**0.225**	**0.138**	**0.165**	**0.197**

scs930_9-25-07-143017.txt								
R2L	1	3	0.467	3.289	7.043	6.424	0.619	0.289
R2L	2	3	0.463	3.236	6.989	6.479	0.510	0.236
R2L	3	3	0.458	3.366	7.349	6.550	0.799	0.366
R2L	4	3	0.438	3.248	7.416	6.849	0.566	0.248
R2L	5	3	0.448	3.252	7.259	6.696	0.563	0.252
L2R	1	3	0.565	3.412	6.039	5.310	0.729	0.412
L2R	2	3	0.562	3.284	5.843	5.338	0.505	0.284
L2R	3	3	0.555	1.815	3.270	5.405	-2.135	-1.185
L2R	4	3	0.548	3.387	6.181	5.474	0.706	0.387
L2R	5	3	0.550	3.393	6.169	5.455	0.715	0.393
Averages			**0.505**	**3.168**	**6.356**	**5.998**	**0.635**	**0.319**
Standard Deviations			**0.054**	**0.480**	**1.236**	**0.646**	**0.882**	**0.480**

Direction	Line Number	Shadow Size	Average Speed	Gap Length	Gap Time	Shadow Time	Relock Time	Relock Distance
scs930_9-25-07-143839.txt								
R2L	1	3	0.707	3.649	5.161	4.243	0.918	0.649
R2L	2	3	0.710	3.376	4.755	4.225	0.530	0.376
R2L	3	3	0.717	3.700	5.160	4.184	0.976	0.700
R2L	4	3	0.706	3.502	4.960	4.249	0.711	0.502
R2L	5	3	0.713	3.821	5.359	4.208	1.151	0.821
L2R	1	3	0.822	3.260	3.966	3.650	0.316	0.260
L2R	2	3	0.829	3.749	4.522	3.619	0.903	0.749
L2R	3	3	0.821	3.571	4.350	3.654	0.695	0.571
L2R	4	3	0.824	3.577	4.341	3.641	0.700	0.577
L2R	5	3	0.816	3.560	4.363	3.676	0.686	0.560
Averages			**0.767**	**3.577**	**4.694**	**3.935**	**0.759**	**0.577**
Standard Deviations			**0.059**	**0.169**	**0.455**	**0.303**	**0.238**	**0.169**

scs930_9-25-07-144230.txt								
R2L	1	3	0.836	3.775	4.516	3.589	0.927	0.775
R2L	2	3	0.879	2.680	3.049	3.413	-0.364	-0.320
R2L	3	3	0.886	2.770	3.126	3.386	-0.260	-0.230
R2L	4	3	0.869	3.791	4.362	3.452	0.910	0.791
R2L	5	3	0.854	3.701	4.334	3.513	0.821	0.701
R2L	6	3	0.867	3.983	4.594	3.460	1.134	0.983
R2L	7	3	0.861	3.703	4.301	3.484	0.816	0.703
L2R	1	3	1.029	3.772	3.666	2.915	0.750	0.772
L2R	2	3	1.025	3.776	3.684	2.927	0.757	0.776
L2R	3	3	1.020	3.663	3.591	2.941	0.650	0.663
L2R	4	3	1.027	3.775	3.676	2.921	0.755	0.775
L2R	5	3	1.023	3.773	3.688	2.933	0.756	0.773
L2R	6	3	1.029	3.772	3.666	2.915	0.750	0.772
L2R	7	3	1.015	3.566	3.513	2.956	0.558	0.566
Averages			**0.944**	**3.607**	**3.840**	**3.200**	**0.640**	**0.607**
Standard Deviations			**0.084**	**0.385**	**0.496**	**0.285**	**0.425**	**0.385**

scs930_9-25-07-144837.txt								
R2L	1	3	0.392	4.110	10.485	7.653	2.832	1.110
R2L	2	3	0.953	3.995	4.192	3.148	1.044	0.995
R2L	3	3	1.028	4.321	4.203	2.918	1.285	1.321
R2L	4	3	1.061	4.097	3.861	2.828	1.034	1.097
R2L	5	3	1.061	3.758	3.542	2.828	0.714	0.758
R2L	6	3	1.073	4.213	3.926	2.796	1.130	1.213
L2R	1	3	1.233	4.077	3.307	2.433	0.873	1.077
L2R	2	3	1.227	4.049	3.300	2.445	0.855	1.049
L2R	3	3	1.210	3.945	3.260	2.479	0.781	0.945
L2R	4	3	1.223	3.951	3.231	2.453	0.778	0.951
L2R	5	3	1.240	3.698	2.982	2.419	0.563	0.698
L2R	6	3	1.206	4.166	3.454	2.488	0.967	1.166

Averages	**1.076**	**4.032**	**4.145**	**3.074**	**0.911**	**1.032**
Standard Deviations	**0.237**	**0.178**	**2.035**	**1.462**	**0.588**	**0.178**

Trimble SPS930 - Single Screen Data Images

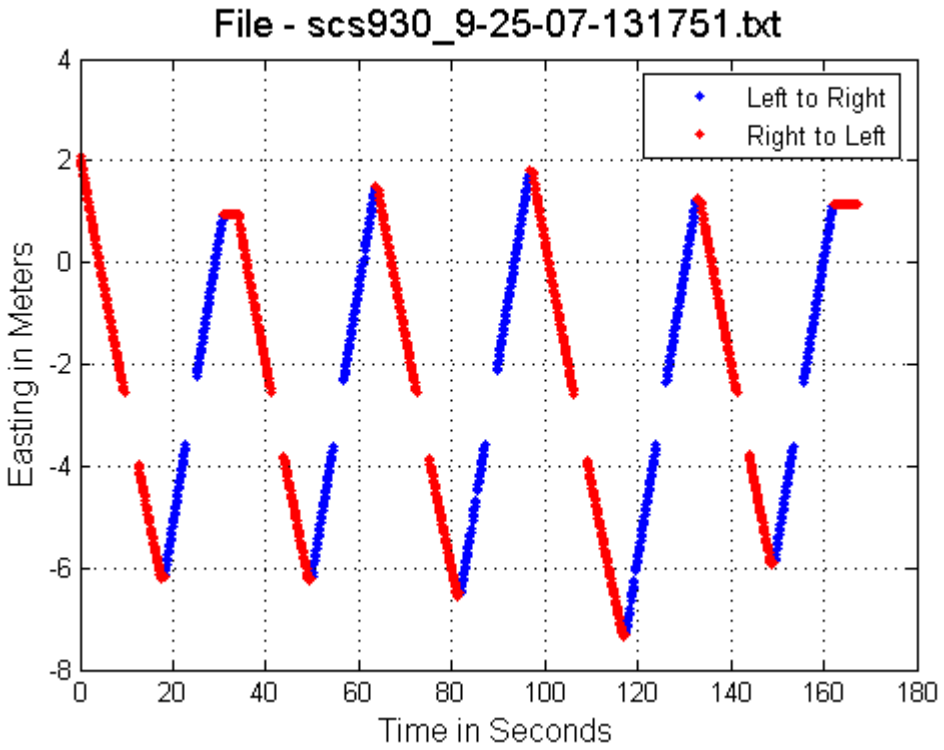

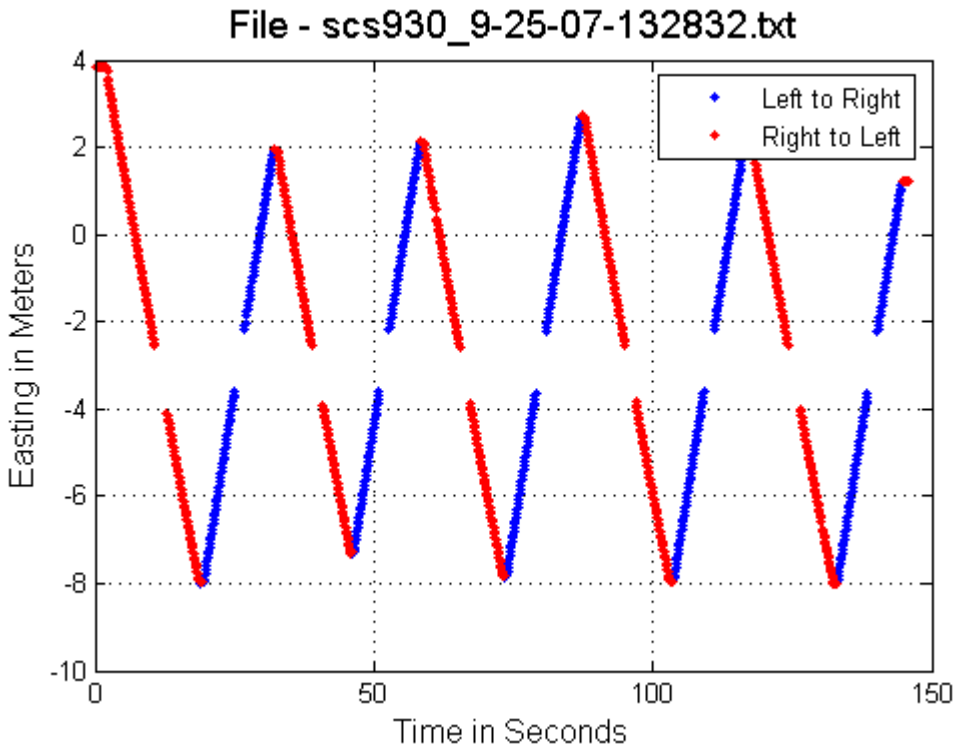

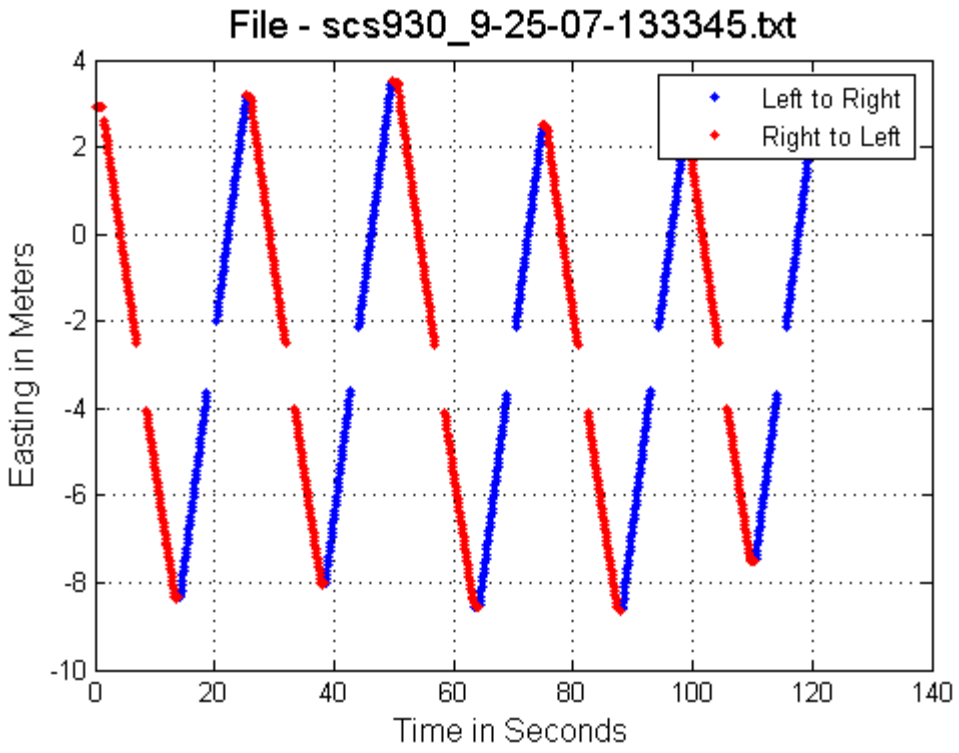
File - scs930_9-25-07-133345.txt
Left to Right
Right to Left
Easting in Meters
Time in Seconds
4
2
0
-2
-4
-6
-8
-10
0
20
40
60
80
100
120
140

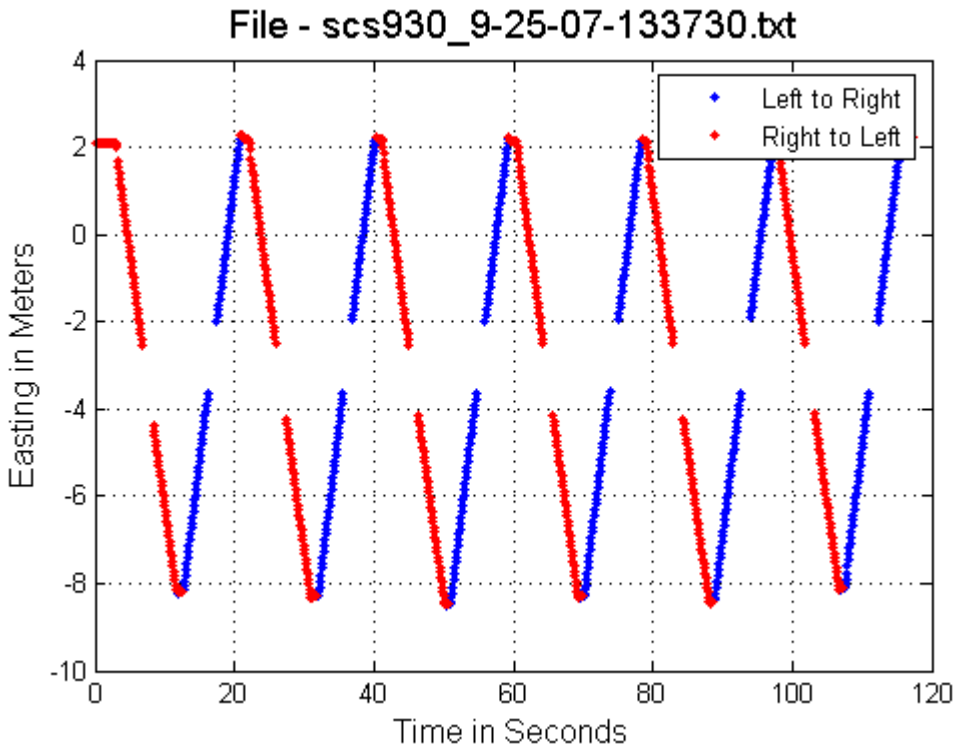
File - scs930_9-25-07-133730.txt
Left to Right
Right to Left
Easting in Meters
Time in Seconds
4
2
0
-2
-4
-6
-8
-10
0
20
40
60
80
100
120

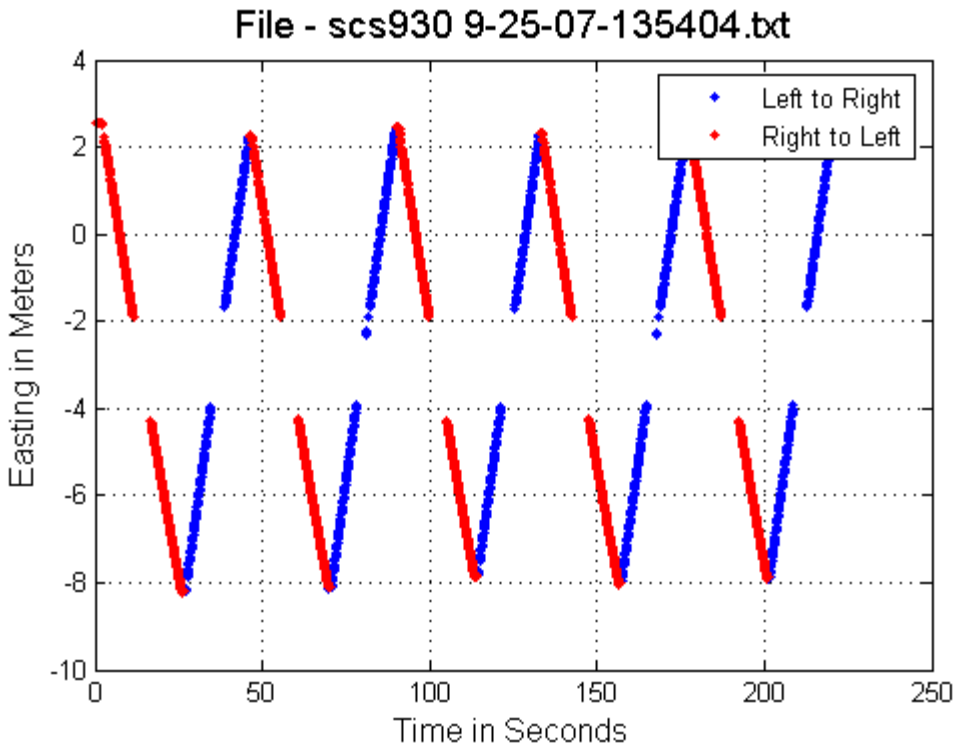
File - scs930 9-25-07-135404.txt
Left to Right
Right to Left
Easting in Meters
Time in Seconds
4
2
0
-2
-4
-6
-8
-10
0
50
100
150
200
250

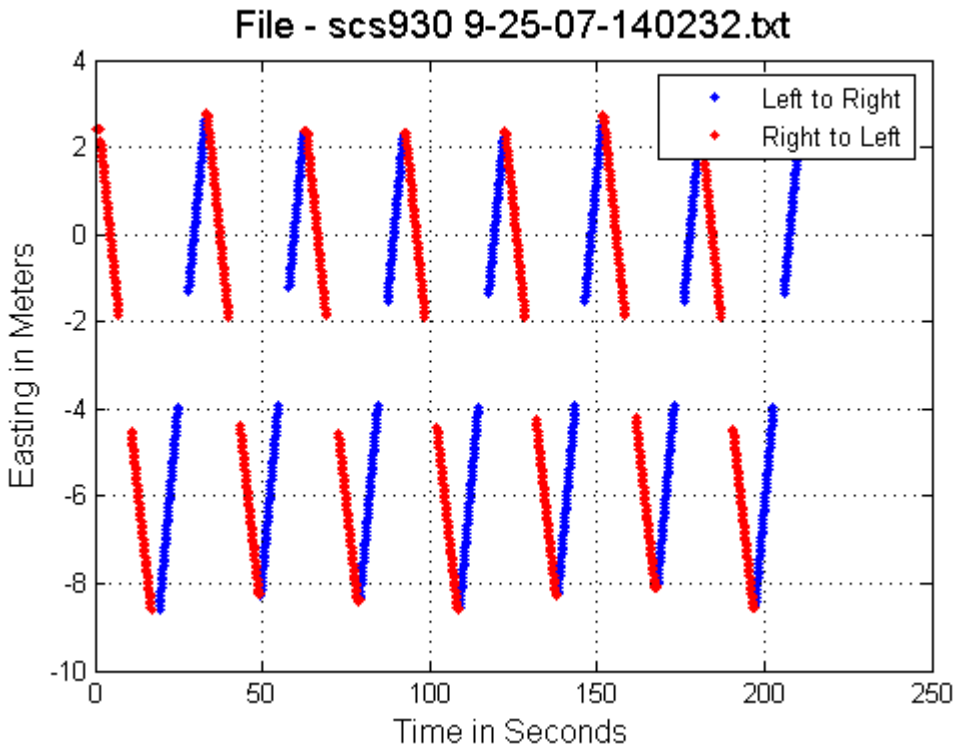
File - scs930 9-25-07-140232.txt
Left to Right
Right to Left
Easting in Meters
Time in Seconds
4
2
0
-2
-4
-6
-8
-10
0
50
100
150
200
250

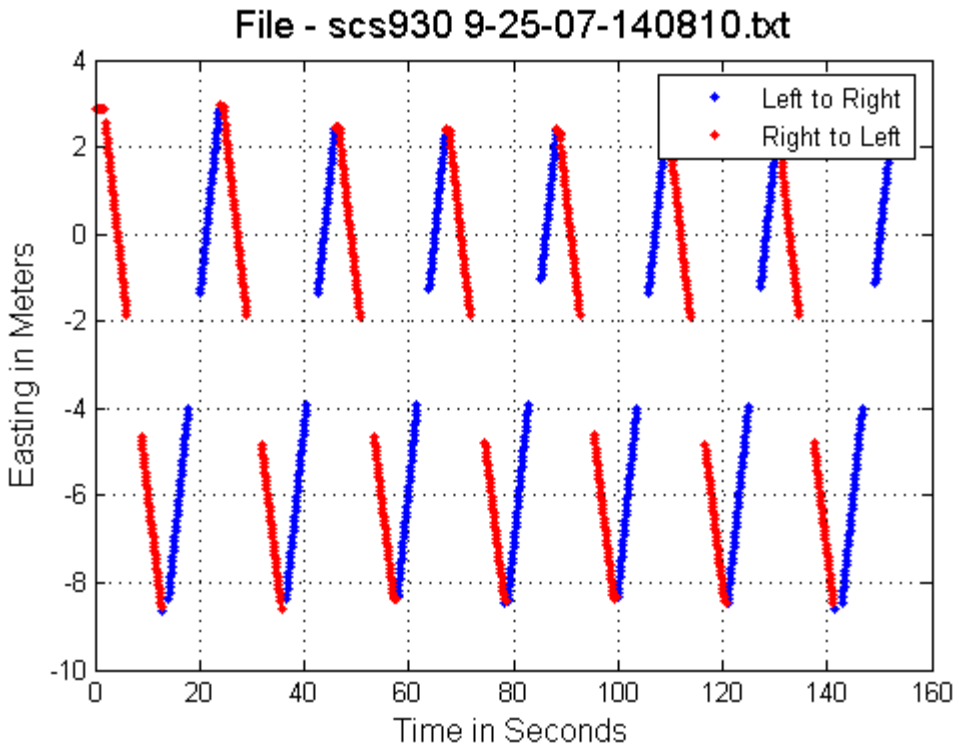
File - scs930 9-25-07-140810.txt
Left to Right
Right to Left
Easting in Meters
Time in Seconds
4
2
0
-2
-4
-6
-8
-10
0
20
40
60
80
100
120
140
160

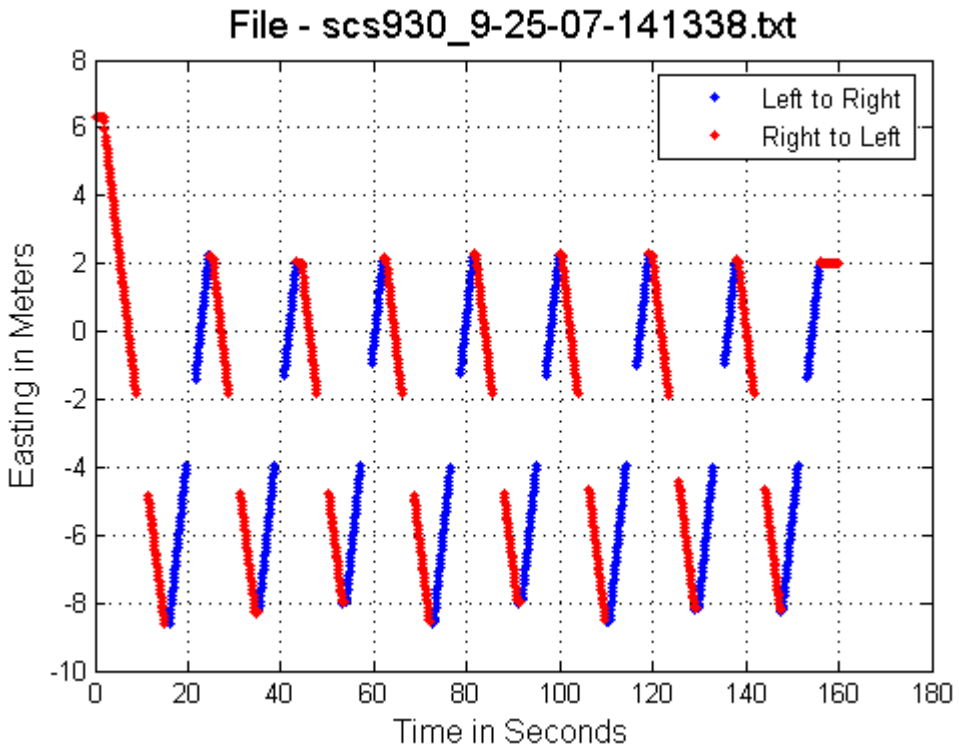
File - scs930_9-25-07-141338.txt
Left to Right
Right to Left
Easting in Meters
Time in Seconds
8
6
4
2
0
-2
-4
-6
-8
-10
0
20
40
60
80
100
120
140
160
180

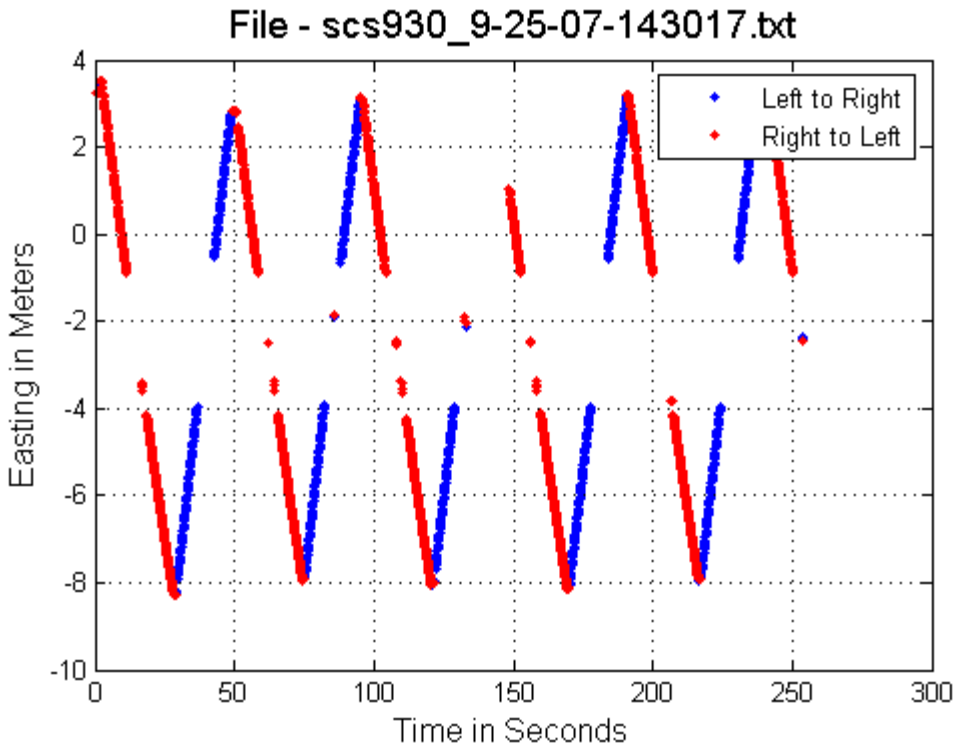
File - scs930_9-25-07-143017.txt
Left to Right
Right to Left
Easting in Meters
Time in Seconds
4
2
0
-2
-4
-6
-8
-10
0
50
100
150
200
250
300

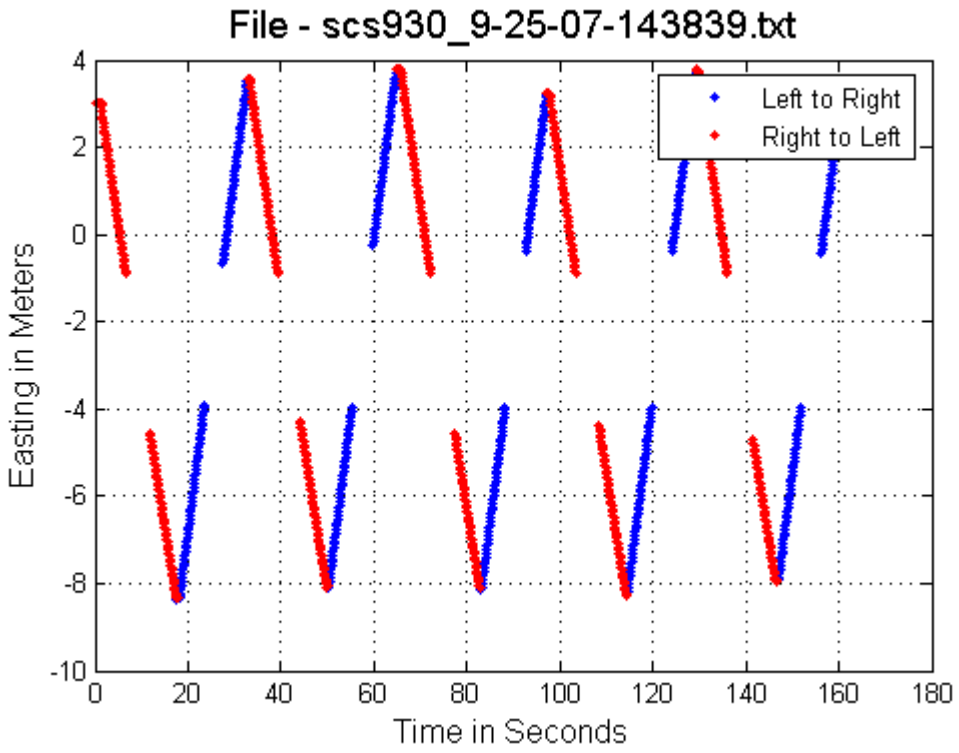
File - scs930_9-25-07-143839.txt
Left to Right
Right to Left
Easting in Meters
Time in Seconds
4
2
0
-2
-4
-6
-8
-10
0
20
40
60
80
100
120
140
160
180

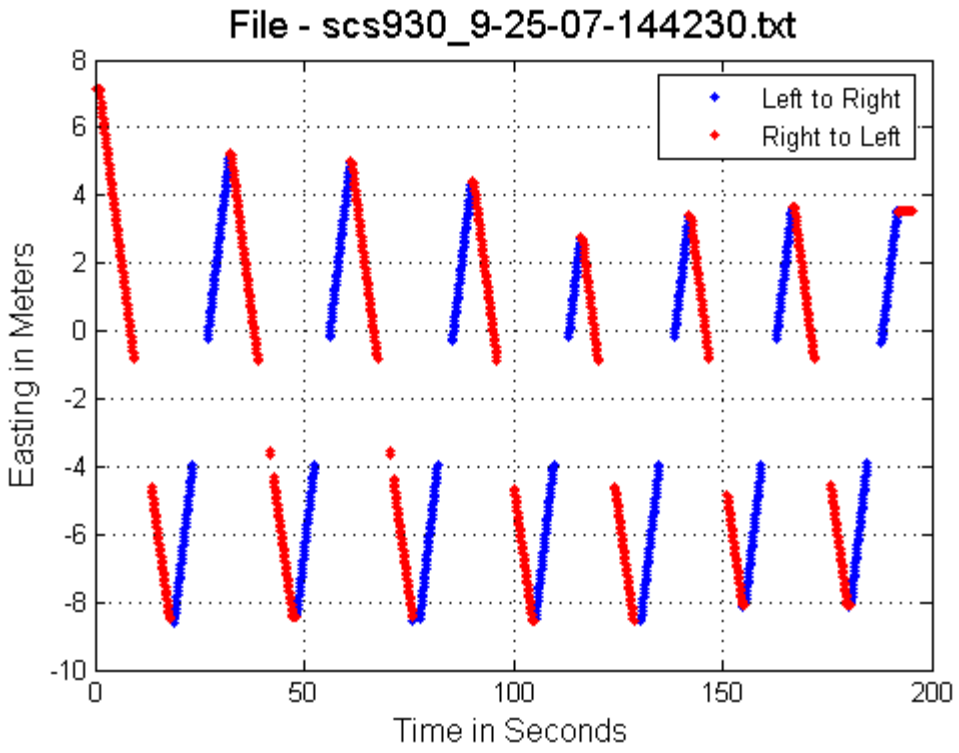
File - scs930_9-25-07-144230.txt
Left to Right
Right to Left
Easting in Meters
Time in Seconds
8
6
4
2
0
-2
-4
-6
-8
-10
0
50
100
150
200

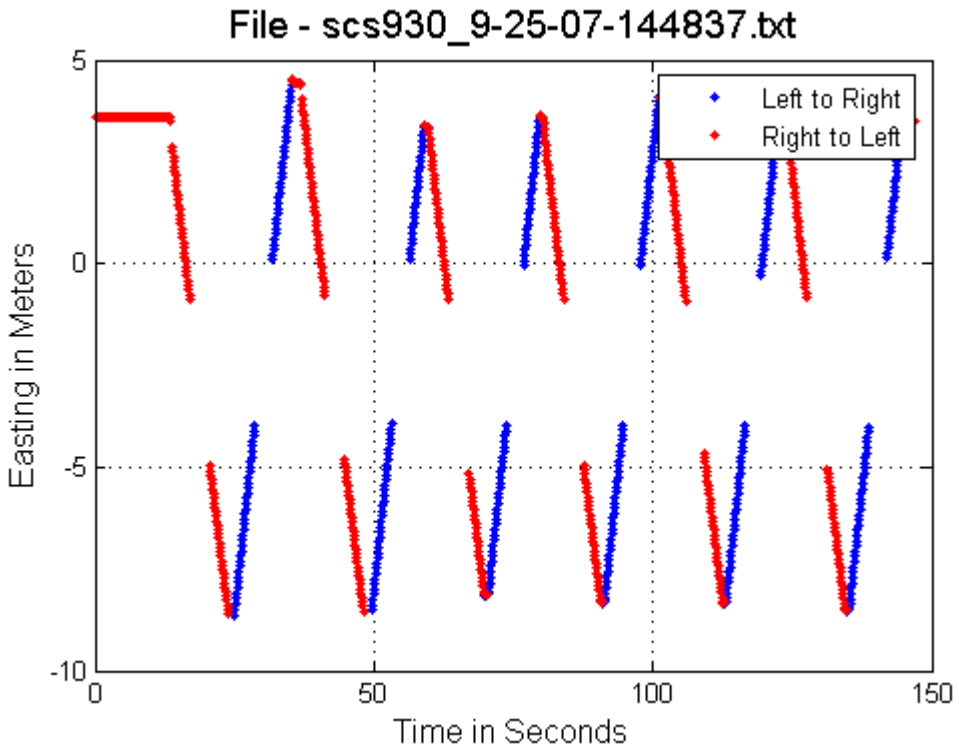
File - scs930_9-25-07-144837.txt
Left to Right
Right to Left
Easting in Meters
Time in Seconds
5
0
-5
-10
0
50
100
150

Trimble SPS930 – Double Screen Summary

				Screen 1				
Filename	Shadow Size	Gap Size	Average Speed	Gap Length	Gap Time	Shadow Time	Relock Time	Relock Distance
-150251.txt	1.6	1.0	0.522	1.949	3.759	3.096	0.663	0.349
-151301.txt	1.6	1.0	0.511	1.956	3.865	3.166	0.700	0.356
-151948.txt	1.6	1.0	0.729	2.115	2.938	2.205	0.733	0.515
-152428.txt	1.6	1.0	1.043	2.371	2.289	1.556	0.733	0.771
-152749.txt	1.6	1.0	1.236	2.430	2.000	1.297	0.703	0.830
-153857.txt	1.6	0.5	0.528	2.028	3.915	3.064	0.851	0.428
-154642.txt	1.6	0.5	0.781	2.065	2.716	2.090	0.626	0.465
-155050.txt	1.6	0.5	0.981	2.086	2.223	1.679	0.544	0.486
-155526.txt	1.6	0.5	1.233	0.000	0.000	0.000	0.000	0.000

				Screen 2					
Filename	Shadow Size	Gap Size	Average Speed	Gap Length	Gap Time	Shadow Time	Relock Time	Relock Distance	Missed Gap
-150251.txt	1.6	1.0	0.522	1.997	3.936	3.096	0.840	0.397	0
-151301.txt	1.6	1.0	0.511	1.932	3.878	3.166	0.713	0.332	0
-151948.txt	1.6	1.0	0.729	2.147	3.045	2.205	0.840	0.547	0
-152428.txt	1.6	1.0	1.043	2.349	2.309	1.556	0.753	0.749	1
-152749.txt	1.6	1.0	1.236	2.506	2.076	1.297	0.779	0.906	0
-153857.txt	1.6	0.5	0.528	2.033	3.995	3.064	0.931	0.433	0
-154642.txt	1.6	0.5	0.781	2.230	2.970	2.090	0.880	0.630	5
-155050.txt	1.6	0.5	0.981	2.360	2.545	1.679	0.867	0.760	6
-155526.txt	1.6	0.5	1.233	4.821	3.980	1.301	0.100	3.221	10

Trimble SPS930 – Double Screen File Results

Left or Right	Line Number	Shadow Size	Gap Size	Average Speed	Screen 1					Screen 2				
					Gap Length	Gap Time	Shadow Time	Relock Time	Relock Distance	Gap Length	Gap Time	Shadow Time	Relock Time	Relock Distance
scs930_9-25-07-150251.txt														
R2L	1	1.6	1	0.471	1.801	3.80	3.40	0.40	0.201	2.005	4.39	3.40	0.99	0.405
R2L	2	1.6	1	0.473	2.042	4.29	3.38	0.91	0.442	1.821	3.98	3.38	0.60	0.221
R2L	3	1.6	1	0.473	1.979	4.21	3.38	0.83	0.379	1.985	4.40	3.38	1.02	0.385
R2L	4	1.6	1	0.465	1.879	4.00	3.44	0.56	0.279	1.892	4.21	3.44	0.77	0.292
R2L	5	1.6	1	0.463	2.014	4.30	3.46	0.85	0.414	1.888	4.20	3.46	0.75	0.288
L2R	1	1.6	1	0.580	1.974	3.41	2.76	0.65	0.374	2.010	3.50	2.76	0.74	0.410
L2R	2	1.6	1	0.580	1.910	3.30	2.76	0.54	0.310	2.003	3.50	2.76	0.74	0.403
L2R	3	1.6	1	0.575	2.115	3.70	2.78	0.92	0.515	2.332	4.09	2.78	1.31	0.732
L2R	4	1.6	1	0.570	1.831	3.19	2.81	0.38	0.231	1.987	3.50	2.81	0.69	0.387
L2R	5	1.6	1	0.571	1.943	3.39	2.80	0.59	0.343	2.049	3.59	2.80	0.79	0.449
Averages				**0.522**	**1.949**	**3.759**	**3.096**	**0.663**	**0.349**	**1.997**	**3.936**	**3.096**	**0.840**	**0.397**
Standard Deviations				**0.056**	**0.097**	**0.426**	**0.333**	**0.201**	**0.097**	**0.137**	**0.377**	**0.333**	**0.209**	**0.137**

scs930_9-25-07-151301.txt														
R2L	1	1.6	1	0.465	1.851	4.00	3.45	0.56	0.251	1.825	4.09	3.45	0.65	0.225
R2L	2	1.6	1	0.460	1.986	4.30	3.48	0.83	0.386	1.872	4.19	3.48	0.72	0.272
R2L	3	1.6	1	0.457	2.018	4.39	3.50	0.89	0.418	1.778	4.00	3.50	0.50	0.178
R2L	4	1.6	1	0.457	1.944	4.30	3.50	0.80	0.344	1.894	4.30	3.50	0.80	0.294
R2L	5	1.6	1	0.455	2.006	4.40	3.52	0.88	0.406	1.855	4.19	3.52	0.67	0.255
R2L	6	1.6	1	0.457	2.016	4.39	3.50	0.89	0.416	1.857	4.18	3.50	0.68	0.257
L2R	1	1.6	1	0.570	2.011	3.50	2.81	0.69	0.411	2.037	3.59	2.81	0.78	0.437
L2R	2	1.6	1	0.566	1.990	3.50	2.83	0.67	0.390	1.967	3.50	2.83	0.67	0.367
L2R	3	1.6	1	0.557	1.955	3.50	2.88	0.63	0.355	1.946	3.50	2.88	0.63	0.346
L2R	4	1.6	1	0.563	1.973	3.50	2.84	0.66	0.373	2.016	3.60	2.84	0.76	0.416
L2R	5	1.6	1	0.561	1.853	3.30	2.85	0.45	0.253	2.120	3.80	2.85	0.95	0.520
L2R	6	1.6	1	0.564	1.865	3.30	2.84	0.46	0.265	2.019	3.60	2.84	0.76	0.419
Averages				**0.511**	**1.956**	**3.865**	**3.166**	**0.700**	**0.356**	**1.932**	**3.878**	**3.166**	**0.713**	**0.332**
Standard Deviations				**0.055**	**0.064**	**0.468**	**0.340**	**0.159**	**0.064**	**0.102**	**0.309**	**0.340**	**0.111**	**0.102**

Left or Right	Line Number	Shadow Size	Gap Size	Average Speed	Screen 1					Screen 2				
					Gap Length	Gap Time	Shadow Time	Relock Time	Relock Distance	Gap Length	Gap Time	Shadow Time	Relock Time	Relock Distance
scs930_9-25-07-152749.txt														
R2L	1	1.6	1	1.189	2.440	2.10	1.35	0.75	0.840	2.629	2.30	1.35	0.95	1.029
R2L	2	1.6	1	1.182	2.548	2.20	1.35	0.85	0.948	2.285	2.00	1.35	0.65	0.685
R2L	3	1.6	1	1.185	2.434	2.10	1.35	0.75	0.834	2.510	2.20	1.35	0.85	0.910
R2L	4	1.6	1	1.189	2.669	2.29	1.35	0.94	1.069	2.624	2.30	1.35	0.95	1.024
R2L	5	1.6	1	1.182	2.557	2.20	1.35	0.85	0.957	1.682	1.50	1.35	0.15	0.082
L2R	1	1.6	1	1.303	2.339	1.81	1.23	0.58	0.739	2.320	1.80	1.23	0.57	0.720
L2R	2	1.6	1	1.290	2.338	1.78	1.24	0.54	0.738	2.707	2.09	1.24	0.85	1.107
L2R	3	1.6	1	1.307	2.340	1.82	1.22	0.60	0.740	2.836	2.19	1.22	0.97	1.236
L2R	4	1.6	1	1.300	2.209	1.70	1.23	0.47	0.609	2.965	2.30	1.23	1.07	1.365
Averages				**1.236**	**2.430**	**2.000**	**1.297**	**0.703**	**0.830**	**2.506**	**2.076**	**1.297**	**0.779**	**0.906**
Standard Deviations				**0.061**	**0.142**	**0.221**	**0.063**	**0.163**	**0.142**	**0.379**	**0.272**	**0.063**	**0.285**	**0.379**

scs930_9-25-07-153857.txt														
R2L	1	1.6	0.5	0.480	2.005	4.21	3.34	0.87	0.405	2.018	4.41	3.34	1.07	0.418
R2L	2	1.6	0.5	0.476	1.995	4.20	3.36	0.84	0.395	1.993	4.30	3.36	0.94	0.393
R2L	3	1.6	0.5	0.478	2.155	4.59	3.35	1.24	0.555	2.019	4.41	3.35	1.06	0.419
R2L	4	1.6	0.5	0.471	1.993	4.20	3.40	0.80	0.393	2.065	4.50	3.40	1.10	0.465
R2L	5	1.6	0.5	0.463	2.051	4.50	3.45	1.05	0.451	1.552	3.69	3.45	0.24	-0.048
R2L	6	1.6	0.5	0.470	1.968	4.20	3.40	0.80	0.368	2.141	4.71	3.40	1.31	0.541
R2L	7	1.6	0.5	0.476	2.126	4.61	3.36	1.25	0.526	2.006	4.41	3.36	1.05	0.406
L2R	1	1.6	0.5	0.590	2.009	3.39	2.71	0.68	0.409	1.930	3.30	2.71	0.59	0.330
L2R	2	1.6	0.5	0.588	1.872	3.21	2.72	0.49	0.272	2.024	3.50	2.72	0.78	0.424
L2R	3	1.6	0.5	0.581	2.048	3.50	2.76	0.74	0.448	2.142	3.69	2.76	0.93	0.542
L2R	4	1.6	0.5	0.579	1.990	3.50	2.76	0.74	0.390	2.296	4.00	2.76	1.24	0.696
L2R	5	1.6	0.5	0.580	2.012	3.50	2.76	0.74	0.412	2.046	3.60	2.76	0.84	0.446
L2R	6	1.6	0.5	0.577	2.084	3.59	2.77	0.82	0.484	2.000	3.50	2.77	0.73	0.400
L2R	7	1.6	0.5	0.584	2.089	3.61	2.74	0.87	0.489	2.229	3.91	2.74	1.17	0.629
Averages				**0.528**	**2.028**	**3.915**	**3.064**	**0.851**	**0.428**	**2.033**	**3.995**	**3.064**	**0.931**	**0.433**
Standard Deviations				**0.057**	**0.071**	**0.488**	**0.330**	**0.207**	**0.071**	**0.171**	**0.456**	**0.330**	**0.284**	**0.171**

Left or Right	Line Number	Shadow Size	Gap Size	Average Speed	Screen 1					Screen 2				
					Gap Length	Gap Time	Shadow Time	Relock Time	Relock Distance	Gap Length	Gap Time	Shadow Time	Relock Time	Relock Distance
scs930_9-25-07-154642.txt														
R2L	1	1.6	0.5	0.726	2.019	2.80	2.20	0.60	0.419	1.962	2.81	2.20	0.61	0.362
R2L	2	1.6	0.5	0.715	2.071	2.90	2.24	0.66	0.471	2.025	2.89	2.24	0.65	0.425
R2L	3	1.6	0.5	0.715	2.071	2.90	2.24	0.66	0.471	2.235	3.20	2.24	0.96	0.635
R2L	4	1.6	0.5	0.719	4.437	6.30	2.22	4.08	2.837					
R2L	5	1.6	0.5	0.716	2.136	3.00	2.23	0.77	0.536	2.304	3.30	2.23	1.07	0.704
R2L	6	1.6	0.5	0.724	4.276	6.11	2.21	3.90	2.676					
L2R	1	1.6	0.5	0.846	4.408	5.31	1.89	3.42	2.808					
L2R	2	1.6	0.5	0.843	2.002	2.41	1.90	0.51	0.402	2.234	2.68	1.90	0.78	0.634
L2R	3	1.6	0.5	0.844	2.086	2.50	1.90	0.60	0.486	2.479	3.00	1.90	1.10	0.879
L2R	4	1.6	0.5	0.843	4.244	5.10	1.90	3.20	2.644					
L2R	5	1.6	0.5	0.834	2.070	2.50	1.92	0.58	0.470	2.374	2.91	1.92	0.99	0.774
L2R	6	1.6	0.5	0.849	4.515	5.41	1.88	3.53	2.915					
Averages				**0.781**	**2.065**	**2.716**	**2.090**	**0.626**	**0.465**	**2.230**	**2.970**	**2.090**	**0.880**	**0.630**
Standard Deviations				**0.065**	**1.192**	**1.552**	**0.171**	**1.560**	**1.192**	**0.184**	**0.217**	**0.174**	**0.200**	**0.184**

scs930_9-25-07-155050.txt														
R2L	1	1.6	0.5	0.902	4.598	5.11	1.77	3.34	2.998					
R2L	2	1.6	0.5	0.927	2.100	2.29	1.73	0.56	0.500	2.420	2.69	1.73	0.96	0.820
R2L	3	1.6	0.5	0.927	2.170	2.40	1.73	0.67	0.570	2.416	2.69	1.73	0.96	0.816
R2L	4	1.6	0.5	0.928	4.500	5.00	1.72	3.28	2.900					
R2L	5	1.6	0.5	0.924	1.989	2.20	1.73	0.47	0.389	2.225	2.50	1.73	0.77	0.625
L2R	1	1.6	0.5	1.047	2.086	2.00	1.53	0.47	0.486	2.379	2.30	1.53	0.77	0.779
L2R	2	1.6	0.5	1.037	4.456	4.30	1.54	2.76	2.856					
L2R	3	1.6	0.5	1.040	4.447	4.31	1.54	2.77	2.847					
L2R	4	1.6	0.5	1.042	4.755	4.61	1.54	3.08	3.155					
L2R	5	1.6	0.5	1.038	4.748	4.60	1.54	3.06	3.148					
Averages				**0.981**	**2.086**	**2.223**	**1.679**	**0.544**	**0.486**	**2.360**	**2.545**	**1.679**	**0.867**	**0.760**
Standard Deviations				**0.063**	**1.295**	**1.285**	**0.106**	**1.306**	**1.295**	**0.092**	**0.186**	**0.100**	**0.111**	**0.092**

Left or Right	Line Number	Shadow Size	Gap Size	Average Speed	Screen 1					Screen 2				
					Gap Length	Gap Time	Shadow Time	Relock Time	Relock Distance	Gap Length	Gap Time	Shadow Time	Relock Time	Relock Distance
scs930_9-25-07-155526.txt														
R2L	1	1.6	0.5	1.132	4.921	4.30	1.41	2.89	3.321					
R2L	2	1.6	0.5	1.177	4.587	4.01	1.36	2.65	2.987					
R2L	3	1.6	0.5	1.178	4.911	4.31	1.36	2.95	3.311					
R2L	4	1.6	0.5	1.175	4.590	4.00	1.36	2.64	2.990					
R2L	5	1.6	0.5	1.172	4.802	4.18	1.37	2.82	3.202					
L2R	1	1.6	0.5	1.301	4.625	3.59	1.23	2.36	3.025					
L2R	2	1.6	0.5	1.299	5.008	3.90	1.23	2.67	3.408					
L2R	3	1.6	0.5	1.304	5.007	3.91	1.23	2.68	3.407					
L2R	4	1.6	0.5	1.298	4.885	3.80	1.23	2.57	3.285					
L2R	5	1.6	0.5	1.298	4.876	3.80	1.23	2.57	3.276					
Averages				**1.233**	**4.821**	**3.980**	**1.301**	**2.679**	**3.221**					
Standard Deviations				**0.071**	**0.164**	**0.231**	**0.076**	**0.172**	**0.164**					

Trimble SPS930 – Double Screen Data Images

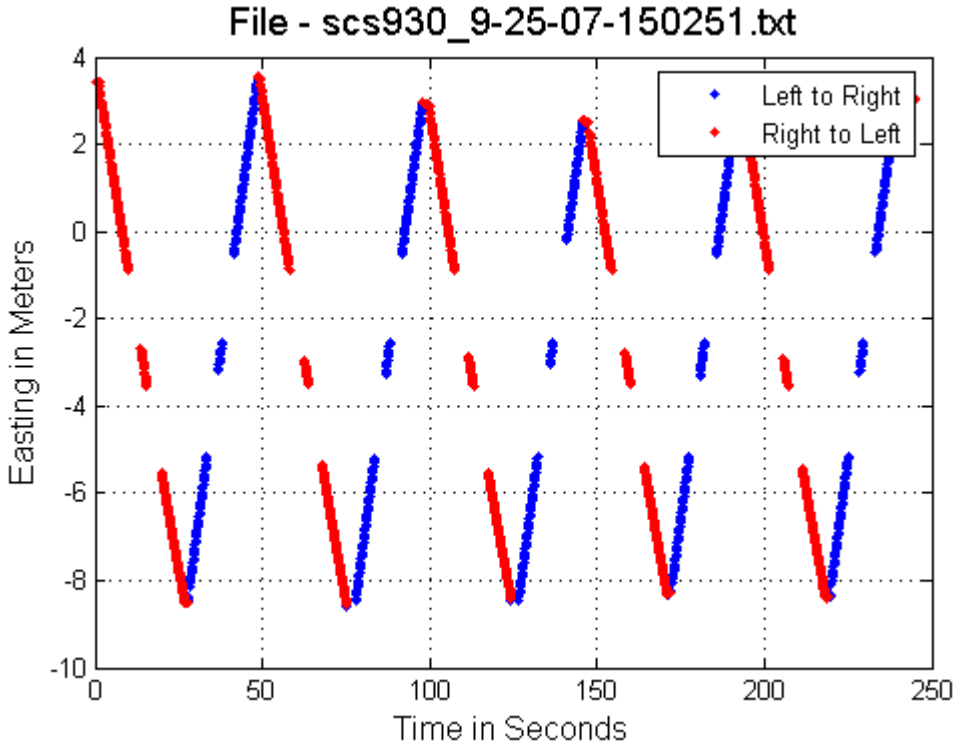

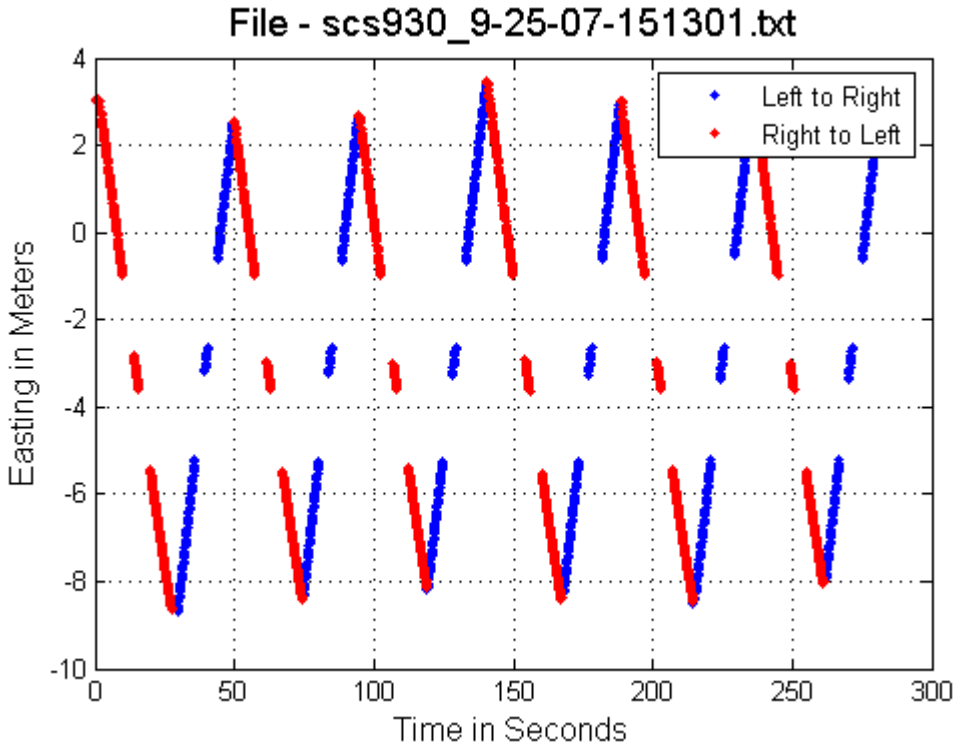

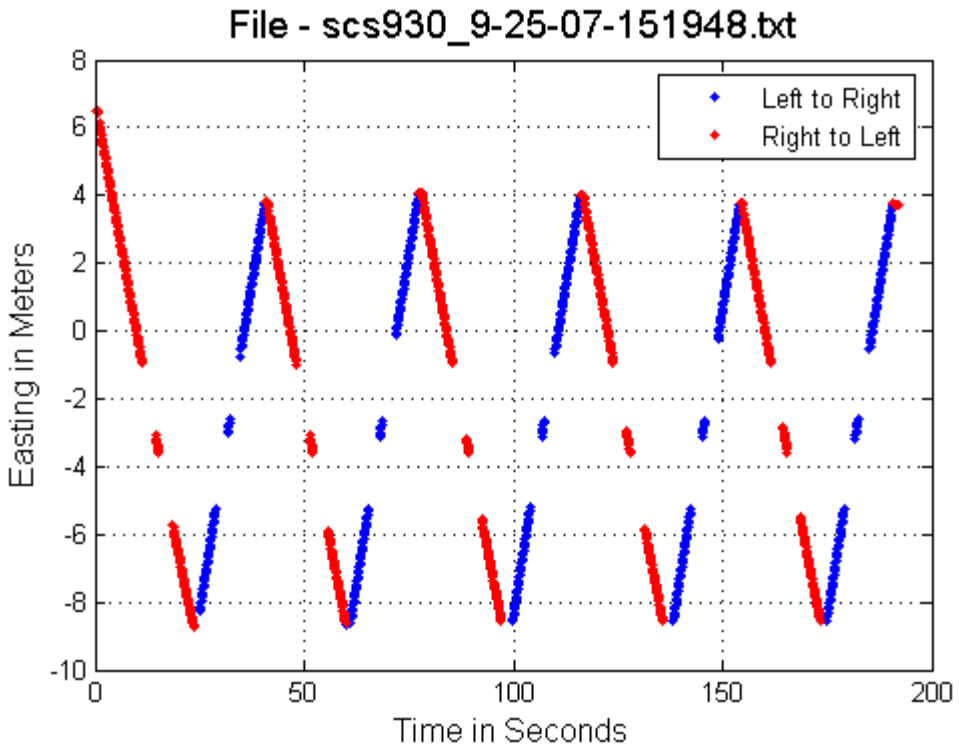
File - scs930_9-25-07-151948.txt
Left to Right
Right to Left
Easting in Meters
Time in Seconds
8
6
4
2
0
-2
-4
-6
-8
-10
0
50
100
150
200

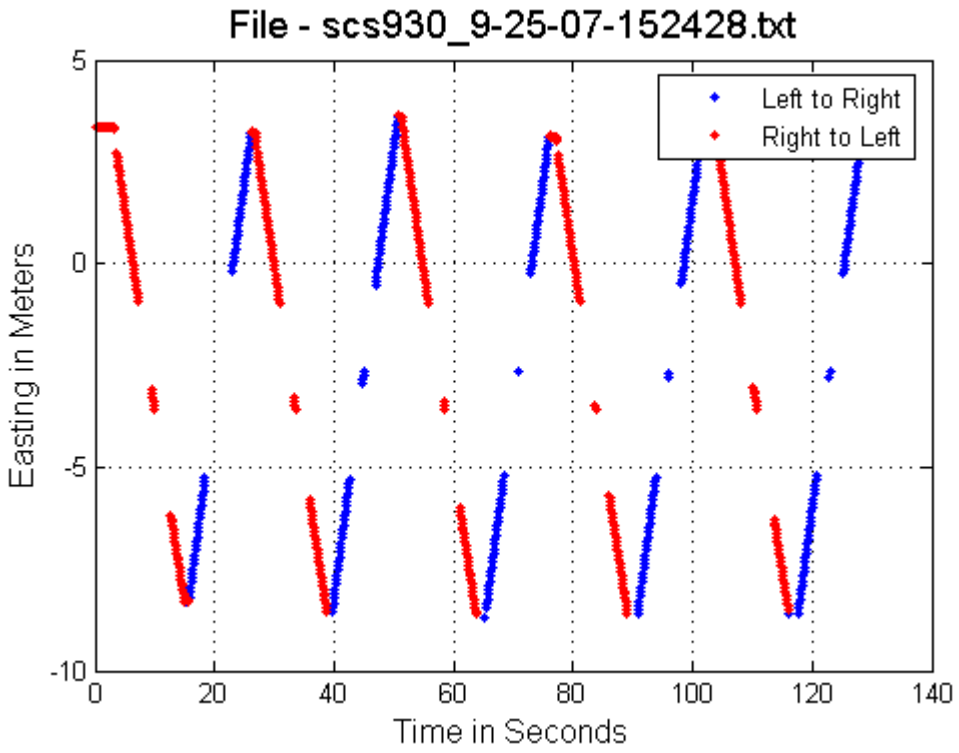
File - scs930_9-25-07-152428.txt
Left to Right
Right to Left
Easting in Meters
Time in Seconds
5
0
-5
-10
0
20
40
60
80
100
120
140

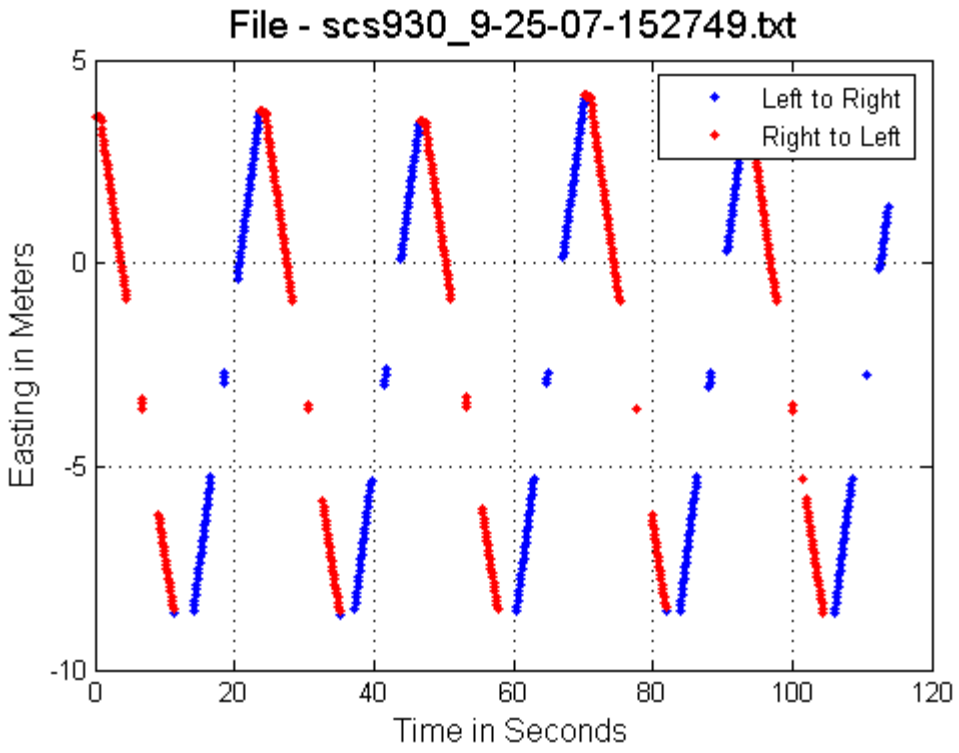
File - scs930_9-25-07-152749.txt
Left to Right
Right to Left
Easting in Meters
Time in Seconds
5
0
-5
-10
0
20
40
60
80
100
120

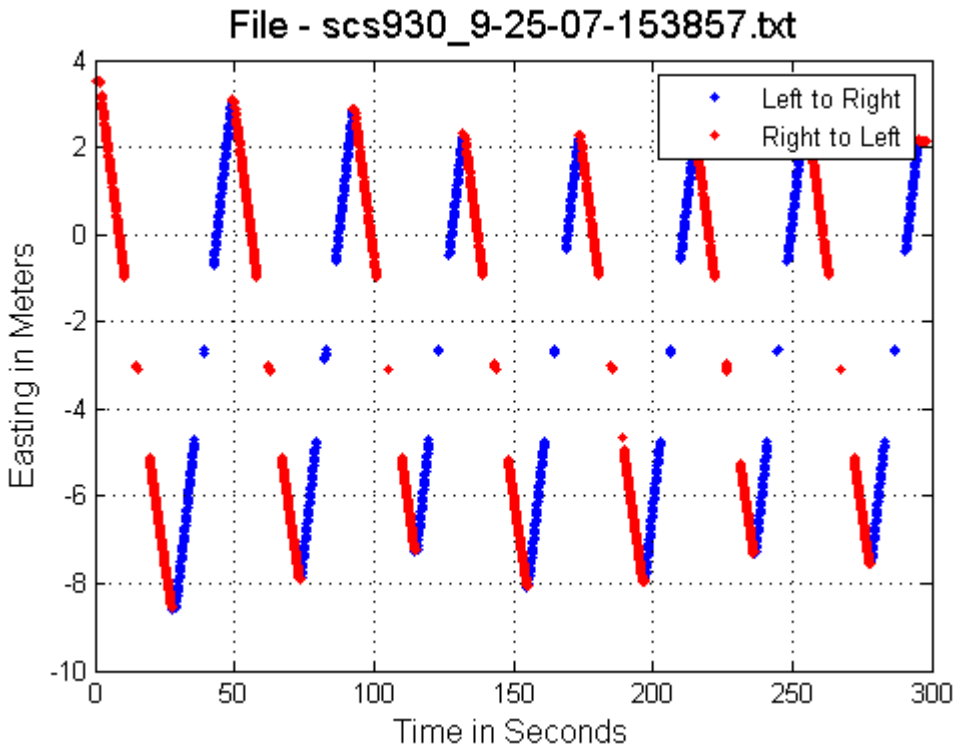
File - scs930_9-25-07-153857.txt
Left to Right
Right to Left
Easting in Meters
Time in Seconds
4
2
0
-2
-4
-6
-8
-10
0
50
100
150
200
250
300

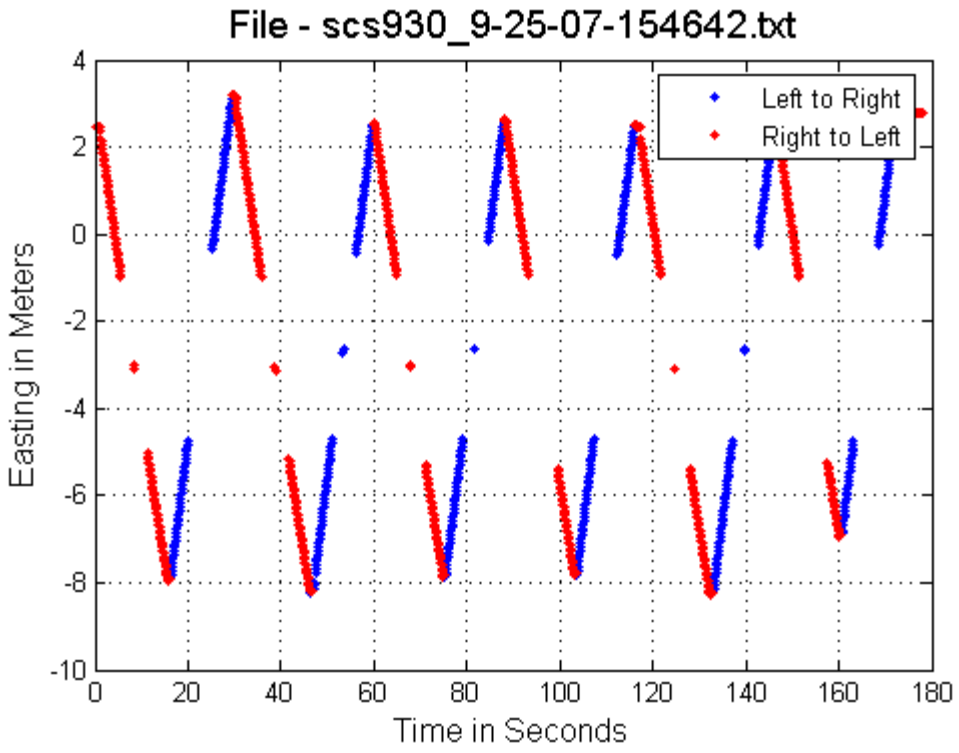
File - scs930_9-25-07-154642.txt
Left to Right
Right to Left
Easting in Meters
Time in Seconds
4
2
0
-2
-4
-6
-8
-10
0
20
40
60
80
100
120
140
160
180

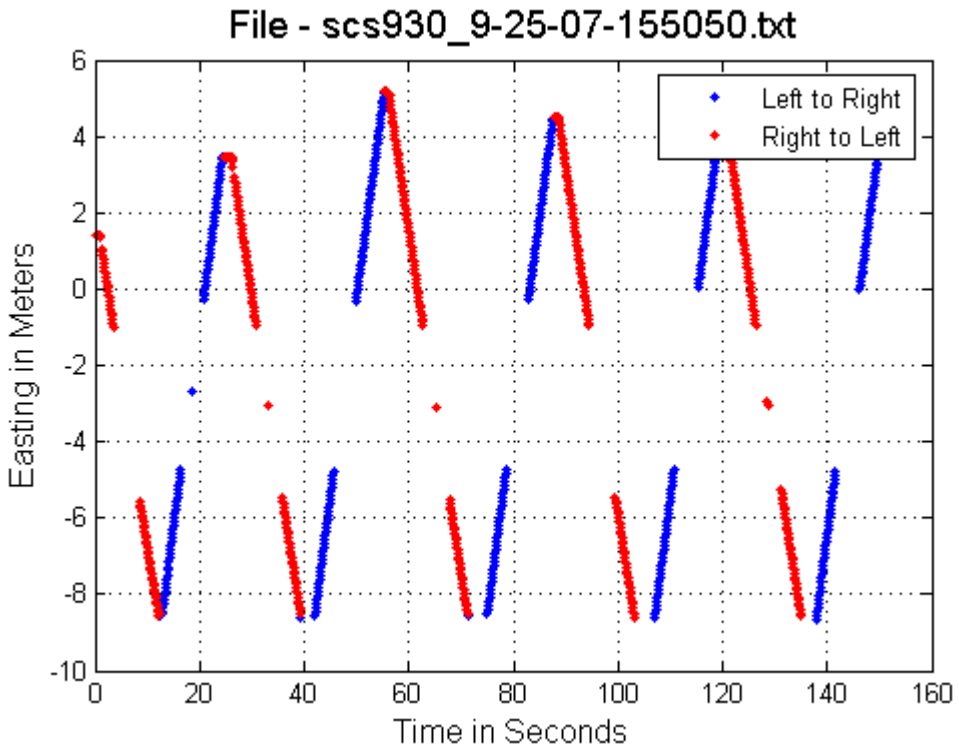
File - scs930_9-25-07-155050.txt
Left to Right
Right to Left
Easting in Meters
Time in Seconds
6
4
2
0
-2
-4
-6
-8
-10
0
20
40
60
80
100
120
140
160

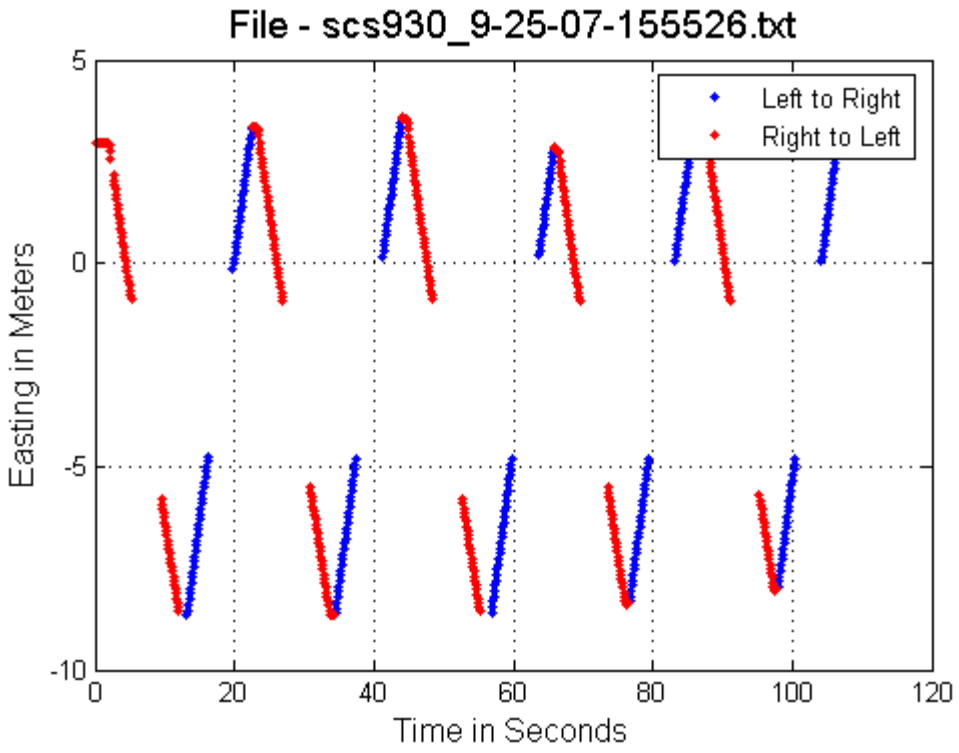
File - scs930_9-25-07-155526.txt
Left to Right
Right to Left
Easting in Meters
Time in Seconds
5
0
-5
-10
0
20
40
60
80
100
120

APPENDIX B

B. LEICA FIRMWARE INVESTIGATIONS

After the Leica moving target tests, it was decided to contact Leica to figure out how to improve the performance. The performance issues of the Leica were the inconsistent prism relock times and the ability of the gun to consistently lock onto a slowly moving prism, so additional investigations were conducted to determine which individual GeoCOM commands were best suited to cause the Leica to regain tracking or to "re-lock" on the prism. For these investigations, a bench-scale system was constructed that included a 0.8 m long motorized linear track. The prism was then placed on a carriage on the linear track driven by a stepper motor. This provided the ability to move the prism back and forth down the track at a speed equivalent to 1 m/s for field applications. In repeated trials, various GeoCOM RS-232 ASCII-type communications were executed from button presses on a software-based graphical user interface (GUI) to evaluate command control over re-lock. This approach permitted simultaneous operation of two units in real time and issuance of new commands the instant a prior command was completed.

B.1. Methods

As described previously, following the LOS tests, additional tests of the Leica system functionality were conducted to better understand the timing and capabilities of the Leica system to relock on a prism following obstruction passage. In order to determine which commands were best suited to cause the Leica to regain tracking or to relock on the prism, a test system was set up that allowed execution of individual GeoCOM commands from button presses on a software-based GUI. The GeoCOM RS-232 and ASCII type communications were used when operating the TPS1203. This approach permitted simultaneous operation of two units in real-time and issuance of new commands the instant a prior command was completed.

For these tests, the TPS1203 tracked a prism moving at a rate of 1 m/s. As the prism approached a point in the middle of the travel path, a command was issued for the gun to stop tracking the prism. This left the gun pointing at the last known location of the prism. Once the prism travel was resumed, the TPS1203 was instructed to attempt to lock on to the moving target. The ability to relock onto the prism before the prism was at the end of the track was evaluated through numerous repeats of this test at the 1 m/s travel rate. This test was then repeated at a slower prism travel rate of 0.66 m/s.

Next, to test the ability to improve the system's capabilities for relocking onto a moving prism, a set of TPS commands were created to command the TPS to first orient the gun to the expected prism location (based upon a calculated position from a second TPS that retained its lock), and

then regain lock. Based on input from Leica engineers, additional testing of prism relock was conducted using the following sequence of commands to attempt to regain lock on a "lost" prism:

1. Move To current prism location (AUT_MakePositioning)
2. Search for prism (AUT_PS_SearchNext)
3. Optimize pointing position (AUT_FineAdjust)
4. Lock on target (AUT_LockIn)
5. Resume taking distance measurement (TMC_QuickDist)

When tested, this approach was found not to work; through trial-and-error, the following sequence of commands was used instead to regain lock on a prism:

1. Turn off lock state (AUS_SetUserLockState)
2. Turn on lock state (AUS_SetUserLockState)
3. Perform a search (AUT_Search)
4. Move to the current prism location (AUT_MakePositioning)
5. Lock on target (AUT_LockIn)
6. Confirm lock by reading lock status (MOT_ReadLockStatus)
7. Resume taking distance measurement (TMC_QuickDist)

The test described above was repeated using this new command sequence and the ability of the system to regain lock on a moving target was quantified.

B.2. Results

Testing of the Leica system to determine the ability to use commands to control relock resulted in a determination that the system could not reliably lock onto the target when it was moving at a rate of 1 m/s. At this velocity, the success rate for relock was approximately 10%. When the prism velocity was slowed to 0.66 m/s, the TPS was successful at regaining lock. Therefore, the system maintains capability to regain lock up to a maximum prism travel speed of 0.66 - 1.0 m/s.

The tests were also conducted using the new sequential set of commands to cause the TPS to first move to the current prism location (based upon a calculated position from a second TPS that retained its lock), and then regain lock while the prism was traveling at a rate equivalent to 1 m/s. While these commands were created to perform the task, the results were inconsistent and determined to be of poor reliability and therefore not an avenue for further investigation into improvements of the Leica's tracking ability. The problems encountered in testing of the Leica commands to perform this function are as follows:

1. The ability to successfully carry out the AUT_LockIn command relied on two seemingly unrelated operations. The first is that a toggling of the Lock State needs to be executed following loss of tracking lock. The second, and more obscure, is that a search must be carried out prior to issuing a LockIn command in order for the LockIn to reliably work; however, the result of the search appears to be irrelevant. The important fact seems to be that a Search command must be executed first or the subsequent LockIn will nearly always fail.

2. The AUT_Lockin command's return value was of little use in determining if a Lockin was successful in terms of regaining the lock on the prism. Often times the return value would be a zero (success) and the subsequent reading of the lock status indicated that the unit was not locked on. Alternatively, an unsuccessful response (typically returning a 512 indicating the Tracking system was not ready, or a 517 indicating that no targets were detected) and testing the lock status would indicate that the system had regained lock and was successfully tracking the prism.
3. The MOT_ReadLockStatus would return either 1 (lock good), 2 (in prediction mode) or 0 (Lock is not good) following reporting of success in step 5 (LockIn). In the algorithm tested for this investigation, if a 2 was returned, repeated sampling of the MOT_ReadLockStatus response would randomly return either a 1 or 0 value.
4. Following a successful response in automatically locking on to the target and reading lock status, the system was only able to estimate the prism travel distance using the (TMC_QuickDist) command about 33 to 50% of the time. Other times, the return value from the TMC_QuickDist command would return a result of 1285 (meaning only angle measurements are valid, and a distance measure is not supplied). Therefore, the Leica's response was unreliable; when the QuickDist command returned a value of 1285, the entire sequence of steps to establish relock had to be reinitiated.
5. In spite of the fact that the automatic tracking was disabled in the TPS (from front panel controls and via GeoCOM commands) and the search area limited to 1.0° when executing the AUT_Search command, the TPS unit would often perform searching or tracking motor movements as part of the execution of the search command. Given the limited size of the search area specified in the search command (1.0° × 1.0°), the TPS should not have moved to complete the search.
6. The simple operation of turning the Lock state on or off often took between 1 and 2 seconds to complete. Also, it was not unusual for the search command to take up to 10 seconds to complete. Again, given that the search area was always specified as 1.0° × 1.0°, this duration was not expected.

B.3. Discussion

Testing of the Leica system to determine the ability to use commands to control relock resulted in a determination that the system could not reliably lock onto the target when it was moving at rate of 1 m/s. At this travel rate, the success rate for relock was approximately 10%. When the prism travel rate was slowed to a travel rate of 0.66 m/s, the TPS was successful at regaining lock. Therefore, the system maintains capability to regain lock up to a maximum prism travel speed of 0.66 - 1.0 m/s.